Investigating Foaming Materials in 3D Printing: An Application for Motorcycle Helmets

Noortje Laureijs

Master thesis
Msc Integrated Product Design
Delft University of Technology

Graduation date: 18th of April, 2023

Author
Eleonora Lieve (Noortje) Laureijs

Master thesis
Master Integrated Product design

Supervisory team
Dr. Ir. Doubrovski, E.L. (Chair)
Dr. Özdemir, M. (Mentor)

Delft University of Technology
Faculty of Industrial Design Engineering
Landbergstraat 15
2628 CE Delft
The Netherlands

Investigating Foaming Materials in 3D Printing: An Application for Motorcycle Helmets

Figure showing the created demonstrator with foaming PLA substituting the impact liner and foaming TPU substituting the comfort liner

Summary

This thesis investigates novel foaming materials for fused deposition modelling (FDM) which have been introduced in 2019. The materials are able to foam by the addition of foaming agents. Foaming materials for FDM printing can be advantageous since they can create lightweight models, and have good impact strength and toughness in relation to their weight (Nofar et al, 2022). The goals of this thesis are to: research the existing knowledge about foaming materials for FDM printing, characterize the different printing parameters that influence the amount of foaming and propose an application for foaming materials for FDM printing. The investigated materials are foaming PLA, ASA, and TPU.

The first goal is reached by conducting a literature review. First, the material properties of foaming materials outside the scope of FDM printing are investigated to better understand the advantages for foaming materials for FDM as well. Second, printing parameters are investigated to understand how these affect final printed products. Third, the available literature for the foaming filaments for FDM printing is investigated. An overview of the material properties in tension is made for the foaming filaments. This shows that most material properties are known for the foaming PLA.

The second goal is reached by conducting three experiments, which investigate the influence of nozzle temperature, fan, printing speed and flow rate. From these experiments it is concluded that the nozzle temperature, printing speed and flow rate influence the expansion of the material, depending on the desired outcome. The fan speed only influences the expansion of the foaming TPU. With the results of these experiments, an overview is made of the influence of the printing parameters on the expansion using the three-link chain model (Doubrovski et al, 2011).

The third goal is reached by conducting a compression experiment in which the foaming PLA is compared with expanded polystyrene (EPS). The results from this experiment and the printing parameters are applied within a motorcycle helmet as demonstrator. This demonstrator shows that the foaming materials for FDM printing could be an interesting area for further research.

This thesis provides a starting point for further research into the influence of printing parameters for foaming materials, as well as the material properties of the foaming filaments. It is recommended to further investigate the influence of more printing parameters on foaming, such as bed temperature, nozzle geometry and type of printer. Second, it is recommended to further investigate the material properties of foaming TPU and ASA as well, since only PLA was tested in the compression experiment. Apart from this, the materials could also be further investigated for tension. Lastly, the proposed foaming PLA sample for the motorcycle helmet could be further investigated for higher strain rates, to confirm the feasibility for the use of motorcycle helmets.

Overall, this thesis investigates the printing parameters for foaming materials which are used to create samples with specific densities for a compression experiment. With the found printing parameters and results from the compression test, a helmet demonstrator is created to show a possible application for the foaming materials.

Preface and acknowledgements

This thesis is about one of my personal interests, 3D printing. Through my high school thesis, the interest for 3D printing was found. While studying in Delft, this interest only grew and I bought my first 3D printer. Therefore, it is no surprise that I chose to write my master thesis about 3D printing. Now, nearing the end of my master, I am writing my thesis while my second 3D printer is printing away. I feel grateful that I am able to conduct my master thesis on a subject which I am passionate about.

First of all, I would like to thank my supervisors, Zjenja and Mehmet, for giving me feedback and support throughout my graduation. Without their support and insights this thesis would not have been what it is now. Secondly, I would like to thank Pim and Mark, for proof reading and giving feedback on my writing. They also supported me when graduation got difficult.

Third, I would like to thank the members of the graduation community “Koffieleutjes”, Dana, Diana, Maaike, Sanne, Clint and Sylvia, that was created during the beginning of the academic year. Without the Koffieleutjes, graduation would have been a lot harder. We provided each other support, feedback and coffee breaks when needed.

Lastly, I would also like to thank the technical support of the Applied labs, Joris and Mascha in particular. Joris who helped me when I had printer problems, and Mascha who helped with conducting my experiments.

I hope that you have as much fun reading my thesis, as I had during my graduation.

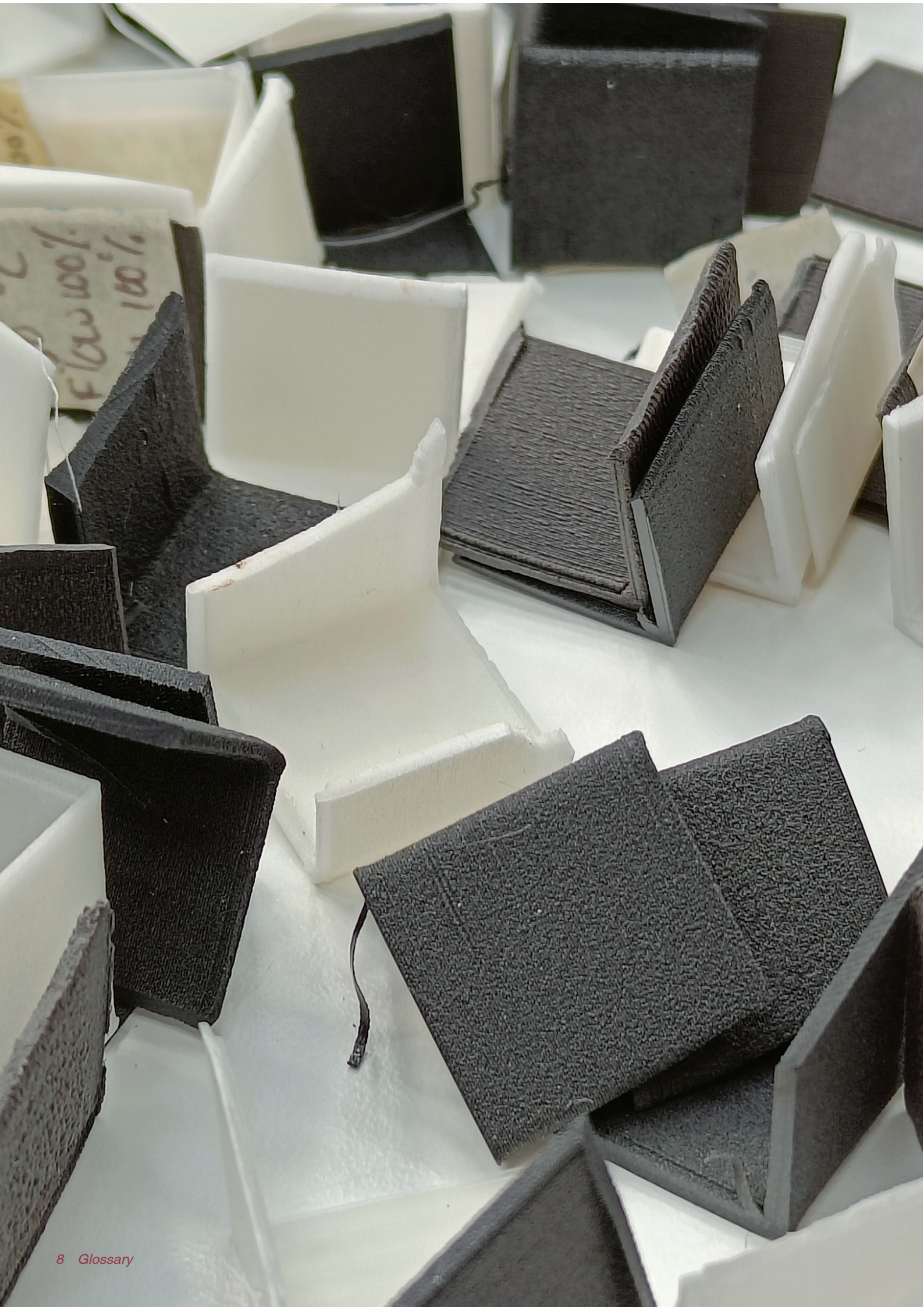

Glossary

ASA	Acrylonitrile styrene acrylate
EPS	Expanded polystyrene
FDM	Fused deposition modelling
LW	Lightweight
PLA	Polylactic acid
TPU	Thermoplastic polyurethane
W/σ ratio	Shoulder point, this describes when a foaming material can absorb the most amount of energy for the minimum amount of stress. (Fuss et al, 2015)
Relative density	This is the density of the foaming material divided by the density of the non-foamed base material of which the foaming material is made (Gibson & Ashby, 1997)
flow rate	The amount of extruded material is multiplied with this value (Ultimaker B.V., 2022)

Table of contents

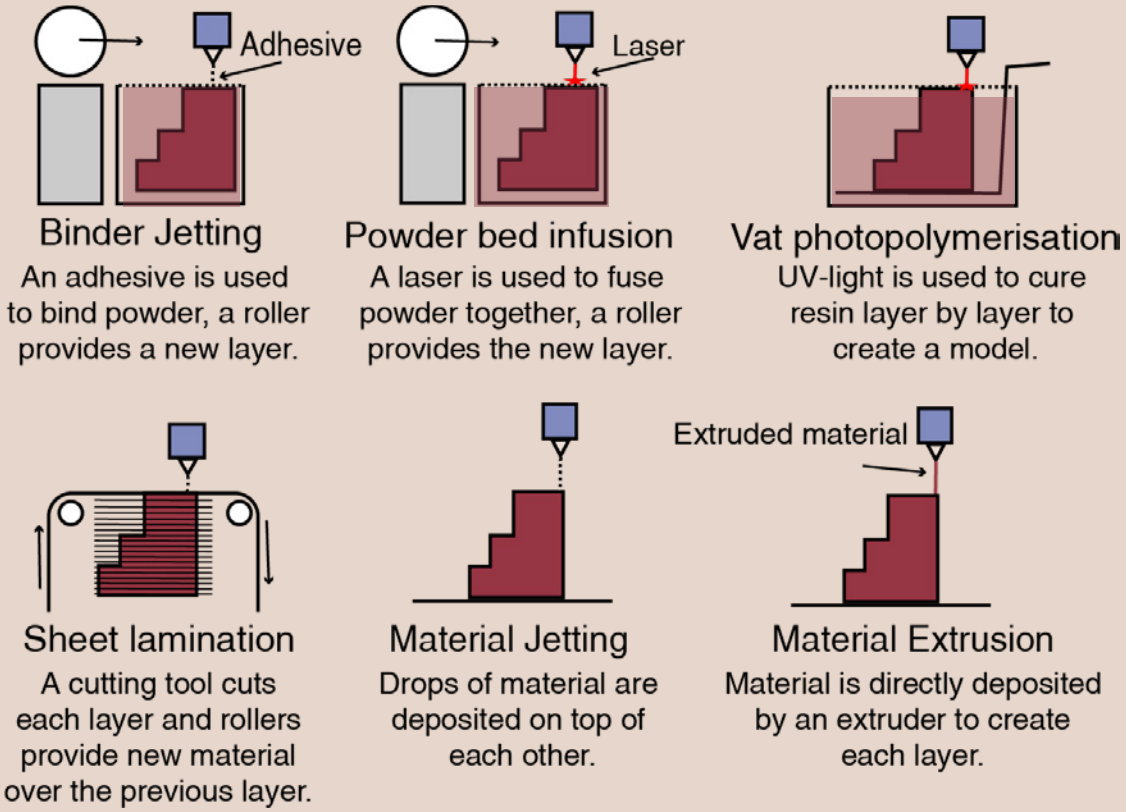

Figure 1.1: Different additive manufacturing techniques, images adapted and information from Loughborough University (n.d.)

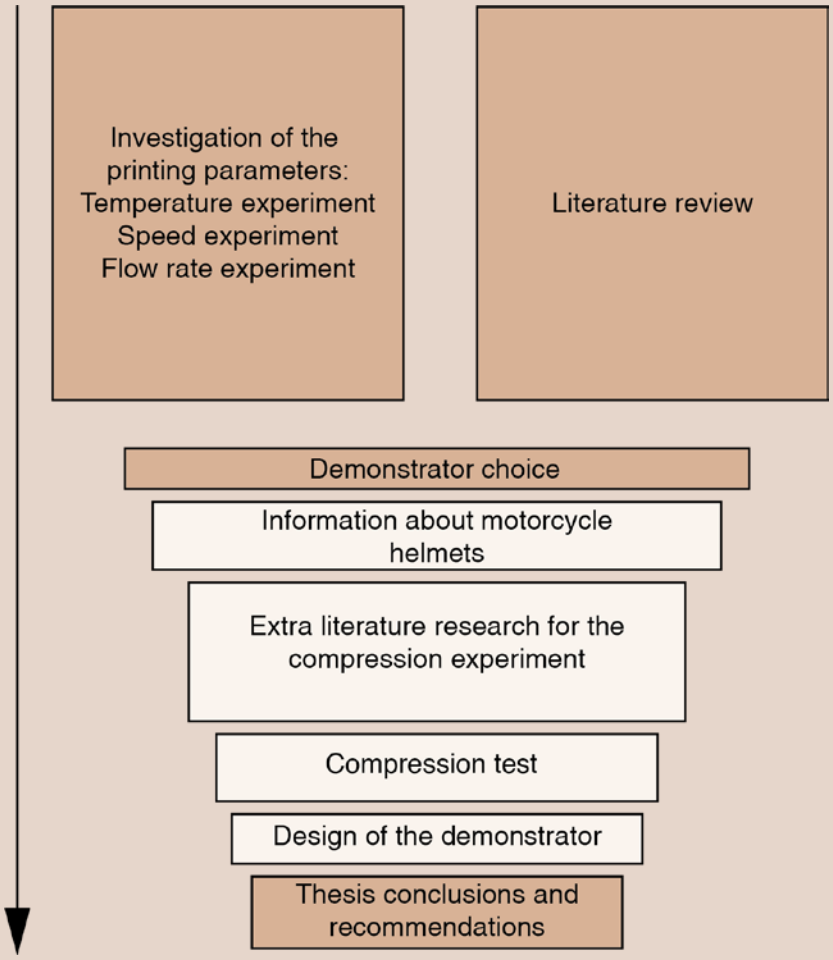

Figure 1.2: Reading guide.

1. Introduction

Three-dimensional printing (3D printing), or additive manufacturing, is the process of joining materials to create physical objects from 3D modelled data (ISO/TC 261, 2021). Many different techniques are available to 3D print, Figure 1.1 shows an overview. 3D printing is becoming a more integral part in most companies and organizations nowadays. Due to the ability to create products and prototypes with high complexity in a short amount of time. One advantage of 3D printing is the ability to create customised products. Another advantage that coincides with this is the amount of design freedom there is for creating products (Nofar et al, 2022). Since a few years, foaming materials for 3D printing have been introduced. These materials foam when they are being printed under certain circumstances. This foaming ability is usually created by adding foaming agents to the materials. Advantages of foaming materials are their lightweight properties and the need for less material to create the same size product (Nofar et al, 2022). Foaming materials also have better impact strength and toughness in relation to their weight (Nofar et al, 2022). Due to the foaming materials for extrusion-based printing, fused deposition modelling (FDM) printing, being new, only a few papers have so far been published about these materials. Therefore, there are still many knowledge gaps regarding the material characteristics of foaming filaments, as well as the influence of printing parameters on the expansion.
The goals of this thesis are:

Research the existing knowledge about foaming filaments.

Characterize the different printing parameters that influence the amount of foaming.

Propose a new application for the foaming materials.

To reach these goals, a literature study is conducted, as well as several experiments to research the print parameters and material properties. The focus during this thesis will be on printing foaming PLA, TPU and ASA with an extrusion-based printer. An extrusion-based printer creates 3D models by placing melted plastic, layer for layer to create a model.

This thesis is divided into three main parts, which are divided in sub-sections. The first part consists of a literature review. This review starts with an overview about the properties of foaming materials outside the scope of FDM printing, followed by in-depth research on different printing parameters and their influence and finally ends with an overview of the available knowledge of lightweight materials. The second part of the thesis focuses on investigating different printing parameters and their influence on the foaming ability of the materials. This part is crucial to understand how to manipulate the foaming rates of the material. The last part of the thesis focusses on the development of a helmet as a demonstrator. First, some general information is given about helmets and their safety standards, after which a test is created and conducted to assess if the material is suitable for this application. The thesis ends with a conclusion and recommendations for further research. Since the order of the thesis is not chronological, a reading guide is made, see Figure 1.2.

Literature review

This part of the report focuses on the collected information; in order to be able to understand foaming materials better, finding knowledge gaps and interesting applications for the foaming materials for FDM printing. First, a general overview of the material properties of foaming materials is given, beyond the scope of FDM printing as well. This is followed by a review about the different printing parameters that influence the outcome of a final print. Third, the information that is available within the literature about foaming materials for FDM printing is presented. Finally, the section ends with an overall conclusion for the literature review

2. Literature review

The goal of the literature review is to understand what knowledge is already available for foaming materials for FDM printing. To understand the characteristics and benefits of foaming materials outside the scope of FDM printing, general information is given first (2.1). This is followed up by the influence of printing parameters on an FDM printed model (2.2) and lastly existing work about foaming filaments (2.3). This chapter ends with a conclusion (2.4). Google Scholar has been used to find different papers and information. The search terms used can be found in Appendix 2.

2.1 Material properties of foaming materials

The goal of this paragraph is to provide a more general overview of the characteristics and benefits of foaming materials, outside the scope of 3D printing as well. This provides a base for understanding where foaming materials in 3D printing can be interesting to use. Firstly, the overall advantages of foaming materials in comparison to non-foaming materials (2.1.1) are discussed. The following section goes into more depth about the energy absorbing properties of foaming materials since they are often used for this application (2.1.2). Lastly, a conclusion is given (2.1.3).

2.1.1 Properties of foaming materials

This paragraph aims to give an overview of properties of foaming materials outside the scope of 3D printing, to better understand the advantages of using foaming materials. Foams can be made from many materials such as, polymers, metals, ceramics, glass and even composites (Gibson & Ashby 1997). Foams are created by adding air into the materials (Gibson & Ashby, 1997). The addition of air can be done in diverse ways. For polymers, this is usually done by adding a blowing agent (Gibson & Ashby, 1997). The blowing agent is either mechanical or a chemical. A physical blowing agent is usually a gas that is forced within the liquid polymer under high pressure, after which the pressure is released (Gibson & Ashby, 1997). A chemical blowing agent is a solution which is mixed within the polymer that will release gas when heated (Gibson & Ashby, 1997). This will create cells within the material which are used to characterize the different foams. If a foam is constructed out of walls, it is called a closed-cell foam. If a foam is constructed out of struts, it is called an open-cell foam (Gibson& Ashby, 1997). Figure 2.1.1 shows the differences between the open- and closed-cell foams. One of the most important properties of foams is the relative density, which is defined by:

$$\frac{\rho^*}{\rho^s}$$

With:

ρ^* = The density of the cellular material [kg/m^3]

ρ^s = The density of the solid material from which the cell walls are made [kg/m^3]

If the value of the relative density is higher than 0,3 the material is not considered a foam (Gibson & Ashby, 1997). Foaming materials provide the ability to create light but stiff structures, cushioning for objects, and energy absorbing structures (Gibson & Ashby, 1997). Depending on the application, the foams can be tailored by adjusting cell size, cell geometry and amount of cells. Foams in compression provide large compressive strengths for little weight (Gibson & Ashby, 1997). This is largely the reason why foams are used in many packaging designs. The following sections will discuss energy absorption in more detail.

2.1.2 Energy absorption of foaming materials

Among other materials, polymer foams are used to absorb energy. Energy-absorbing structures and materials undergo significant changes in their geometry to withstand intense impact loads, strains and various combinations between bending and stretching (Lu & Yu, 2003). Energy absorption can be defined as the area below the load-displacement curve (Topçu and Unverdi, 2018 & Nurul et al, 2018). Soe et al (2022) and Ashby et al (2014) define energy

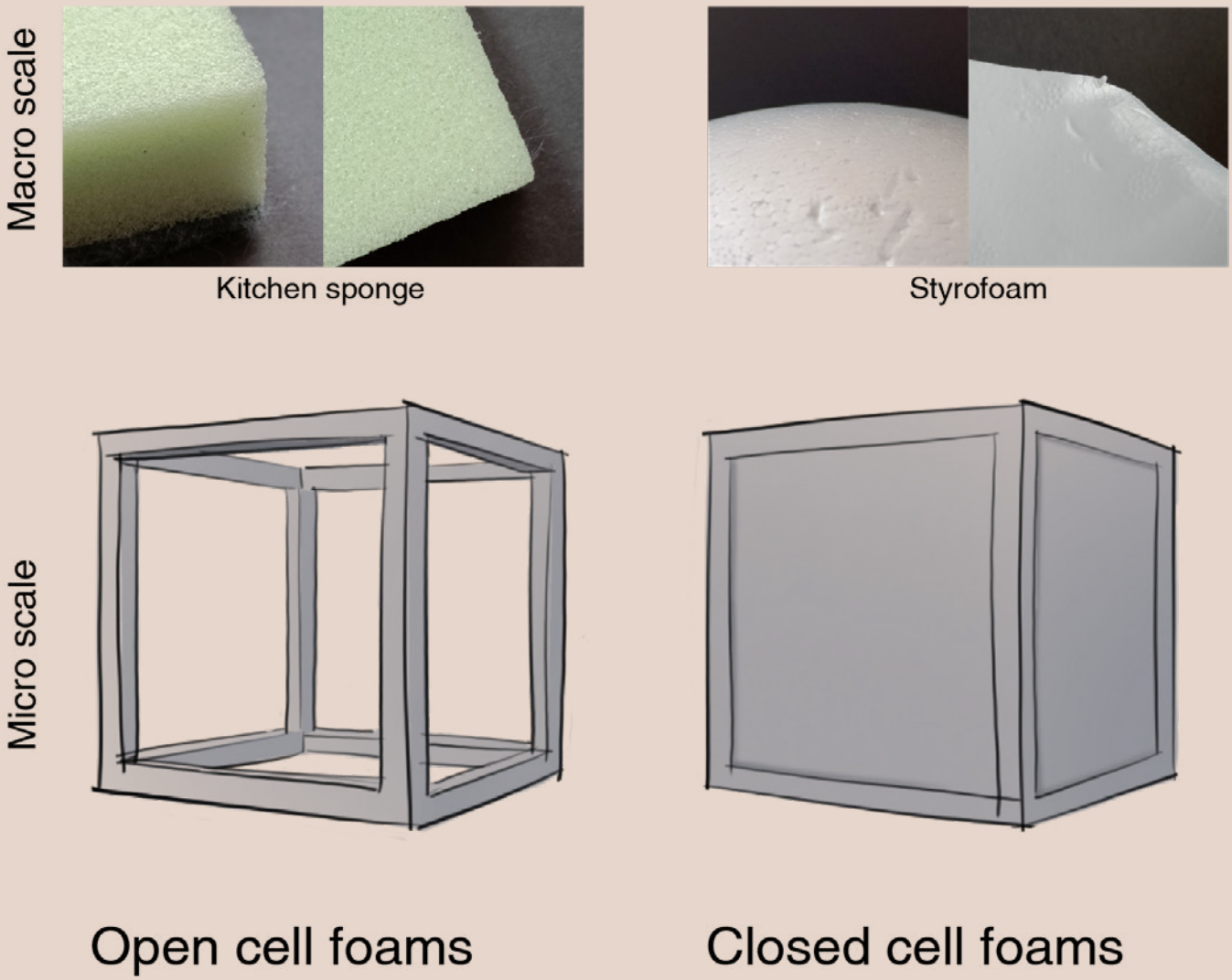

Figure 2.1.1: This figure shows the main difference between an open- and closed cell foam on macro and micro scale. The micro scale represents a schematic of individual cells.

absorption as the amount of energy absorbed by a specimen during fracture within an impact test. Energy absorption is also known as toughness (Topçu and Unverdi, 2018), which is defined by Ashby et al (2014) as:

$$Toughness = \frac{(Fracture\ toughness)^2}{Young's\ modulus}$$

According to Lu & Yu (2003) a desirable characteristic for the energy absorbing structure is that the energy conversion is irreversible. This means that the energy is not released after impact and cause damage to the person or product that the structure is supposed to protect (Lu & Yu, 2003). There are two definitions for energy absorption within the literature. These are, specific energy absorption, which is the total absorbed energy per unit mass (Nurul et al, 2018). Secondly, there is volumetric energy absorption, which is the absorbed energy per unit distance (Nurul et al, 2018). As briefly mentioned in Section 2.1.1, different applications for energy absorption can be found within the literature. An overview of these examples is given Figure 2.1.2, further explanation can be found in Appendix 3. Materials should be able to aid in the transformation of energy. The review of Qiao et al (2008) provides an overview of some high-energy-absorbing materials. Qiao et al (2008) discussed the use of; fibre composites, foams, magnetorheological fluids and porous materials. Apart from these materials, they also investigate the use of sandwich structures and lattice structures for high energy absorption. The advantages of using sandwich structures and lattice systems is that one can combine the right material choice with design for high impact or material absorption (Qiao et al, 2008). The advantages of using polymeric foams is that they are able to absorb significant amounts of specific energy, due to the collapsing of the cell walls. In line with this, Avalle et al. (2001) found that polymeric foams have a higher energy efficiency than their non-foaming counterparts.

2.1.3 Conclusion

Within this paragraph the properties of foaming materials were discussed to understand the potential advantages for the foaming materials for FDM printing. Energy absorption, also known as toughness, refers to the energy that is absorbed by a material before it fails. This is the area under the load displacement curve. Energy absorbing materials, foams, and structures are able to sustain large amounts of energy and convert this into geometrical change. Foaming materials also have a higher specific energy absorption than their non-foaming counterparts. Which means that foams can absorb relatively large

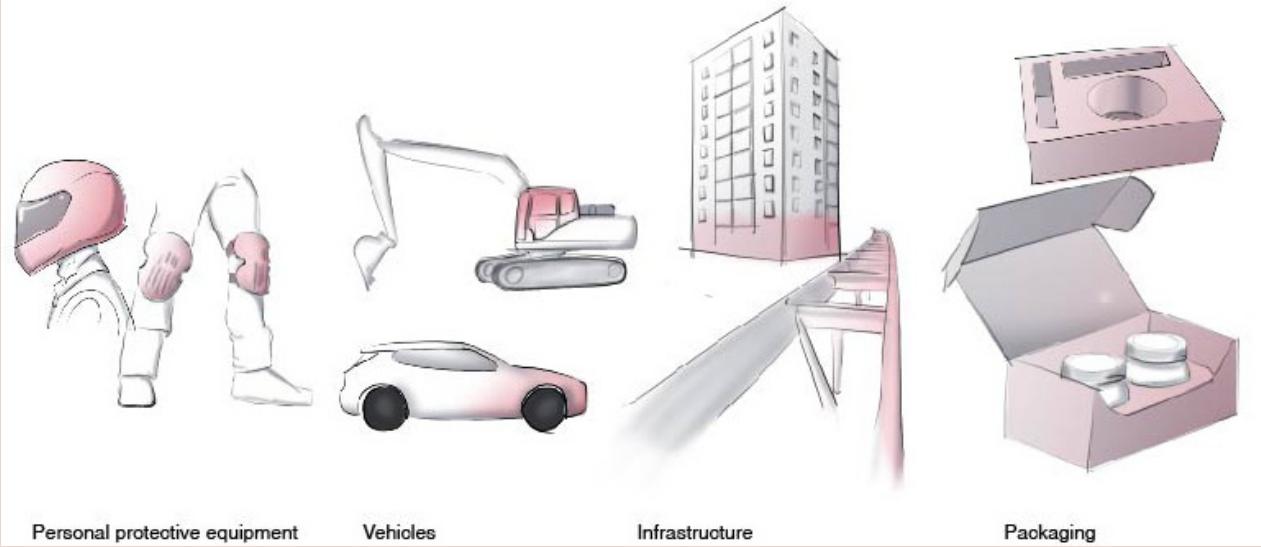

Figure 2.1.2: The different areas of application in which energy absorption is needed according to Lu & Yu, 2003, Personal protective equipment, vehicles, infrastructure and packaging. The parts that are coloured red will need to absorb (the most) energy.

amounts of energy while maintaining a low weight. Therefore, it can be concluded that materials such as foams and cellular structures are used in different fields to protect users or products, due to the fact that they are lightweight and provide a high specific energy absorption. The foaming materials for FDM printing could also potentially hold these properties. Further research into the foaming materials for FDM printing could give insights in their potential as lightweight and energy absorbing materials for protective applications.

2.2 Influence of printing parameters on FDM prints

This paragraph will discuss the influence of different printing parameters found in the literature. One can modify the printing parameters, also known as machine settings, of an FDM printer to be able to influence the way a product is printed. Khan, et al (2021) further define four printing parameters and their influence: layer resolution, build orientation, nozzle temperature, raster angle and air gap. Apart from these parameters, Solomon et al (2020) investigated the printing parameters, printing speed, infill density, infill pattern, raster width, extrusion temperature and nozzle diameter as well. This paragraph will focus on the following four printing parameters: the printing path (2.2.1), the influence of temperature (2.2.2), printing speed (2.2.3) and nozzle height (2.2.4). Lastly, a conclusion will be given about the advantages of each parameter that is found (2.2.5).

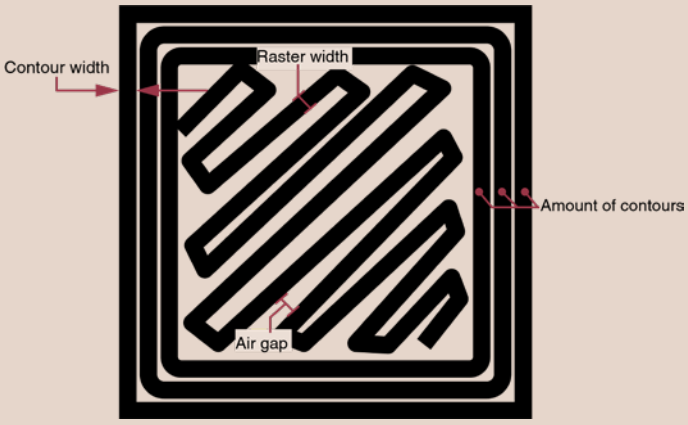

Figure 2.2.1: Tool path parameters, image adapted from Kristiawan et al, 2021

2.2.1 Printing path

The tool path of a 3D printer describes the way the nozzle moves while extruding material (Kristiawan et al, 2021). This is influenced by parameters such as contour width, raster width, air gap, and number of contours (as shown in Figure 2.2.1) (Kristiawan et al, 2021). To be able to customize the toolpath, one needs to adjust or write Gcode. Gcode is instructions for the printer (Horvath, 2014). For example, it includes instructions for the movement, extrusion amount, and speed. Gcode is usually generated by slicing software such as Cura or Slic3r (Horvath, 2014). To be able to customize the printing path, among others, one will need to write Gcode. Pezutti-Dyer & Buechley (2022) simplified this by creating a Python class and Grasshopper plugin which lets you move a turtle to write Gcode. Another technique that influences the printing path, is printing in a continuous line. This technique is most often seen in printed materials that are soft, like clay (Zhong et al., 2020). Dong et al. (2021) have used continuous printing to make a Kevlar-reinforced product. They printed with a continuous fibre that was inserted in the filament. Because the fibre is in one piece, the authors had to define continuous paths to be able to print with it. They gave suggestions for multiple continuous infill paths as shown in Figure 2.2.2.

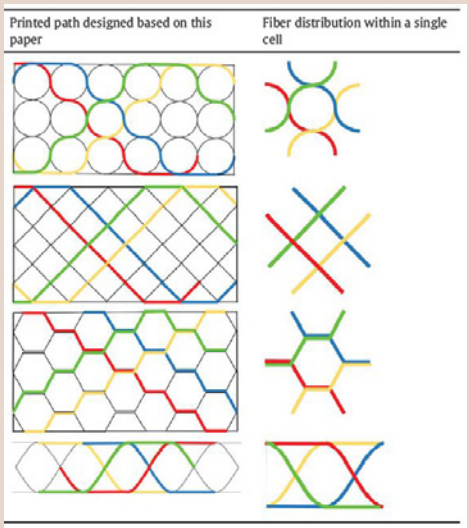

Figure 2.2.2: Different continious infill paths as proposed by Dong et al, 2021. (Image from Dong et al, 2021).

2.2.2 Temperature

There are two parts on the printer that are affected by temperature, the nozzle and the build plate. The nozzle temperature, or extrusion temperature, is the temperature that the nozzle reaches to heat the material inside of it (Dey and Yodo, 2019). The extrusion temperature is also affected by the printing speed (Khan et al, 2021; Dey & Yodo, 2019). This temperature of the nozzle affects the viscosity of the material, which can affect the stresses that occur within the nozzle (Solomon et al, 2020). These internal stresses can lead to deformations between layers or fabrication failure. The build plate temperature, is the temperature of the heated bed on which the printed model is created. In the case for materials such as ABS, it is important to heat the build plate to avoid shrinkage from the part cooling down too quickly (Agarwal, et al. 2022). Bhavsar et al (2020) studied the bonding of the first layer of a print. In this study they found that higher temperatures for build plate and material allow for better adhesion of the printed part. Spoerk et al (2018) found that prints stick better if the bed temperature is slightly above the glass transition temperature of the material. Adhesion is crucial to make sure the print does not come loose when printing, resulting in a failed print.

2.2.3 Layer Height

The layer height, layer resolution, or layer thickness, describes the amount of material that is placed in one pass (Solomon et al, 2020). The layer thickness is influenced by the nozzle diameter as well as the accuracy of the printer (Kristiawan, 2021). The height of a layer will always be less than the diameter of the used extruder (Solomon et al, 2020). To obtain prints that are more dimensionally accurate, a lower layer height is desired (Polák et al, 2017). Agarwal et al (2022) found that layer thickness was one of the main contributors in being able to obtain dimensionally accurate prints. In addition to dimensional accuracy, surface roughness also influences the choice of layer height. When the layer height increases, the staircasing effect also becomes more visible (Khan, et al. 2021). Figure 2.2.3 gives an example of staircasing effect within 3D printing, which is the fact that the individual layers can be seen. Pérez et al (2018) found that layer height and wall thickness are the most important for creating a good surface finish. Kim et al (2018) found that an FDM part will have the smoothest surface finish if the distance to the nozzle and the line width are the same. By adjusting the nozzle height, one can also decide to create really textured prints. Takahashi & Miyashita (2016 & 2017) explored this within their two papers. They investigated how the different distances of the nozzle height influenced the resulting texture of the printed part, Figure 2.2.4.

2.2.4 Printing Speed

The printing speed is how fast the nozzle moves on the horizontal plane of the FDM printer and is usually measured in mm/s (Dey & Yodo, 2019). When increasing the print speed, the nozzle will make faster travel movements. Printers that operate at higher speeds will extrude more material than printers that operate at lower speeds (Doshi et al, 2022). Due to the faster speeds and the need to extrude more, the stress within the nozzle to extrude increases (Solomon et al, 2020). Agarwal et al, (2022) found in their research that when ABS is printed faster, e.g. with a higher print speed, the dimensional accuracy improves. Zarko et al (2017), also found that higher printing speed improves the dimensional accuracy but resulted in surface cracks.

2.2.5 Conclusion

The goal of this paragraph was to create a better understanding of the influence of printing parameters on the final printed product. Apart from the four discussed, there are many more printing parameters that can influence the final print. To conclude, Table 2.2.1 has been made as overview of the influence of the discussed printing parameters. With this overview, experiments can be defined to research the discussed printing parameters for the foaming filaments in particular.

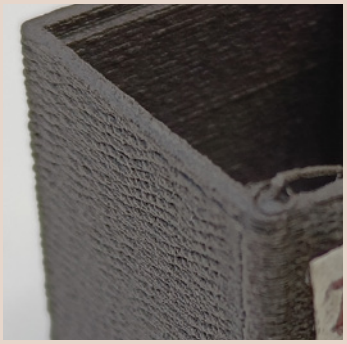

Figure 2.2.3: Staircasing effect on a 3D printed part

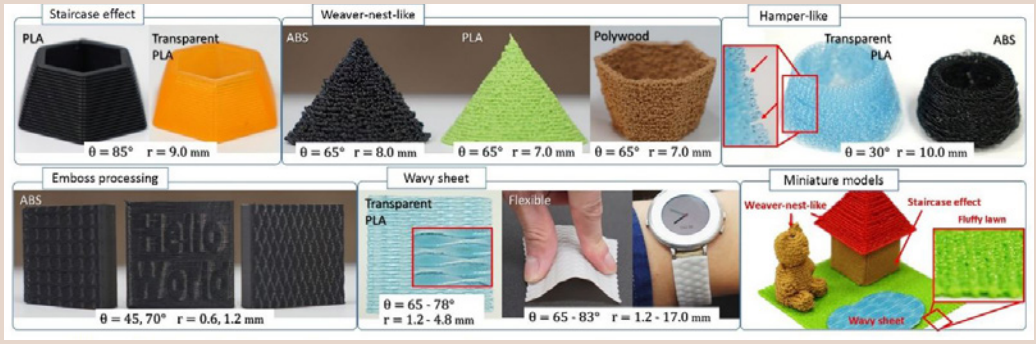

Figure 2.2.4: Different textures created by Takahashi & Miyashita (2016) by changing the nozzle height. (Image from Takakashi & Miyashita, 2016)

Table 2.2.1: Overview of the printing parameters and their influences

Printing parameter	Definition	Influence on the printed model
Printing path	The movement of a nozzle while extruding material.	It determines the way a printed object is build. When one wants to personalize this path, Gcode needs to be manually written. Usually, printing paths are not continuous. Having continuous printing paths is important for soft materials were retraction is not available
Nozzle Temperature	The temperature at which the nozzle is heated, to extrude material. The print speed influences the nozzle temperature.	The nozzle temperature affects the viscosity of the material. This viscosity depends on the material. Because the viscosity of the material is affected, the stress within the nozzle also change.
Bed Temperature	The temperature at which the build plate is heated.	The heated bed helps the print to stick to the build plate. If this is not the case, the print can fail.
Layer height	The amount of the material extruded within one pass. The layer height is influenced by the nozzle size.	The dimensional accuracy is influenced by the layer height. A smaller layer height gives more accurate prints. The layer height also influences the surface texture of the printed model.
Printing Speed	How fast the nozzle moves in the horizontal plane.	Higher print speed can lead to higher residual stresses within the nozzle. It is found that higher speeds result in better dimensional accuracy.

Table 2.3.1, Properties of PLA, ASA, TPU and their actively foaming counterpart. Stresses are in tension.

	PLA (Ansys inc, 2022b)	Foaming PLA	ASA (Ansys inc, 2022a)	Foaming ASA	TPU (Ansys inc, 2022c)	Foaming TPU
Youngs modulus [GPa]	3,3 – 3,6	0,598 – 2,586 (Kanani et al, 2022) 3,33 (at 200°C, ColorFabb, 2022b) 0,86 (at 250°C, ColorFabb, 2022b) ~0,4 – 1,9 (Damanpack et al, 2021)	1,51 – 2,34	0,69 (at 260°C Colorfabb, 2022a)	1,31 – 2,07	
Yield strength [MPa]	50 – 55	7,5 – 61 (Kanani et al, 2022) 43,07 (at 250°C, ColorFabb, 2022b)	35,9 – 38,6		36 – 42	
Tensile strength [MPa]	55 – 72	7,7 – 25,89 (Kanani et al, 2022) 43,07 (at 200°C, ColorFabb, 2022b) 10,83 (at 250°C , ColorFabb, 2022b) 32,2 (Esun, 2021) ~7 – 32 (Damanpack et al, 2021)	27,6 – 51,7	8,91 (at 260°C ColorFabb, 2022a)	31 – 62	58,6 (no foaming activated, ColorFabb, 2019)
Shear modulus [GPa]	1,2 – 1,29		0,538 – 0,833		0,465 – 0,735	
Toughness (G) [KJ/m^2]	3,32 – 6,49		1,49 – 9,19		2,39 – 12,8	
Density [Kg/ m^3]	1240 – 1270	400 – 1240 (ColorFabb,2022b) 1200 (Esun, 2021)	1050 – 1060	400 – 1070 (ColorFabb, 2022a)	1120 – 1240	1220 (ColorFabb, 2019)
Melting point [°C]	145 – 175		220 – 260			
Glass temperature [°C]	52 – 60	55-60 (ColorFabb, 2022b)	101 – 116		77 – 107	-20

2.3 Foaming materials for FDM printing

This section focuses on the available literature and knowledge concerning the foaming filaments. First, material properties are discussed with the available information (2.3.1). Secondly, some summaries of applications of the lightweight filaments are given (2.3.2). The section ends with a conclusion (2.3.3).

2.3.1 Material properties of foaming materials for FDM printing

Since this thesis focusses on printing with foaming materials for the FDM printer, the literature review in this section is also constrained to FDM printers. Colorfabb released their first lightweight filament in 2019, LW-PLA, as well as the Varioshore TPU. LW-ASA was introduced later. These materials all have in common that they foam when extruded under a certain temperature (ColorFabb, 2022a, 2022b, 2019), see Figure 2.3.1. Apart from ColorFabb, there are also other manufacturers that have introduced foaming materials. For example Esun, of which the ePLA-LW was first released in 2021 (Esun, 2022) and Polylite LW-PLA, which was introduced in 2019 (Polymaker, 2019). The main difference between the brands is that Polylite is not temperature depended, it always foams when extruded. The foaming ability of the materials from ColorFabb and Esun affect the material properties, for example the translucency, the dimensions, and the outside texture of the final products.

Table 2.3.1 shows key material properties of the lightweight filaments in comparison to their non-foaming counterparts. All the information that was available during time of writing for the foaming materials is shown in the table. Table 2.3.1 shows, that the range of the Youngs modulus of the LW-PLA (0,598 -3,3 GPa) is broader than that of the regular PLA (3,3-3,6 GPa). Kanani et al (2022) found that foamed PLA with low-infill performed slightly better in compression than the non-foamed specimens. This can be explained by the presence of the bubbles, in tension the bubbles tend to crack and in compression they absorb energy (Kanani et al, 2022). Damanpack et al (2021) found that the material was stiffer in tension when the density increased. Due to the foaming ability of the materials and the high printing temperatures, the material can droop from the nozzle

Figure 2.3.1 A non-foaming cube (left) and a foaming cube (right) printed with LW-PLA

causing a lot of stringing (Knackmuhs et al, 2022). Therefore, one should consider the printing path of the nozzle when making a model.

2.3.2 Applications of foaming materials

Only a few applications for these lightweight materials have been described in the literature. Most prominent is the application of the foaming PLA and TPU for model aeroplanes or drones (Knackmuhs et al, 2022 & Gotthans et al, 2021). These two materials are suitable for this application since they can print with less material (ColorFabb, 2022b & 2019), giving the ability to make lightweight models. Foaming PLA was also used for the shell of a bicycle helmet (Prosperi, 2021), which has the advantage that the foaming PLA was able to absorb slightly more energy (44,102 J) than the previously used foam, expanded polystyrene (37,723 J)(EPS). Williams et al's (2021) bone model for wire navigation training used the foaming characteristic to more accurately mimic bone. Foaming TPU is mostly applied for shoe soles in literature (Chen & Lee, 2022a & b and Michau, 2021). This has the advantage that the soles can be personalised because one can determine the amount of foaming for each place on the sole. For the foaming ASA there are few applications available in the literature. On the internet people printed model airplanes (Igor Gaspar [My Tech Fun], 2021) or cosplay[1] props (Daniel [ModBot], 2021) with it. An overview of the examples found in literature can be found in Figure 2.3.2

2.3.3 Conclusion

The goal of this section was to get an overview of the available literature of the foaming materials. An overview of the available mechanical properties of foaming materials was given in Table 2.3.1. It was revealed that most is known about the mechanical properties of the foaming PLA such as young's modulus and tensile strength. For the foaming ASA and TPU, the mechanical properties are mostly unknown. The technical data sheets of the manufacturers do provide some insights, but only for few temperatures. Overall, mechanical properties that are known, are only measured in tension. This means that the compressive properties of the materials could be further investigated. Table 2.3.1 also gives an overview of the knowledge gaps for the mechanical properties for the foaming materials. The foaming materials provide the advantage to be able to be printed with less material due to their foaming property. We can conclude from the found applications that most of them focused on the materials' lightweight properties. Therefore, for the thesis it can be interesting to look into different areas for application for the materials than just their lightweight features. For example, changing the appearance and energy absorption of the materials.

1 *Cosplay is a form of costume making where people dress-up as characters from movies or series.*

Bone stimulant for wire navigation training, printed on a FDM printer with foaming PLA (Williams et al., 2021)

Bicycle helmet printed on a FDM printer with foaming PLA (Prosperi, 2021)

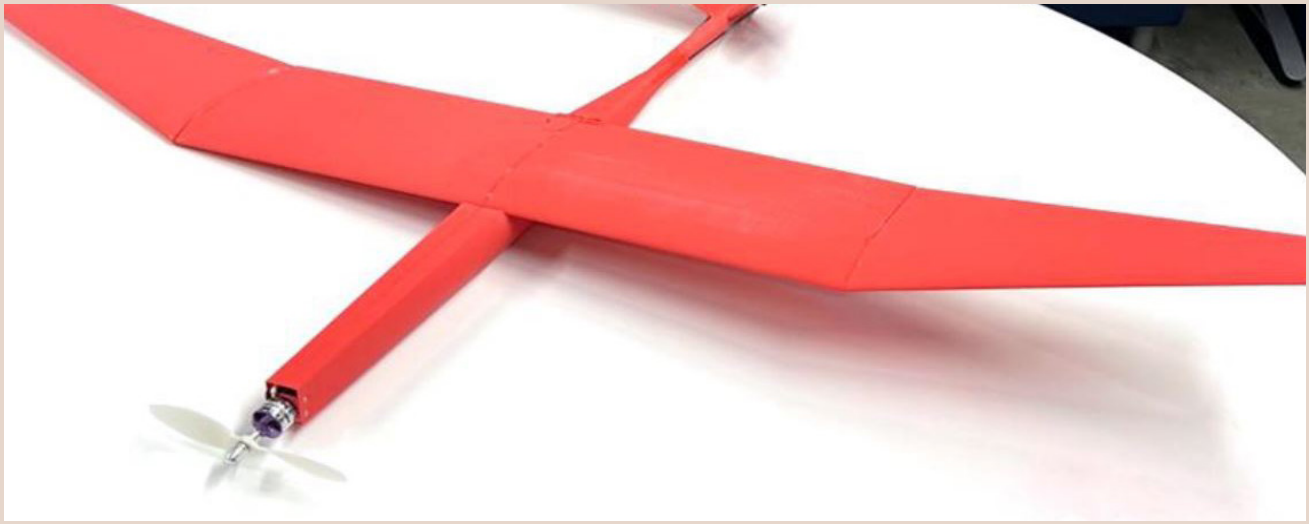

Printed model airplane using foaming PLA (Knackmuhs et al., 2022)

Printed shoe. Printed on a FDM printer with foaming TPU (Michau, 2021)

Printed shoesoles. Printed on a FDM printer with foaming TPU (Chen & Lee, 2022)

Figure 2.3.2: Examples of the applications of the foaming filaments

2.4 Overall conclusion of the literature review

The goal of the literature review was to get an understanding of; foaming materials beyond 3D printing, the influence of printing parameters and the knowledge that is already available for foaming filaments. First of all, it can be concluded that foaming materials and cellular structures beyond the scope of 3D printing have been used to protect users and products since they have a high specific energy absorption. Therefore, further research into the mechanical properties of foaming materials for FDM printing can give insights into their potential energy absorbing qualities. Secondly, printing parameters for FDM printing have been further researched which resulted in Table 2.2.1 that gives an overview of printing parameters and their influence on the final print. It can be concluded that the found printing parameters all have their own influence on the final print as well as on each other. For example, the printing speed does not only affect the time it takes to print a model, but also the nozzle temperature. For the continuation for the thesis the table can be used as a reference for researching the influence of the printing parameters on the foaming materials. Lastly, the knowledge concerning the foaming filaments has been researched which resulted in Table 2.3.1. Most material knowledge is available for the foaming PLA, followed by the TPU. Since ASA is the newest foaming material, the least material knowledge is available for it. From the available applications within literature, the foaming filaments have mostly been used for their lightweight properties. Some studies investigated the energy absorbing aspects of the materials.

Overall it can be concluded that it would be interesting to further look into the energy absorbing properties of the foaming materials for FDM printing, since it will give more insights into material properties. The investigation of the energy absorption will be done in the context of a motorcycle helmet with the focus of the foaming PLA as impact liner. The foaming PLA bike helmet with a TPU cover made by Prosperi (2021) demonstrated the ability to reach a realistic value of absorbing impacts for a helmet. Prosperi (2021) was able to reach a similar amount of absorbed energy (44,102 J) in her printed helmet as a regular EPS helmet (37,723 J). Even though the difference is not much, it shows that the material could reach the same standards. Chapter 8 will explain the requirements and scope of the demonstrator more in depth.

Investigation of printing parameters

In this chapter the influence of three different printing parameters on the foaming filaments is further investigated. It is important to understand the influence of printing parameters so the correct settings can be chosen for the desired outcome. The chapter describes three experiments and concludes with guidelines for printing with foaming filaments for the continuation of this thesis.


250°C
260°C

3. The effect of printing parameters on the material expansion

The following chapter investigates the influence of different printing parameters on the expansion of the foaming materials, PLA, ASA and TPU. The effect of temperature is investigated for each material. Due to specific application of a motorcycle helmet, the speed and the flow are only investigated further for the PLA and TPU. The goal of these experiments is to investigate under which conditions the materials expand the most, as well as what the best printing conditions are. This chapter is divided into the following paragraphs: an overall introduction to the experiments (3.1), the methods of the experiments (3.2), the results of the experiments (3.3), the discussions and recommendations of the experiments (3.4). The chapter will end with the conclusions and an overview of the found guidelines (3.5).

3.1 Introduction to the experiments

By investigating the effects of printing parameters on the expansion of the materials, one can create guidelines for designers and researchers on how to print with the foaming materials. Based on Table 2.3.1 in Chapter 2, three printing parameters are chosen to further investigate upon their influence on the overall expansion. For these experiments the foaming filaments of ColorFabb are used: LW-PLA, LW-ASA and Varioshore TPU. The Cura slicer, as well as 3D printers from Ultimaker, are used to prepare the printed samples. For each experiment and material an overview is given of the machine settings, such as type of machine and printcore. Apart from the hardware settings, the relevant printing parameters are also given such as; print speed, layer thickness, and type of adhesion.

The first printing parameter that is investigated is the nozzle temperature. Table 2.3.1 shows that the temperature of the nozzle will affect the viscosity of the material, which in turn could affect the forming of the bubbles. This is followed up by the second printing parameter, which is printing speed. Table 2.3.1 shows that a higher speed may lead to a higher dimensional accuracy, which can also be different depending on the amount of foaming of the material. Lastly, the flow rate of the TPU and PLA are investigated, to compensate for the amount of foaming to get the correct dimensional accuracy. The next sub-section gives an in-depth overview of the slicing progress within FDM printing to understand the movements of 3D printers and the influence of the printing parameters on these.

3.1.1 Slicing

Before one can print, the desired model first needs to be converted into Gcode as was discussed in Chapter 2. Figure 3.1.1 gives an overview of the process of slicing and printing a model. Within the slicer, the model is divided into layers and movements of the nozzle. The number of layers is determined

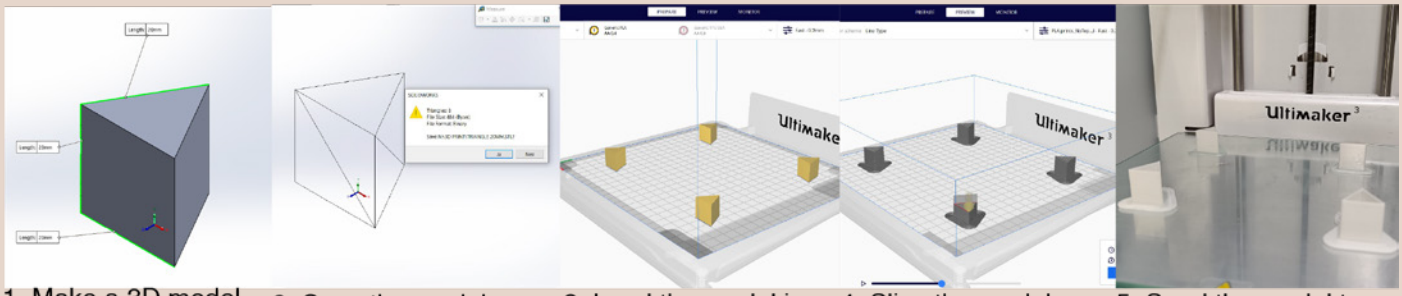

1. Make a 3D model.
2. Save the model as a mesh (.STL, .OBJ, .STEP, .3mf etc).
3. Load the model in your preferred slicer and choose the desired values for the printing parameters.
4. Slice the model.
5. Send the model to the printer, and print it.

Figure 3.1.1, The process of preparing a model for 3D printing.

by the individual layer height and the total height of the model. The layer height partly determines the resolution of the print as well as the printing speed (Wu, 2018). The layer height itself is constrained by the height of the nozzle. The toolpath determines the path the nozzle will take (Kristiawan et al, 2021). This can be influenced in the slicer. It can be chosen to print in a continuous path to get thin-walled and hollow prints. Within the following experiments, the option "spiralize outer contour" within Cura was used. This option prints any object with only the outer contour without retracting or stopping. This function is desired for measuring the expansion of the foaming materials, since only one contour line is printed continuously without top or bottom layers.
A printing parameter that very directly influences the wall thickness is the contour width of the extruded line. This thickness can be set within the slicer. It is important to take into account the nozzle size when choosing the contour width of the line. The line width should correspond with the nozzle size according to the Cura slicer (Ultimaker B.V., 2022). If your desired line width is bigger or smaller than the nozzle, then the flow rate of the material needs to be adjusted. The flow rate determines the amount of material that leaves the nozzle when printing (Ultimaker B.V., 2022). When all the printing parameters are set, the model can be sliced and is ready to print.

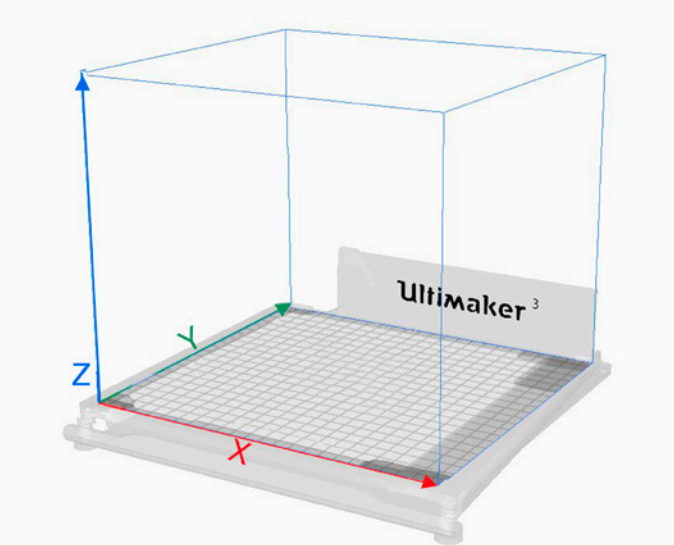

Figure 3.1.2, Axis to define the different planes within the buildplate of the printer.

3.1.2 Research questions

The first printing parameter that is investigated is the nozzle temperature. The second parameter that is investigated is the printing speed. Lastly, the amount of flow is found for different temperatures for TPU and PLA to obtain dimensionally accurate prints. The research questions within this experiment are therefore:

How do printing temperature and fan cooling influence material expansion of TPU, PLA and ASA?

How does the printing speed influence the material expansion of TPU and PLA?

What amount of flow is needed to obtain dimensionally accurate prints for TPU and PLA?

The experiment from Hermann (2020a) and the technical datasheets of Colorfabb (2022a, 2022b and 2019) were used as a reference to determine the minimum and maximum printing temperatures. To be able to measure the expansion of the materials, the wall thickness was measured. Measuring the thicknesses can help explain the expansion in the XY-plane, Figure 3.2.1 shows the plane definitions.

3.2 Method

The method section is divided into two parts, first the manufacturing of all the test samples is discussed (3.2.1). It covers the manufacturing of the samples for all the experiments. This is followed up by a section that explains how the samples of each experiment are measured (3.2.2).

3.2.1 Manufacturing the test samples

The materials that were used to conduct the experiments were ColorFabb's LW-PLA, LW-ASA and Varioshore TPU. The model that was printed for the temperature and flow rate experiments was a 20 mm x 20 mm x 20 mm triangle, designed in Solidworks (Figure 3.2.1). For the printing speed experiment the model was scaled to 140 mm x 140 mm x 140 mm to ensure that the desired printing speed was

reached. The models were sliced in Cura and printed using the setting “spiralize outer contour”, which ensures the prints have a single wall. This is to be able to measure the expansion. To make the overall measuring easier, the top and bottom layers were not printed by disabling them in the slicer. The triangles were printed with different materials, which all need their own printing settings. The Ultimaker printers have pre-set printing profiles which make it convenient to print with different materials. Since the LW-PLA, LW-ASA and Varioshore TPU were not available as printing profile for the Ultimaker 3 or Ultimaker s3, the most similar ones were chosen instead, which can be found in Table 3.2.1 and 3.2.2. Since there was no ASA profile available, the generic nylon profile was chosen, Table 3.2.3. This profile matches the printing temperatures of ASA the best. The overall settings per experiment and material can be found in Table 3.2.1, 3.2.2 and 3.2.3 on the next pages. All the models were printed with a brim to ensure they adhered to the build plate. The printing temperatures for the materials were chosen based on Colorfabb’s recommendations (Colorfabb, n.d. a,b & c).

Within the temperature experiment, the first batch of samples was printed without fan speed, after which the second batch was printed with 100% fan speed for all the materials. Multiple models were placed on one build plate, to make the printing process more efficient, as can be seen from Figure 3.2.2. To achieve this, the appropriate settings were chosen, sliced in Cura and saved as a Gcode file. Later, this file was modified so each triangle had a different printing temperature. Within the Gcode file, the Gcode M109 S”temperature” was added before the start of each model. This meant that the nozzle waited and heated up before extruding. For example, M109 S220 means that the hot end waits and heats up to 220 °C before continuing with printing (Marlinfw, n.d.). An example Gcode file in which this is applied, can be found in Appendix 4.

For the printing speed experiment, four of the big triangles were printed under different printing speeds, with the temperature that gave the most amount of foaming according to the temperature experiment. For the flow rate experiment four temperatures, including the temperature at which the most expansion occurs, were printed. The flow was tweaked each time until the wall thicknesses was accurate. The flow rate was calculated using:

$$Flow\ rate = \frac{Flow\ rate_{used} * Thickness_{desired}}{Thickness\ _{measured}}$$

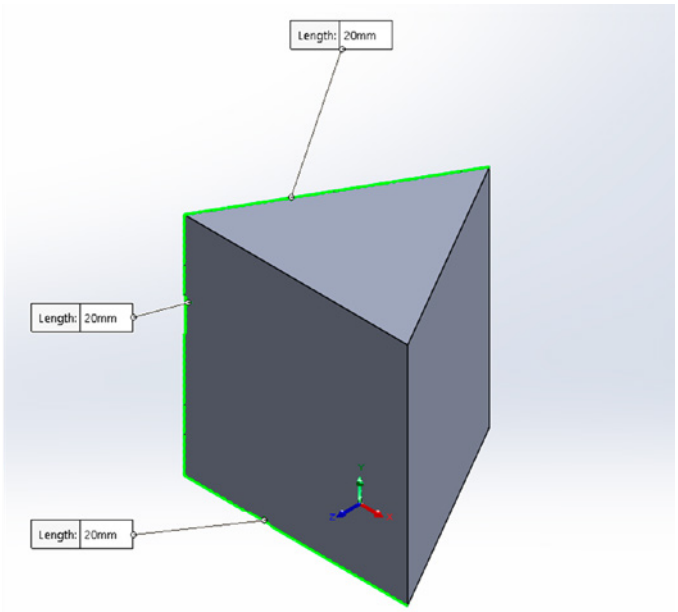

Figure 3.2.1, Dimensions of the print sample for the flow and temperature experiment. This sample is scaled up to 700 % to obtain a triangle of 140 x 140 x 140 mm.

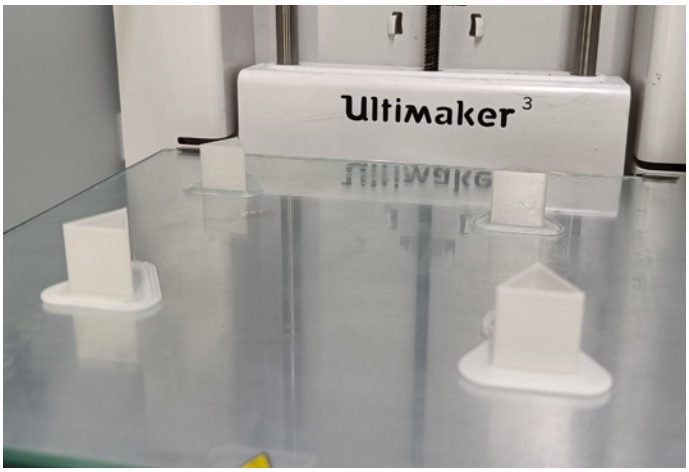

Figure 3.2.2, Printing of four PLA models with different temperatures on the same build plate.

Table 3.2.1, Printer settings for the temperature experiment.

Material	**LW-PLA**	**Varioshore TPU**	**LW-ASA**
Printer Model	**UM3**	**UMS3**	**UM3**
Printing profile	**Generic PLA**	**Generic TPU 95A**	**Generic Nylon**
Printcore	**AA 0,4**	**AA 0,8**	**AA 0,4**
Nozzle Temperature [°C]	190 -270	180 -270	230-270
Bed Temperature [°C]	60	20	100
Fan Speed [%]	100% or 0%	100% or 0%	100% or 0%
Flow rate [%]	100%	100%	100%
Wall line count [-]	1 (0,4 mm)	1 (0,8 mm)	1 (0,4 mm)
Layer height [mm]	0,2	0,2	0,2
Infill [%]	0%	0%	0%
Printing Speed [mm/s]	50	30	40
Initial Bed Temperature [°C]	60	20	105
Initial layer speed [mm/s]	15	15	20
Brim Width [mm]	7	8,75	15
Brim Speed [mm/s]	15	15	15

Table 3.2.2, Printer settings for the printing speed experiment.

Material	**LW-PLA**	**Varioshore TPU**
Printer Model	**UM3**	**UM3**
Printing profile	**Generic PLA**	**Generic TPU 95A**
Printcore	**AA 0,4**	**AA 0,8**
Nozzle Temperature [°C]	220	210
Bed Temperature [°C]	60	20
Fan Speed [%]	100%	100%
Flow rate [%]	100%	100%
Wall line count [-]	1 (0,4 mm)	1 (0,8 mm)
Layer height [mm]	0,2	0,2
Infill [%]	0%	0%
Printing Speed [mm/s]	25-50-75-100	25-50-75-100
Initial Bed Temperature [°C]	60	20
Initial layer speed [mm/s]	15	15
Brim Width [mm]	7	8,75
Brim Speed [mm/s]	15	15

Table 3.2.3, Printer settings for the flow rate experiment.

Material	**LW-PLA**	**Varioshore TPU**
Printer Model	**UM3**	**UM3**
Printing profile	**Generic PLA**	**Generic TPU 95A**
Printcore	**AA 0,4**	**AA 0,8**
Nozzle Temperature [°C]	220	210
Bed Temperature [°C]	60	20
Fan Speed [%]	100%	100%
Flow rate [%]	Deviates per sample	Deviates per sample
Wall line count [-]	1 (0,4 mm)	1 (0,8 mm)
Layer height [mm]	0,2	0,2
Infill [%]	0%	0%
Printing Speed [mm/s]	50	30
Initial Bed Temperature [°C]	60	20
Initial layer speed [mm/s]	15	15
Brim Width [mm]	7	8,75
Brim Speed [mm/s]	15	15

3.2.2 Measuring the results

Before being able to measure the expansion of the triangles, the brims were removed. They were cut as closely to the print as possible, to make sure that there are no bumps when measuring the thickness. This is done for all the experiments. Since the speed experiment had bigger triangles, the middle of a side of the triangle was cut to measure. The middle was chosen since the printer does not (de)accelerate at that point, which could influence the results. The expansion of all the samples were measured by using the Heidenhain thickness-gauge (Figure 3.2.3). From each sample, four measurements were taken (Figure 3.2.4). From these four measurements the average was calculated. The expected wall thickness was the same as the nozzle size. Therefore, the nozzle size was taken as a reference for the wall thickness. To calculate the maximum expansion of the foam for the temperature experiment, the expected wall thickness of 0,4 (for ASA and PLA), or 0,8 (for TPU) were taken as reference (C_{ref}). The measured wall thickness was variable (C_{var}) due to the printing temperature. The following calculation was used to calculate the expansion in percentages of the material:

$$Expansion = \frac{C_{var} - C_{ref}}{C_{ref}} * 100$$

For finding the correct flow rate, there were three iterations done. After each iteration the expansion was measured and the flow rate was calculated. If the right amount of flow rate was found, no recalculations were made. The right amount of flow rate was found if the average value of the measurements was 0,8 mm or 0,4 mm ±0,01 mm. If this was not reached within the three iterations, the flow that gave the closest result to 0,8 or 0,4 mm was chosen.

3.3 Results

The results section is split into three parts, each part describes the results of each individual experiment. First, the temperature experiment is discussed (3.3.1), followed by the speed experiment (3.3.2) and the flow experiment (3.3.3).

Figure 3.2.3: Heidenhain thickness-gauge

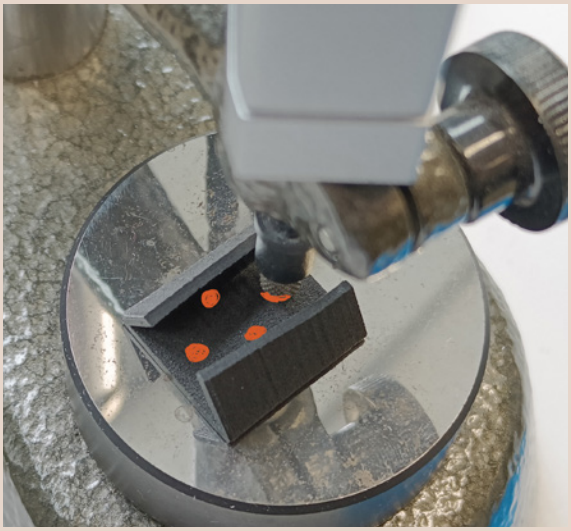

Figure 3.2.4: The orange dots show the four measuring points used for the temperature and flow experiments. The speed experiment used approximatly the same placement.

3.3.1 Results temperature experiment

PLA

The results for the wall thickness measurements of the series with and without fan cooling can be seen in Figure 3.3.1. The maximum amount of foaming was achieved at 220 °C for both series. The PLA with fan cooling appeared to have a second optimum at 250 °C. The maximum expansion that was achieved in comparison to the starting wall thickness of both series was 114,4% with and without fan cooling for 220 °C, Table 3.3.1. For both samples this maximum thickness was 0,858 mm.

TPU

The results of the wall thickness for both series of TPU prints can be found in Figure 3.3.2 and Table 3.3.2. The series with cooling had an optimum at 210 °C, afterwards the thickness declined. The series without fan cooling appeared to have two optima, a small one at 200 °C and a higher one at 250 °C. The wall thickness was the highest at 250 °C without fan cooling, it had an expansion of 103,3%.

ASA

The results for the wall thickness measurements can be found in Figure 3.3.3 and Table 3.3.3. Both series are quite similar in terms of wall thickness. The thickness of the walls declines and did not increase, but they were already higher than the expected nozzle size. The biggest increase was on 240 °C with fan cooling (119,7 %). The highest increase without a fan was at 230 °C (111,6%).

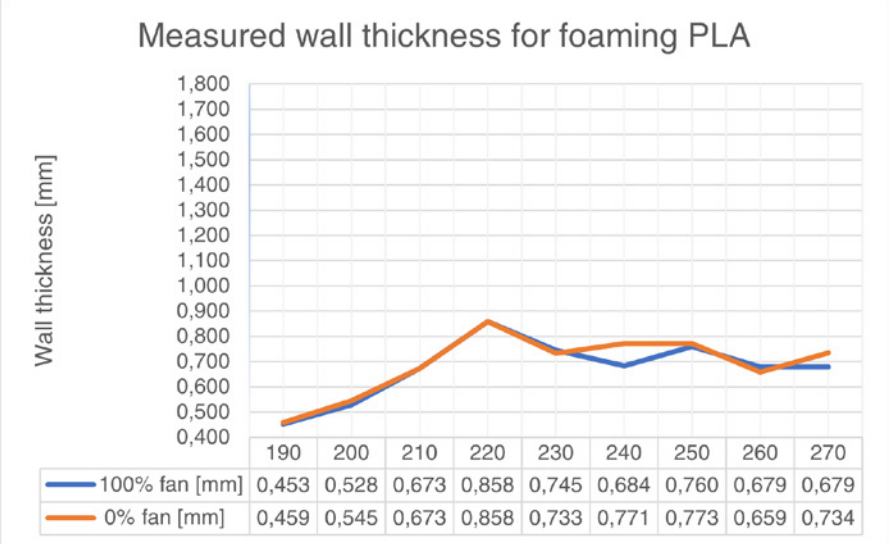

Figure 3.3.1: Graph which shows the measured wall thicknesses of the foaming PLA at different temperatures, withput fan cooling (orange line) and with fan cooling (blue line).

Table 3.3.1, Wall expansion foaming PLA

Temperature [°C]	190	200	210	220	230	240	250	260	270
Expansion with fan 100% [%]	13,1	31,9	68,1	114,4	86,3	70,9	90,0	69,7	69,7
Expansion with fan 0% [%]	14,7	36,3	68,1	114,4	83,1	92,8	83,1	64,7	83,4

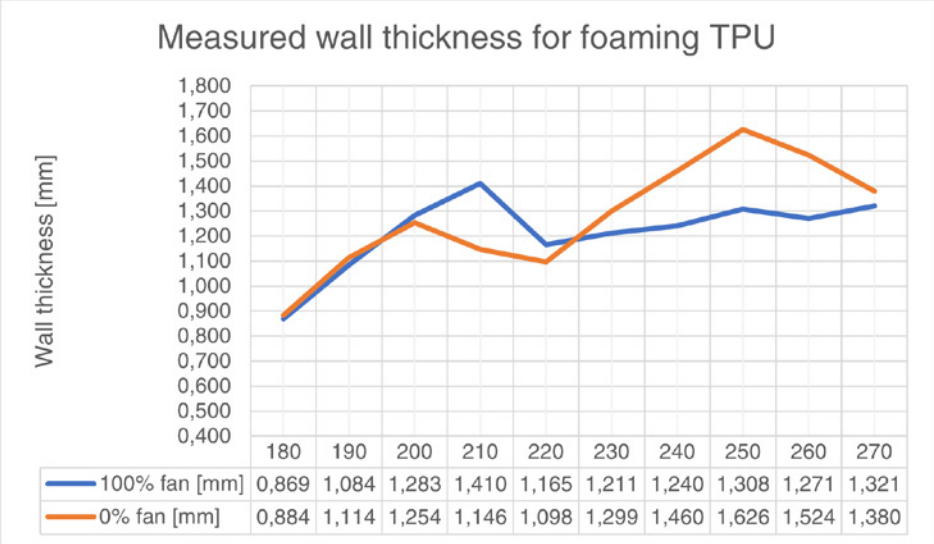

Figure 3.3.2: Graph which shows the measured wall thicknesses of the foaming TPU at different temperatures, withput fan cooling (orange line) and with fan cooling (blue line).

Table 3.3.2, Wall expansion foaming TPU

Temperature [°C]	180	190	200	210	220	230	240	250	260	270
Expansion with fan 100% [%]	8,6	35,5	60,3	76,3	45,6	51,4	55,0	63,4	58,9	65,2
Expansion with fan 0% [%]	10,5	39,2	56,7	43,3	37,2	62,3	82,5	103,3	90,5	72,5

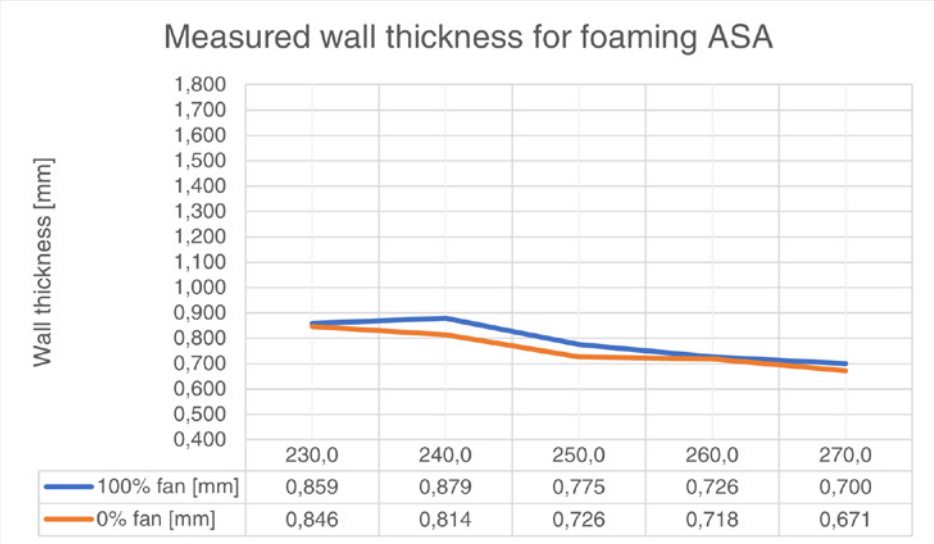

Figure 3.3.3: Graph which shows the measured wall thicknesses of the foaming ASA at different temperatures, withput fan cooling (orange line) and with fan cooling (blue line).

Table 3.3.3, Wall expansion fomaming ASA

Temperature [°C]	230	240	250	260	270
Expansion with fan 100% [%]	114,7	119,7	93,8	81,6	75,0
Expansion with fan 0% [%]	11,6	103,5	81,6	79,4	67,8

3.3.2 Results speed experiment

PLA

The PLA was able to print successfully over all the print speeds. It did get thinner when the print head moved more quickly, as well as making the part look more translucent, Figure 3.3.4. The surface did not appear to get rougher. When the speed increased, the wall thickness decreased, Figure 3.3.7. When the print head moved four times faster, the wall thickness was almost halved. For example, at 25 mm/s the wall thickness was about 0,8 mm and at 100 mm/s it was 0,5 mm approximately.

TPU

The TPU was able to print up until a speed of 50 mm/s. At 75 mm/s and higher, the triangle was extruded in a spider web like way, Figure 3.3.5. At 75 mm/s it appeared that the printer was able to print correctly up until half the height of the model, afterwards the material became spiderweb. For the triangle printed at 100 mm/s, the printer was not even able to print a wall, it immediately turned into a spiderweb like structure. The wall thickness of the different triangles decreased when the print speed increased, Figure 3.3.7. Due to the amount of spider web like structure the 100 mm/s print had, the wall thickness was determined 0 mm. The last few layers of the TPU printed with 50 mm/ s were thicker in the middle, it appeared like they had two lines. This was not the case at the corners, Figure 3.3.6.

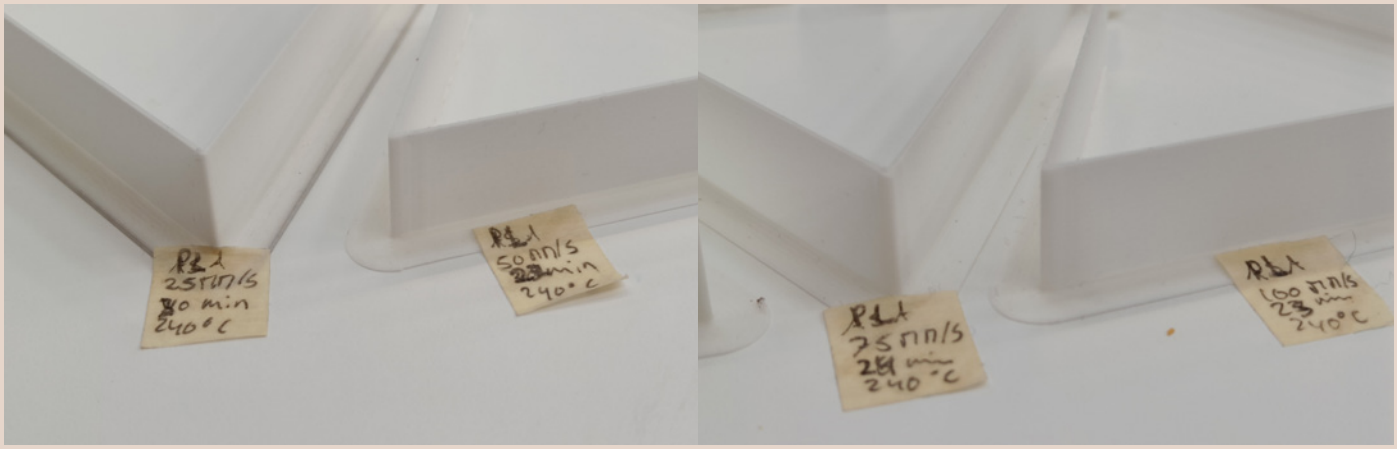

Figure 3.3.4 Visual results of the speed experiment for foamingPLA From left to right, 25 mm/s, 50 mm/ s, 75 mm/s and 100 mm/s

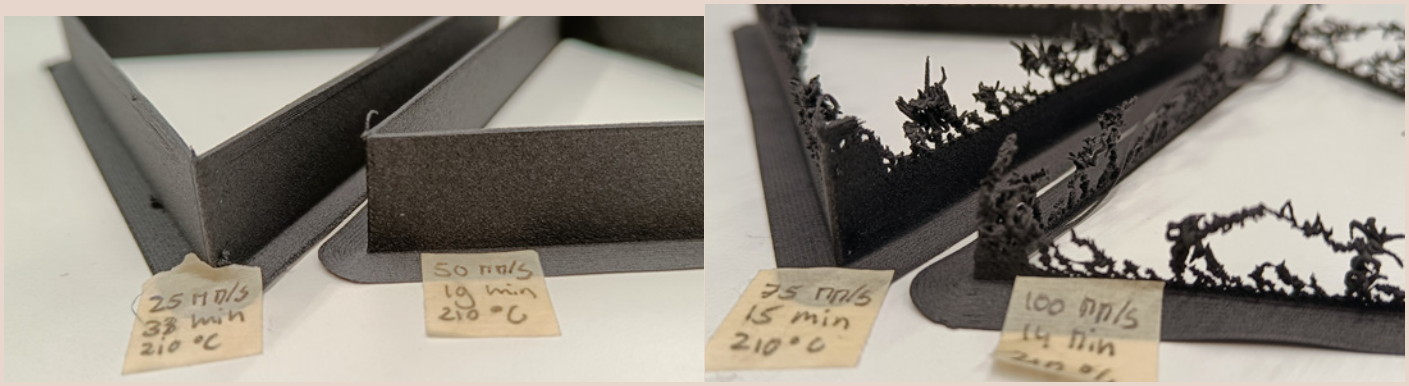

Figure 3.3.5 Visual results of the speed experiment for foaming TPU. From left to right, top to bottom; 25 mm/s, 50 mm/ s, 75 mm/s and 100 mm/s

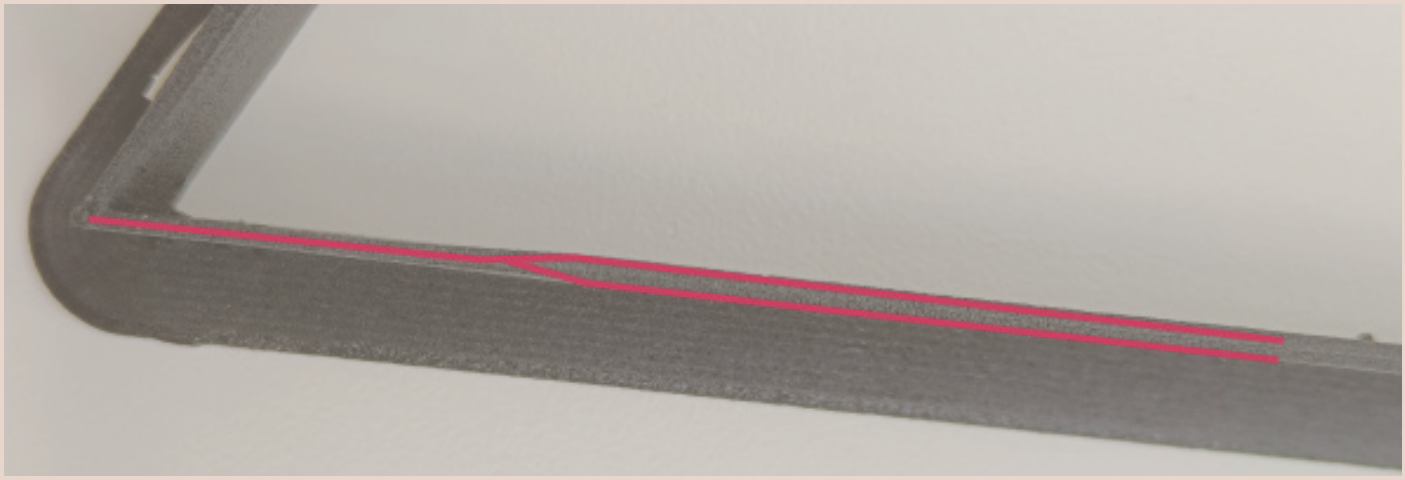

Figure 3.3.6 Double lines created in the last few layers of the 50 mm/s printed TPU triangle

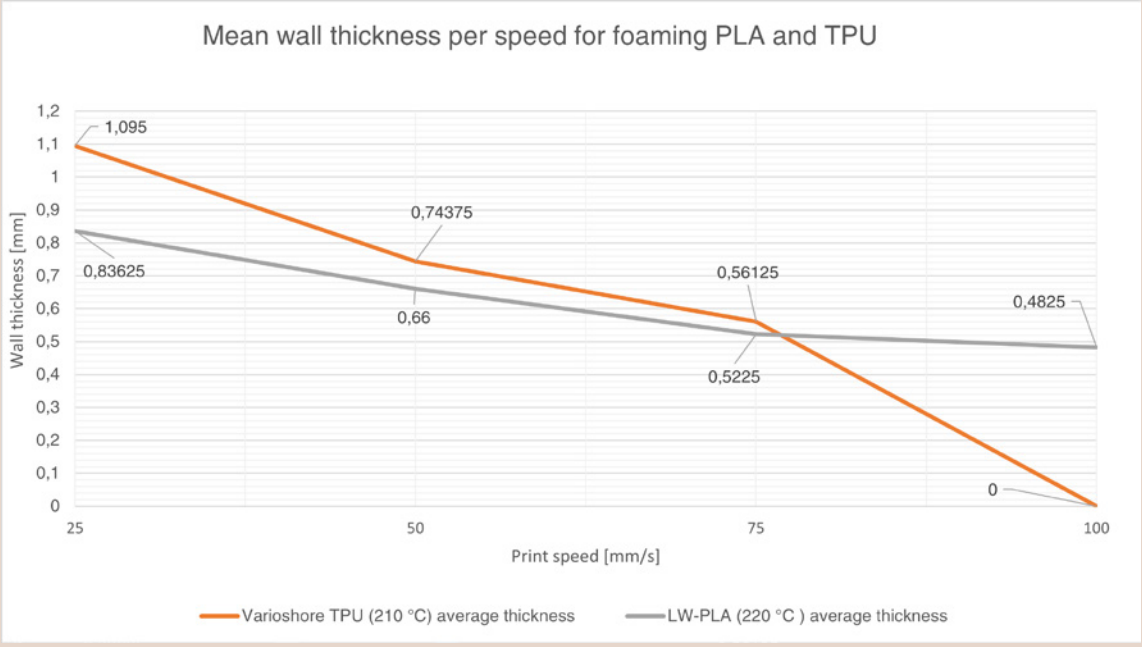

Figure 3.3.7 Measured wall thicknesses for the different speeds and materials

Table 3.3.4 Final found flow rates for foaming PLA

Temperature [°C]	190	220	250	270
Flow [%]	88	41	49	59
Measurement [mm]	0,386	0,411	0,380	0,374

Table 3.3.5 Final found flow rates for foaming TPU

Temperature [°C]	180	210	240	270
Flow [%]	98	64	65	71
Measurement [mm]	0,785	0,821	0,808	0,833

1.3.3 Results flow rate experiment

The different flow rates used in each iteration can be found in Figure 3.3.8 and 3.3.9 for each material. The final best flow rates and their results can be found in Table 3.3.4 and 3.3.5. The total average of each iteration of the measured expansion is shown with a yellow dotted line.

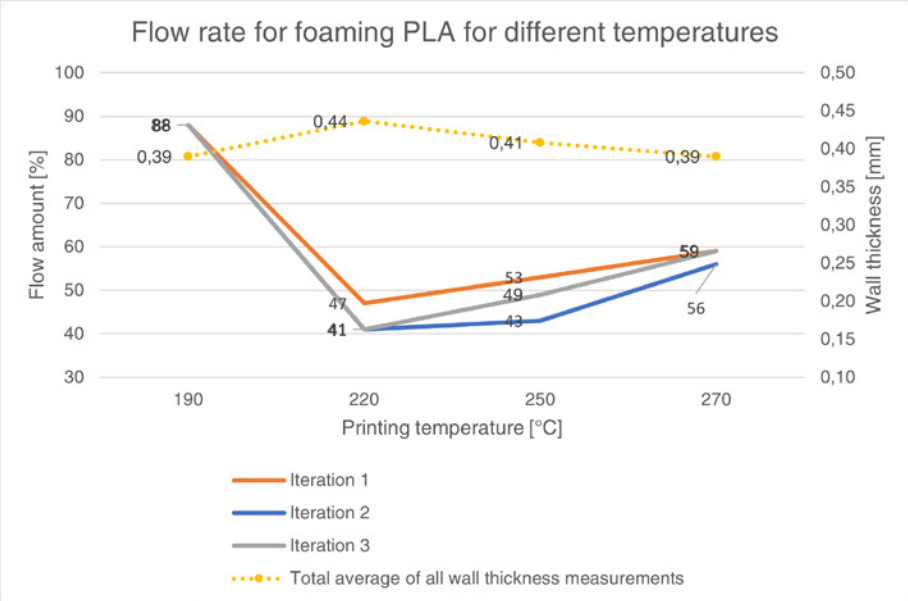

Figure 3.3.8, Flow rate for the different iterations and temperatures of the foaming PLA.

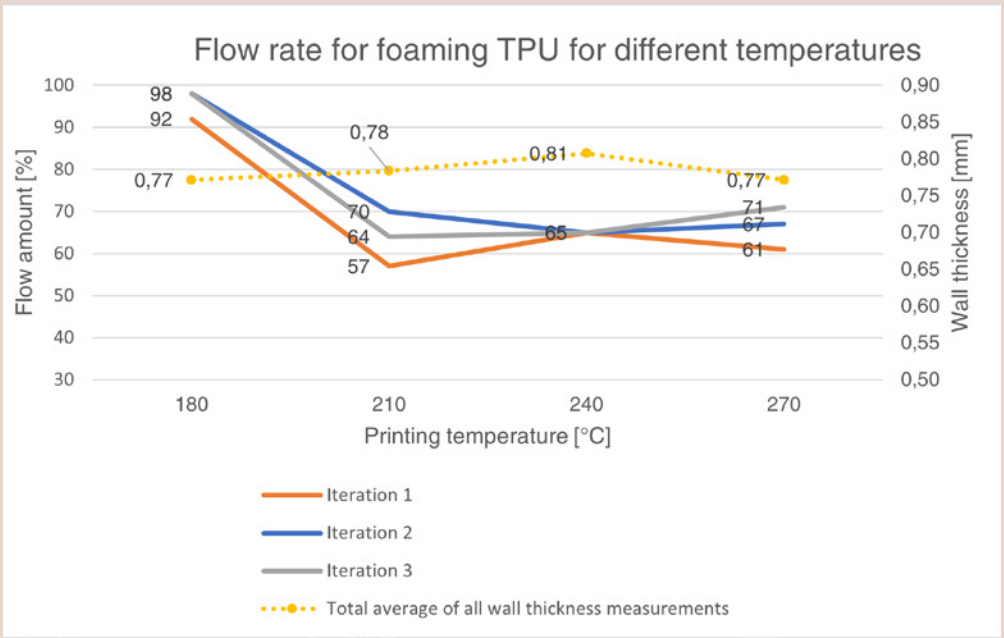

Figure 3.3.9, Flow rate for the different iterations and temperatures of the foaming TPU

3.4 Discussions and recommendations

The discussion is divided by the three conducted experiments. First, the temperature experiment is discussed (3.4.1), followed by the speed experiment (3.4.2) and lastly the flow experiment (3.4.3).

3.4.1 Discussion and recommendations temperature experiment

From the experiments can be concluded that the maximum expansion for each material is achieved under different circumstances. The influence of the fan cooling is also different for each material. Depending on the desired outcome, both the fan cooling and nozzle temperature can be adjusted. For the expansion in the XY-plane, PLA expanded the most significantly at 220 °C regardless of fan cooling, TPU expanded the most significantly at 250 °C without the fan cooling. ASA expanded the most significantly at 240 °C with fan cooling.

The PLA was not able to achieve the same amount of expansions as Hermann (2020a&b). The fact that the materials did not foam as much as Hermann's (2020a&b) results could be for several reasons. First of all, the used printer was different than the one Hermann (2020a&b) used. Hermann used a Prusa Printer which has no enclosure. Ultimakers have an enclosure which could influence the airflow around the print bed, which in turn could influence the results of the printed samples. Secondly, different printing settings can cause different outcomes. For example, various print speeds can have an impact on the amount of expansion, as can be seen from the results of the speed experiment. Moreover, the nozzle geometry can affect the material expansion. The material is only heated when it is inside the nozzle. The moment when the material leaves the nozzle, it will immediately cool down. Figure 3.4.1 shows a schematic of this phenomenon. Therefore, the time frame for the material to foam is fairly small. There are several different nozzles on the market which vary in length. A longer nozzle (Figure 3.4.2) could give the material more time to be heated before being extruded. Further research could investigate the influence of the length of the nozzle on the ability of the material to foam. Since Ultimaker has a dedicated printcore, it would be recommended to test the influence of the nozzle length on a printer which allows the changing of nozzles, such as an Ender 3 or a Prusa Printer.

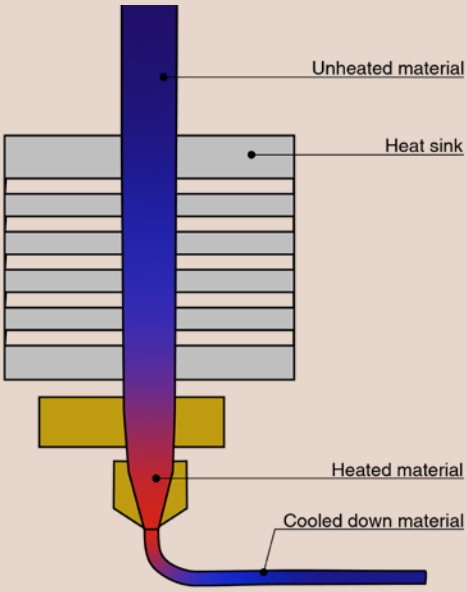

Figure 3.4.1, Schematic of the geometry of an extruding nozzle. The red colour indicates that the material is hot, blue indicates that the material is cooled down

The results show that the wall thickness of ASA decreased. This can be attributed to the fact that ASA already reached the maximum foaming temperature, at a temperature lower than was set. The expected minimum wall thickness for this experiment was around 0,4 mm, as the nozzle size was also 0,4 mm. However, the measured wall thickness for both series at the lowest temperature was around 0,8 mm. A potential follow-up experiment could investigate printing the LW-ASA below 230 °C to see if the expected wall thickness of around 0,4 mm can be achieved.

The addition of the fan had very little effect for PLA and ASA. For TPU, the fan did affect the amount of foaming of the material. For PLA the biggest difference between using the fan or not was at 240 °C with a difference of 0,087 mm, and for ASA this

Figure 3.4.2: Different Nozzle lengths, images from 123-3D.nl (n.d)

was 0,065 mm at 240°C as well. The fan has very little to no influence on the expansion of the PLA and ASA filaments. The biggest difference for using a fan or not was observed for the wall thickness of the Varioshore TPU at 250°C with a difference of 0,318mm. At 210°C, 240°C and 260°C the difference between using a fan and no fan was 0,264mm, 0,220 mm, and 0,253 mm, respectively. Besides the foaming, the fan could have also influenced the shrinkage of the material. Turner and Gold (2015) found that FDM printed parts can have dimensional inaccuracies due to shrinkage. The fan may have accelerated this effect for the TPU. Therefore, it can be concluded that the fan had an influence on the wall thickness of the TPU, but it is not clear how much influence it has on foaming in particular. This could be further researched by printing the TPU at different fan speeds with the temperature that causes the most amount of foaming. The differences in expansion for each increase in fan speed can be measured to determine the influence of fan speed on the foaming. An additional printer was used to improve the efficiency of the printing process. The main difference between the printer used to print the TPU with and the other printer is that it is a newer model and has a door. The door may have limited the amount of airflow which could have influenced the results.

3.4.2 Discussion and recommendations printing speed experiment

It can be concluded from the results that a higher printing speed for both materials influences the final printed product. TPU obtained a rougher surface when the speed increased. For the highest speeds, TPU was not able to print properly. There might be several reasons why the TPU at higher speeds (75 mm/s and 100 mm/s) was not able to print properly. First of all, it could be due to the fact that the material did not have enough time to stick to the previous layer. As found by Kacergis et al. (2019) the material will built-up stress due to it stretching. Every time the material adheres, it gets pulled slightly, but when it breaks there is a possibility that it shoots back into the nozzle due to the stress. Secondly, the pressure within the nozzle could have also been too high, making it difficult for the printer to push the material trough the nozzle, causing under-extrusion. This might have to do with the elasticity of the TPU. It is more difficult for the feeder to push the TPU trough the nozzle, as it needs to travel a relatively long distance. Ultimakers do not have a direct drive feeder, like printers such as the Ender-3 s1 (Alternate, n.d.), where the feeder is just above the print head. Figure 3.4.3 shows the difference between these feeders. The two reasons above can also cause the nozzle to clog, since the TPU does not move through the nozzle, resulting in failed prints.

An interesting observation was made for TPU, the top layers printed at 50 mm/s speed were not printed on top of each other, but next to each other. Which resulted in an increased thickness at the top. This could be explained due to the fact that TPU is flexible and might move a bit when the nozzle goes over it. If the printer nozzle moves faster and the TPU material shifts, it has less time to align with the previous layer properly. On the other hand, this phenomenon can also be attributed by the thin and high walls of the models. For further research I recommend to further look into where the exact cut-off is per material for the maximum printing speeds, since this could be interesting to know if one wants to print very quickly. For TPU one could look in the range between 50 mm/s

and 75 mm/s. For PLA it would have to be above 100 mm/s. I also recommend to further research the reason the TPU model printed double lines the last few layers at 50 mm/s.

PLA was able to print successfully on all the different speeds. The surface quality for each print appeared to be about the same, and the material did not slip. The results indicated that the speed affected the wall thickness of the PLA. The high speeds may have prevented the bubbles within the material from reaching their maximum size, which could be another reason why the expansion of the material decreased with speed. The material spends less time in the print head due to the movement and the correction that Cura makes to the extrusion speed. This might give the material less time to be heated and for bubbles to form. A nozzle of a different length could affect this as well, so it is also recommended to further investigate the influence of the nozzle length on the wall thickness. This can be done by repeating the experiment with nozzles of different sizes. As mentioned in the discussion for temperature, this would have to be done on another printer.

3.4.3 Discussion and recommendations flow rate experiment

From the flow rate experiment, it can be concluded what the optimal amounts of flow rate would be for TPU and PLA for different temperatures. Depending on the desired amount of foaming or density, a different flow rate can be chosen. These flow rates are specific to the used printer, the settings, and the environmental conditions. The expansion for the material can be influenced by other printing parameters such as bed temperature and printing speed. For the samples, a limited number of iterations were performed to determine the right amount of flow rate. Each flow rate sample was only printed once. Therefore, it is recommended for future experiments to print more samples to ensure the chosen flow rate is appropriate, since each sample can vary between prints.

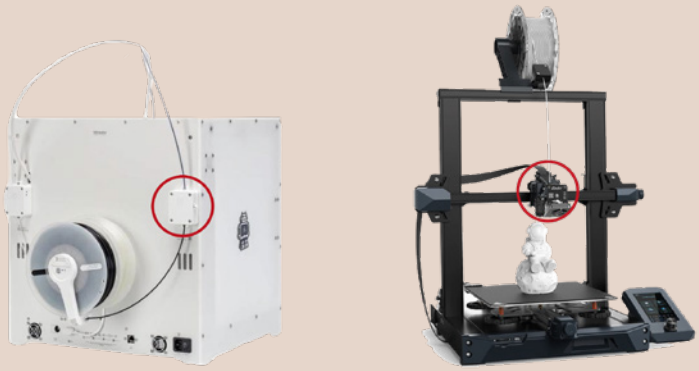

Figure 3.4.3: The red circles shows the placement of the feeder. As can be seen from the Ultimaker on the left, the feeder is much further away from the nozzle than for the Ender on the right. Image of the Ultimaker from 3D Ninja, (n.d.) and image of the Ender from Alternate (n.d.).

3.5 Conclusions for the experiments

The following sections discuss the conclusions of the experiments. First, each experiment is concluded separately, after which an overall conclusion is given for all the printing parameters. This overall conclusion discusses guidelines for printing with the lightweight materials as well as recommendations for future work.

3.5.1 Conclusion temperature experiment

The aim of this experiment was to investigate the maximum expansions of the lightweight materials as well as to investigate how the fan influenced these expansions. Based on the results, it can be concluded that the fan did not have a big impact on the expansion of the foaming PLA and foaming ASA. Foaming TPU was more affected by it. The experiment demonstrated that the extent of foaming of the materials can be controlled by adjusting the nozzle temperature in the first place. For the TPU the fan can also be used. These findings help with selecting the appropriate printing temperatures for a desired outcome. The experiment proves to be valuable in understanding the influence of the nozzle temperature on the expansion of the material. The expansion for the materials for different temperatures are shown in Figure 3.3.1, 3.3.2, 3.3.3

3.5.2 Conclusion printing speed experiment

The speed experiment concludes that the speed influenced the expansion of the foaming PLA and foaming TPU. For TPU the surface got rougher, above 75 mm/s it was not even able to extrude, causing a clogged nozzle. The foaming PLA was able to print up to 100 mm/s. With this experiment it was clear that the recommended speed for TPU was between 25 and 50 mm/s, while PLA was able to print between 25 and 100 mm/s. In general, lower print speeds provided prints that were more expanded, Figure 3.3.7. Depending on the desired outcome and available time, one can choose a speed to accommodate their wishes. The results of this experiment are valuable in determining the appropriate speed for printing with foaming PLA and foaming TPU.

3.5.3 Conclusion flow rate experiment

The goal of the flow rate experiment was to find the appropriate flow rate for the expansion of four temperatures for foaming PLA and foaming TPU. The conclusion can be drawn, that the flow rate differs per material and for each expansion. The prints with the most amount of expansion, needed the highest amount of flow rate. The found flow rates in Tables 3.3.4 and 3.3.5 are useful for being able to print dimensionally accurate prints or get the lightest prints as possible.

3.5.4 Future work

For future work, one could investigate the influence of nozzle geometry on the expansion of the materials. The experiments above could be conducted in the same way, but then instead on a printer which allows switching nozzles with different geometries more easily. The outcomes of the experiments with different nozzles can then be compared to each other.

Secondly, the influence of the fan cooling on the expansion of the foaming TPU can be further investigated. The biggest amount of expansion without fan cooling would first need to be determined, after which samples can be printed with this temperature. For each sample, the fan speed is increased until it reaches 100%. Each sample is then measured as described in the temperature experiment. Subsequently, the influence of the fan can be more accurately determined.

Third, one could further investigate the minimum expansion of foaming ASA by printing samples at temperatures lower than 230 °C according to the settings of the temperature experiment.

Fourth, the cut-off speed for the foaming PLA and TPU could be further investigated. Within the experiment that had been conducted, the material stopped extruding properly at 50 mm/s for foaming TPU. For foaming TPU one could conduct the printing speed experiment again and take smaller steps for the print speed from 50 mm/s onwards. For foaming PLA the speed experiment can also be repeated, but then increasing the print speed from 100 mm/s onwards to investigate after which speed the material is not able to print anymore. This way, a more exact cut-off speed can be found.

Fifth, the flow rate for the foaming TPU and PLA can be investigated more extensively. Within this experiment only four temperatures were investigated for each material. For future work, the remaining temperatures can also be investigated. Apart from investigating more temperatures, it would also be recommended to print more than one sample of a certain flow rate to make sure the right amount is found.

Sixth, the influence of the printing speed and flow rate can also be further investigated for the foaming ASA material. This can be done by repeating the described flow rate and printing speed experiments again, but then for the foaming ASA.

Lastly, since the printing speed has an effect on the amount of foaming, it is also recommended to repeat the temperature experiment with different printing speeds. By repeating the temperature experiment under different printing speeds.

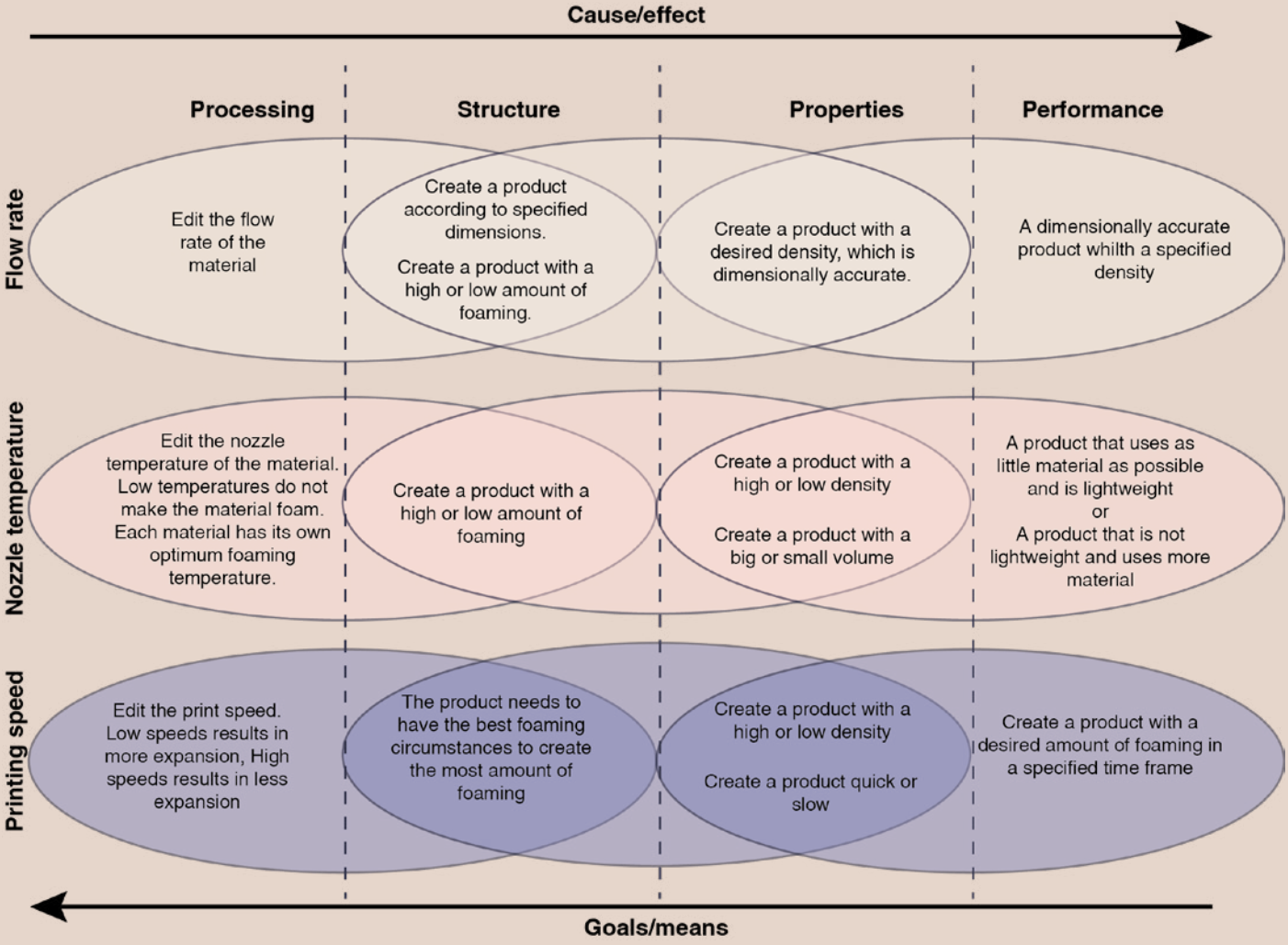

Figure 3.6.1 Overview of the investigated applied to the 3-link chain model

3.6 Overall conclusions and guidelines for the printing parameters

The goal of the experiments was to get a better understanding of how to print with the different lightweight materials. Nozzle temperature and fan speed were investigated to see their influence on the amount of foaming. The flow rate of the material was adjusted to get dimensionally accurate prints. From these experiments several practical printing parameters were obtained which will be useful for designing with the lightweight materials for the rest of the thesis. It can be concluded that the tested printing parameters all influenced the expansion of the materials in their own way. Depending on the goal or desired outcome of the print, these printing parameters can be adjusted to achieve this goal. The 3-link chain model (Doubrovski et al, 2011) is used to give an overview of the influence of the researched parameters on the final outcome of the print, Figure 3.6.1. The knowledge from these experiments will be used in the final demonstrator.

Demonstrator

This last phase covers the investigation process for the creation of the final demonstrator, which is a recreation of the inner linings of a motorcycle helmet with the foaming materials. This section starts with an overview of the proposal for the application. This is followed by a benchmarking experiment of the foaming PLA and the expanded polystyrene (EPS) which is currently used in motorcycle helmets. During this test, several foaming PLA samples are compressed and compared to the EPS. This benchmarking experiment is conducted as an initial test to see if the foaming PLA is able to gain comparable results as the EPS. Lastly, the creation of the demonstrator is reported and concluded.

4. Introduction to motorcycle helmets

The goal of this chapter is to highlight the importance of motorcycle helmets, understand their safety standards and the possible advantages of 3D printing a motorcycle helmet. First, information about motorcycle helmets is given to understand their importance (4.1). Secondly, an overview of different testing standards for motorcycle helmets is given (4.2). Third, the advantages of a 3D printed helmet is explored (4.3). Finally, the chapter ends with a conclusion and design goal for the demonstrator (4.4).

4.1 The importance of motorcycle helmets

Motorcycles do not have a crumple zone or any protection from the vehicle, therefore it is important for motorcyclists to wear protective gear. The helmet might be one of the most important parts of the set. Wearing a helmet helps to prevent mortality in case of an accident (Liu et al, 2008). Ramli & Oxley (2016) found that a helmet should fit well on the head to be able to provide good protection. An user wearing an ill-fitting helmet was four times more likely to sustain a severe head injury (Ramli & Oxley, 2016). To be more specific, Urréchaga et al. (2022) found that wearing a full-face helmet was highly recommended in reducing brain injury, facial fractures and other severe injuries to the head. Motorcyclists can choose from many different types of helmets that are available on the market, as shown in Figure 4.1.1. These all serve a different use case, but in Europe, they all must meet the ECE-22 standard. This standard describes guidelines of testing a helmet in terms of safety, the next section discusses this matter in more depth. All ECE-22 approved helmets consist of three layers, which are shown in Figure 4.1.2

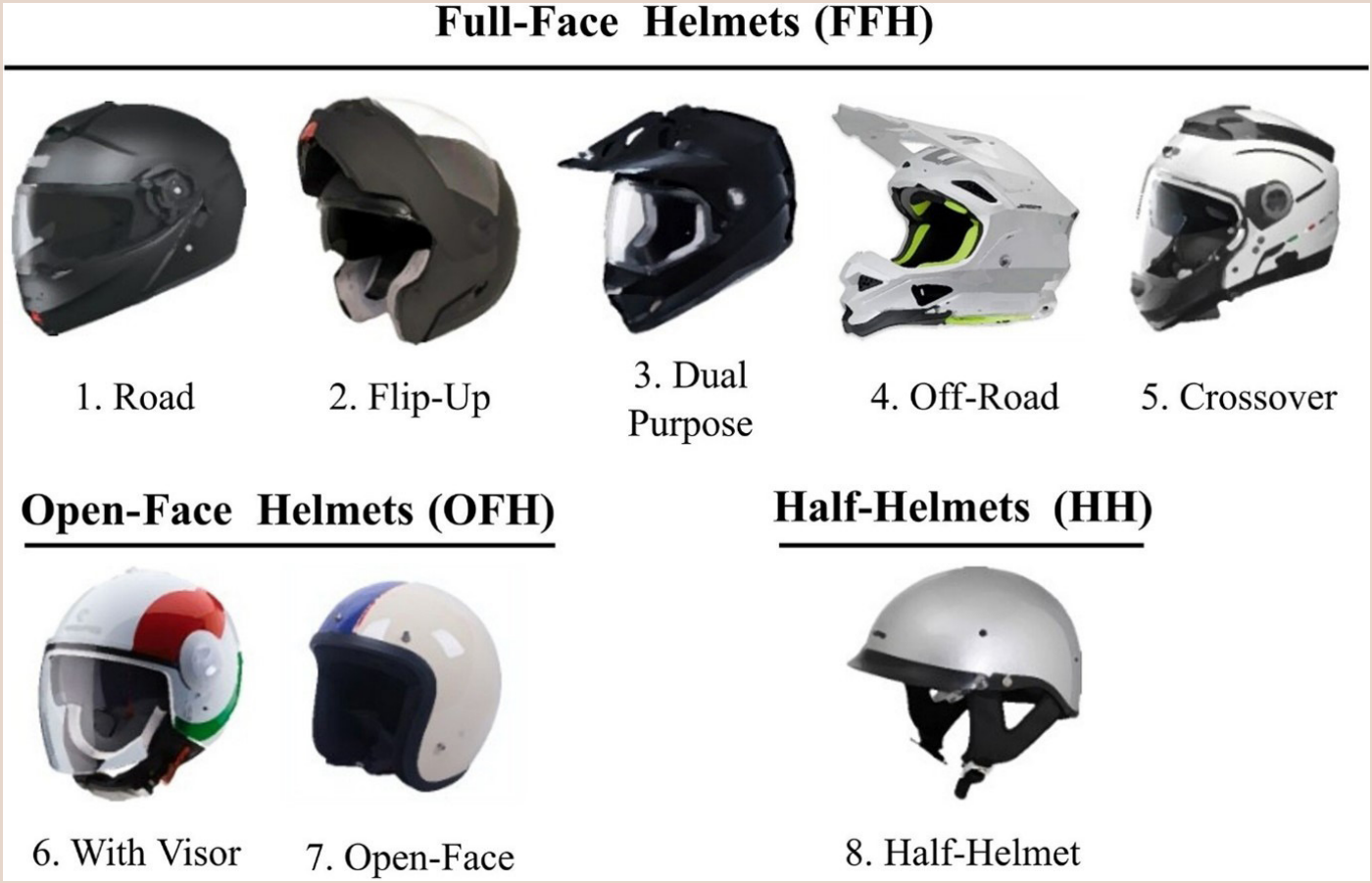

Figure 4.1.1, Types of motorcycle helmets, image by Lucci et al, 2021.

The outer shell, which is the outer most layer (UNECE, 2021), must be able to distribute the load in case of a crash and prevent anything from piercing the helmet. It is typically made from a composite (Roof, n.d.) or other impact plastics such as polycarbonate (pc) (Nolan, n.d.). The second layer is the protective impact padding which absorbs the impact in case of a crash (UNECE, 2021). This impact layer is most often made from EPS. The EPS foam irreversibly deforms when an impact occurs (Dainese, N.D). The last layer is the comfort padding, which sits against the head and provides wearer comfort (UNECE, 2021). To accommodate different head sizes, manufacturers usually produce a few outer shell sizes and adjust the padding within this shell. Figure 4.1.3 presents the sizing chart of the Nolan helmet manufacturer. As can be seen only two shell sizes exist for the sizes XXS to XXXL. This means that if you have a XXS head, you may wear a medium shell size with more padding to fill it, until a good fit is achieved. This makes the helmet potentially heavier and look bigger than for someone with a medium head. Figure 4.1.2 shows this phenomenon

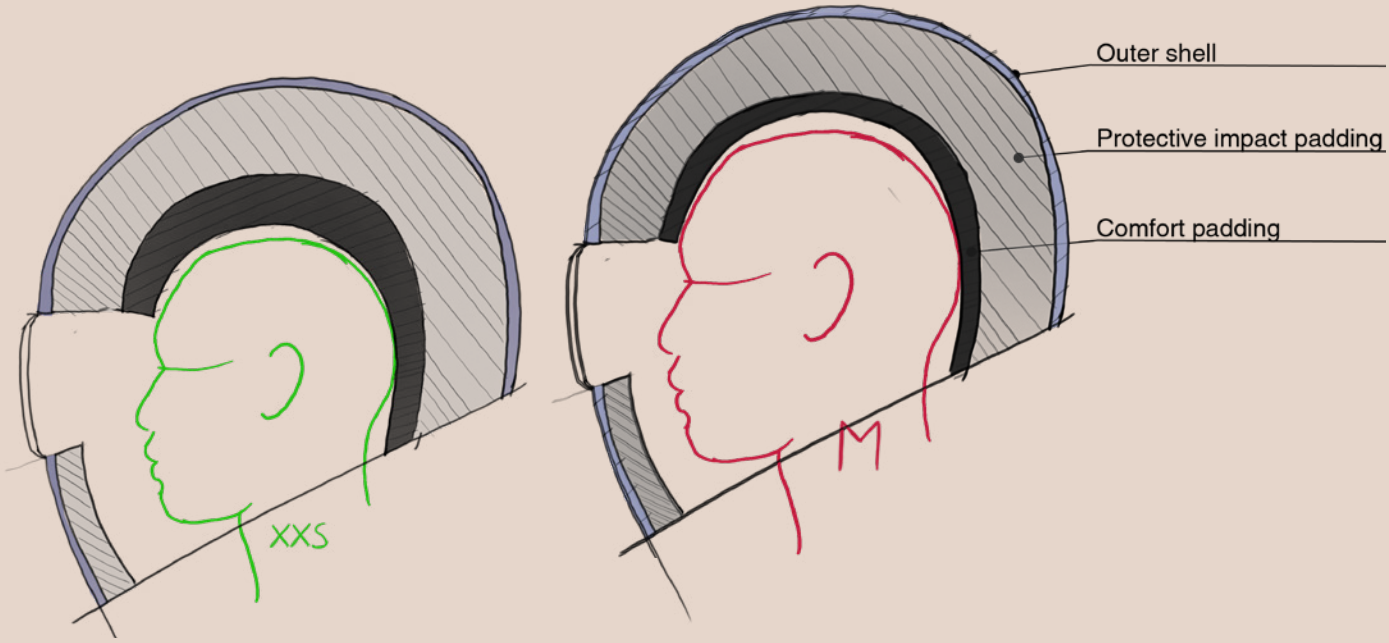

Figure 4.1.2, A schematic cross section to illustrate the difference between shell sizes as well as the different layers within a helmet

SIZES	8	XXXS	XXS	XS	ST	M	L	XL	XXL	XXXL
CAPS	2									
CIRCUMF.	CM		54	55	56	58	60	62	64	65

Figure 4.1.3, A size chart from helmet manufacturer Nolan (n.d.), indicating the different sizes with the corresponding head circumference and shell. The image shows that for sizes XXS-M the same outer shell is used and for sizes L-XXXL another outer shell is used.

4.2 Testing standards for motorcycle helmets

Apart from the ECE-22 standard, efforts by other independent groups have been made to standardize impact testing for helmets as well. However, simulating actual conditions remains a challenge. The differences between each accident vary significantly with different speeds and drop heights. Additionally, polymers are strain, temperature and pressure dependent (Siviour & Jordan, 2016). Therefore, depending on the weather and place you live, the helmet could potentially provide slightly different material properties.

To get an idea what the differences are between the testing standards, three standards for motorcycle helmets have been consulted. They all are set-up in a same manner, a helmet is dropped on an anvil on which the impact force is measured, Figure 4.2.1. The most prominent variations between the testing standards is the maximum residual force on the anvil as well as the speed at which they fall. These differences between the standards are shown in Table 4.2.1. Several values can be seen for the drop speed and the peak residual force, this is because different situations are tested within the standards. All these standards require that the extra accessories, such as peaks and visors, need to be mounted when testing. The outer shell and visor must not fail in such a way that they inflict damage on the wearer. For this project, we will focus on the ECE-22 standard. This standard also tests different impact points and drops.

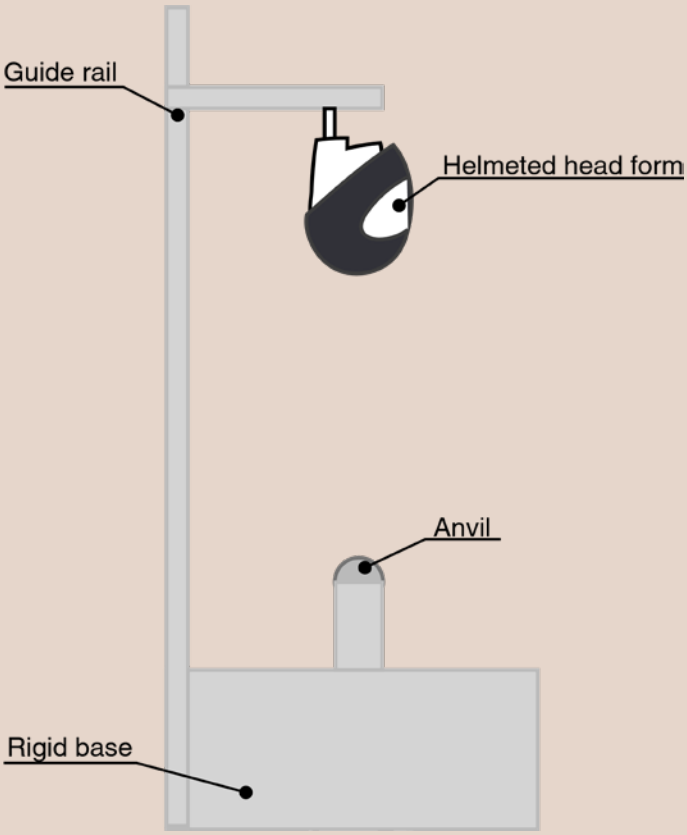

Figure 4.2.1, Schematic of a drop testing rig typically used to test motorcycle helmets.

4.3 Advantages of a printed motorcycle helmet

There are several potential advantages to using 3D printing for manufacturing a motorcycle helmet. First of all, one can make a custom-fit helmet with the help of 3D scanning. By creating a 3D scan of an individual's head, a more accurate fit can be achieved. Ellena et al (2018), researched a frame work for the mass customization of bicycle helmets. It was found that with 3D scanning the fit accuracy of the helmets increased (Ellena et al, 2018). Having a more accurate fitted helmet is potentially safer due to the helmet being more comfortable, reducing fatigue. Currently, the process of custom-fit helmets involves manually measuring the individual's head and testing the fit. A personal fitted helmet by Shoei, a helmet manufacturer, starts at around €450 for the helmet (Voordeelhelmen.nl, n.d.a) alone. According to Shoei Europe (n.d.), the recommended price for the fitting process is €60, though the actual price varies depending on factors such as, time needed for fitting, the type of cushions needed and whether an existing helmet is brought along (Shoei Europe, n.d.). Therefore, the total price of a custom-fit helmet by Shoei could vary vastly. With 3D printing and scanning, the price for a custom-fit helmet could be lowered since less time is needed to get a correct fit. 3D printing offers the opportunity for helmet shops to print the parts they need locally, possibly reducing the cost of transporting different helmet parts. The bicycle helmet manufacturers Hexr already implement the process of 3D scanning and manufacturing bicycle

helmets on demand with 3D printing (Hexr, n.d.). Kav Sports (n.d.), another bicycle helmet company also already manufacturers 3D printed bicycle helmets.
Non-printed foaming materials are used within a helmet because they are able to keep the weight low while still being able to absorb significant amounts of specific energy (Avalle et al, 2001). X-lite is a brand specialized in creating ultra-light motorcycle helmets, a helmet of theirs starts at a price of around €500 according to the retailer,Voordeelhelmen.nl (n.d.b). The helmet manufacturer Arai (n.d.) has developed multi-density EPS foam liners in which they tune the density to the place of impact. Foam with a higher density, collapses slower meaning that it can better protect the wearer in the context of a high-speed crashes. When the foam has a lower density, it collapses quicker which is better suited for low-speed crashes (Parrotte, n.d.). With the 3D printed foaming materials, a multi-density foam liner can be created which can be printed in one piece, instead of multiple.

4.4 Conclusion and design goal

Within this chapter the importance of motorcycle helmets for a riders' safety have been highlighted, the safety standards helmets need to meet, and the potential benefits of 3D printing motorcycle helmets have been discussed. In conclusion, wearing a helmet that fits and is fastened correctly can significantly reduce the mortality and severity in case of a crash. Within Europe the ECE-22 standard is used to test the minimum safety requirements for motorcycle helmets. Different parts of the world use different standards. It could also be concluded that, 3D printing can be advantageous over current manufacturing processes, since it provides the ability to create custom-fit helmets faster, and possibly more affordably. Prosperi (2021) showed that printing a foaming PLA bicycle helmet could be feasible and therefore it will be interesting to further investigate the possibilities of 3D printing parts of a motorcycle helmet. Since the outer shell needs to be made of non-pierceable material, this will not be redesigned with the foaming materials for 3D printing. Instead, the impact padding that is currently made out of EPS as well as the comfort padding, will be redesigned. Before assuming if the foaming PLA will work for the application of a motorcycle helmet, a benchmark test will be done first. The main goal for this benchmark is to see if the foaming PLA is close to energy absorbing values of the EPS. If this is the case, the foaming PLA can thus possibly be feasible for the use within a motorcycle helmet. Since the foaming TPU will substitute the comfort padding which is not a critical part, it will not be benchmarked or further tested. Finally, from this chapter the design goal is concluded, the design goal for the final demonstrator will be to investigate the application of 3D printed foaming materials inside a motorcycle helmet.

Table 4.2.1, Differences between drop speed and peak residual force between standards

Standard	Drop speed [km/h]	Peak residual force on the anvil [N]
ECE-22 (UNECE, 2021)	21,6 - 29,52	2500, 3500
Snell (Snell Foundation, 2019)	19,94 - 27,91	2384, 2590, 2698
Dot (571.218 Standard No.218; Motorcycle helmets, 2022)	20,88 - 22,32	1472, 1962, 3924

5. Compression testing foaming PLA and EPS

The goal of this chapter is to investigate the feasibility of the use of foaming PLA within motorcycle helmets. To do this a compression test is carried out. For this project a derivative of the test set-ups from Gibson & Ashby (1997) and Van den Hazel, (2015) are used. Different densities are compressed and measured under different strain-rates until all the cells within the sample collapse. With this information, energy absorption graphs can be created to compare the foaming PLA with the EPS. First, some background information on the behaviour of (foaming) materials in compression is given (5.1). This is followed by an introduction to the benchmarking test (5.2), the method (5.3), results (5.4), discussion (5.5) and conclusion (5.6).

5.1 Introduction to materials in compression

This paragraph aims to provide background information on the behaviour of materials in compression, in order to better understand the benchmarking tests that will be conducted. First, the general behaviour of a sample being compressed is discussed (5.1.1). This is followed by a paragraph that goes into more detail about what happens to the foaming material when it is compressed (5.1.2). Lastly, information is given about how one could measure the behaviour of polymeric foams in compression (5.1.3).

5.1.1 Behaviour of material when compressing a sample

The stress-strain properties for metals in compression are comparable to those in tension. Plastics are typically 1,2 times stronger in compression than in tension (Ashby, 2016). The compressive behaviour for foams in compression are different, and is discussed in the following section. A schematic overview of a generic sample in compression in a free space is shown in Figure 5.1.1. In this situation, the force will only be applied at the top and bottom of the sample and the sides are free as shown. It is assumed that the sample subjected to compression is short enough, so it does not buckle (Height < 4*Diameter) (Tempelman et al, 2014). If the sample is too long, it will buckle, as shown in Figure 5.1.1. When compressing a sample with height < 4* diameter, the volume will remain constant, causing the diameter of the sample to increase. The increasing cross-sectional area results in an increasing force needed to compress the sample (Tempelman et al, 2014). This causes friction which acts radially inward. This friction creates multiaxial stresses which make the material more resistant to deformation in that spot. The deformation of the area here is close to zero (Tempelman et al, 2014). This is called the dead metal zone, shown in Figure 5.1.1. Since the volume stays consistent, the deformation of the material will act outside of this zone. This phenomenon is known as “barrelling” (Tempelman et al, 2014).

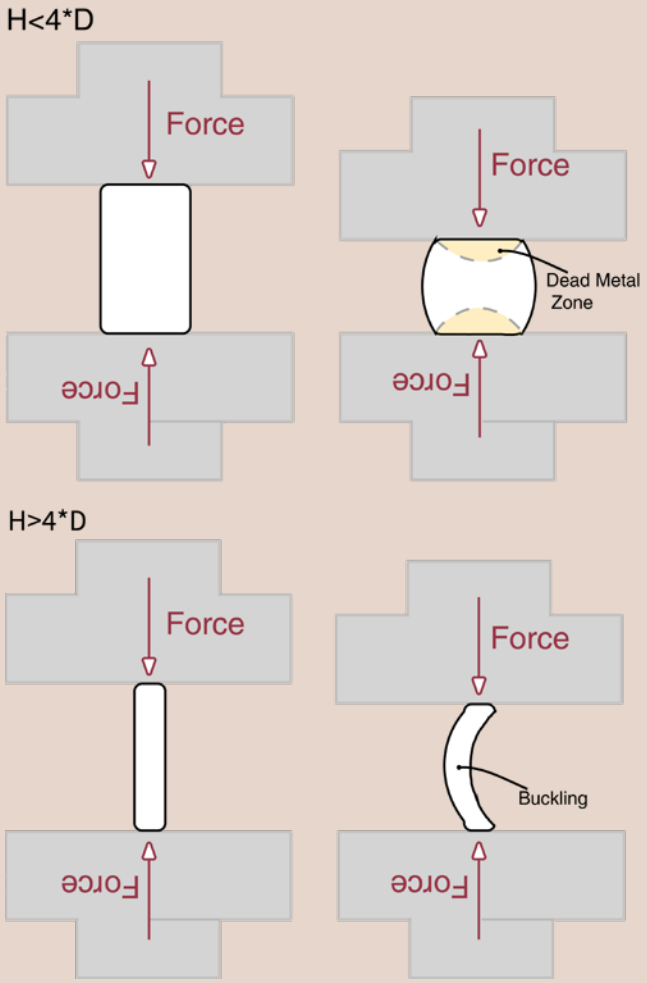

*Figure 5.1.1: Schematic of two samples in compression. The top row presents a sample that conforms to the Height < * diameter rule, and does not buckle. The bottom row shows a sample which does not adhere to this rule, and buckles.*

5.1.2 Properties of foams in compression

When foam samples are compressed, their mechanical response differs from that of solid materials. Before conducting any tests with foams, it is crucial to understand these mechanisms. When a foam sample is exposed to a compressive force, three stages describe the overall behaviour. In the first stage, at low stresses, linear elasticity can be observed (Figure 5.1.2 (1)) (Gibson & Ashby, 1997). This is followed by a plateau which differs for the overall material category (Figure 5.1.2 (2)). An elastomeric foam, such as rubbers, will buckle elastically (Figure 5.1.2 (red)). An elastic-plastic foam, such as metals, will plastically yield (Figure 5.1.2 (blue)) and an elastic brittle foam, such as ceramics, will brittlely crush (Figure 5.1.2 (green)) (Gibson & Ashby, 1997). After the cell walls have completely collapsed, the walls or struts will come into contact with each other. This is when the densification stage will commence (Figure 5.1.2 (3)). The stress will rise steeply again (Gibson & Ashby, 1997). Van den Hazel (2015) describes the densification stage as the point at which the foam starts to behave like a solid again, since all the cells collapsed.

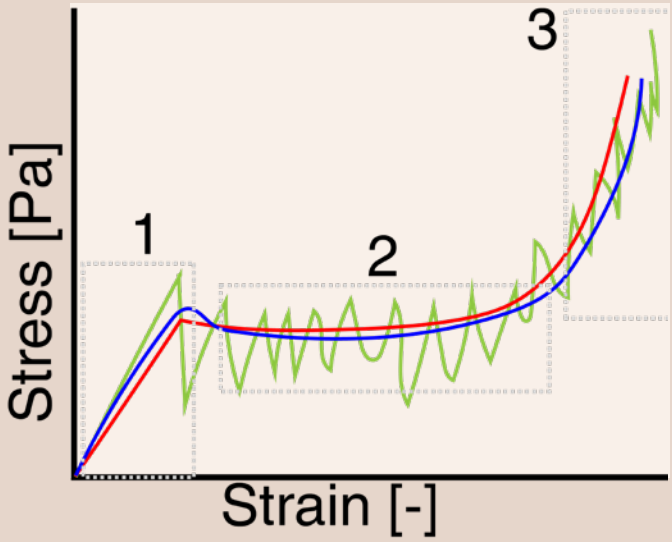

Figure 5.1.2: Stress-Strain curve of foam samples in compression. 1 represents the linear elasticity, 2 represents the plateau, 3 represents the densification. The red line is for elastomeric foam samples, blue is for elastic-plastic foam samples and green is for brittle foam samples. Image adapted from Gibson & Ashby, 1997

In addition to the material, the type of foam can also influence the behaviour of the sample, see Figure 2.1.1 in Chapter 2. With open-cell foams, the compressive force exerts on the struts of the foam, causing them to buckle (Gibson & Ashby, 1997). In the case of most closed-cell foams, the cell-faces that connect the struts are so thin that they do not really contribute to the stiffness. Therefore, making the cell edges the main contributors to the overall stiffness (Gibson & Ashby, 1997). Some closed-cell foams however, do contain a lot of the material in the cell-faces, and can contribute to the stiffness (Gibson & Ashby, 1997). Another difference between closed- and open-cell foams, is that closed-cell foams can behave differently in compression due to the compression of a fluid, usually a gas, within the cells of the foam. This gives an additional force that can resist the compression (Gibson & Ashby, 1997).

5.1.3 Measuring the forces of foams in compression

Gibson & Ashby (1997) argue that constructing energy absorption graphs can be a promising method for choosing the right material for impact absorbing applications. These graphs provide an overview of all the relevant material properties important to energy absorption. The energy absorption graph is a function of peak-stress, strain-rate, density, and foam type that is summarized within a unified plot. To be able to construct this graph, a prerequisite is to construct a stress-strain curve until the densification part (Gibson & Ashby, 1997). The moment of densification is chosen by finding the highest absorbed energy to stress (W/σ) ratio (Fuss et al, 2015). By calculating the area under the curve up until densification, the energy absorption graph can be constructed. The absorbed energy (W) is plotted against the stress (σ). Figure 5.1.3 shows the described steps using graphs. The found values for the energy that is absorbed are normalised with the elasticity modulus of the solid material. This is important for constructing these graphs since the strain-rate dependence is removed, and different materials can be plotted in the same graph (Gibson & Ashby, 1997). The highest W/σ ratio provides the highest absorbed energy for the minimum applied stress (Fuss et al, 2015),

known as the shoulder point. This point is used for energy absorbing applications since it maximises the absorbed energy while minimising the amount of stress (Fuss et al, 2015). This point is usually just before the densification of the material, therefore giving $\sigma_{densification} = \sigma_{peakstress}$(Gibson & Ashby, 1997). By testing several densities of the foam at one strain-rate, an envelope can be drawn from the energy absorption graphs. This line that is retrieved indicates the maximum envelope of peak stress the material can handle before densification (Gibson & Ashby, 1997). This process is repeated for different strain-rates to create a more complete view of the material properties. The energy absorption graphs can also be constructed for different temperatures (Gibson & Ashby, 1997).

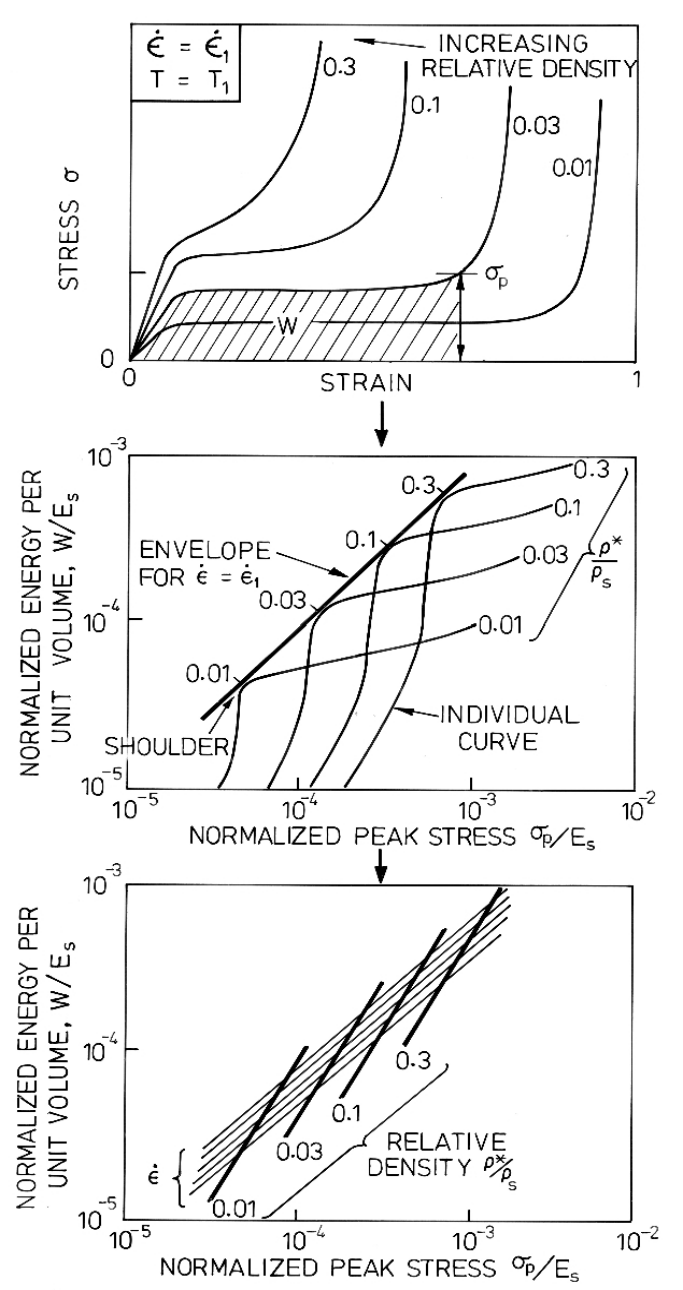

Figure 5.1.3: The steps for converting a stress strain curve into an energy absorption curve (image from Gibson and Ashby, 1997)

5.2 Research questions

The goal of this initial research is to compare the foaming PLA foam with the EPS, this gives an idea of the feasibility of using 3D printed foamed PLA as an impact absorbing material. When considering the information from Chapter 2, Section 2.1.1 and the microscopic images from Damanpack et al (2021), Figure 5.2.1, the conclusion can be made that the foaming PLA is a closed-cell foam. EPS is also a closed cell foam (Ansys, 2022d). Taking in consideration the goal of comparing the materials, as well as the feasibility for the envisioned application, the research questions are:

Is the foamed PLA able to absorb a similar amount of energy as the already existing EPS used in a helmets?

How will the foamed PLA deform under compression?

What advantage does the foamed PLA have over the not foamed PLA?

To be able to quantify the first research question, the strain-rate and density are set as boundaries. Within these boundaries, the different foaming PLA samples can be compared to the EPS. The strain must not be lower than that of EPS with a tolerance of 0,05 [-], otherwise the material will not deform enough to be able to absorb enough energy in the form of deformation. Ideally, the samples should not have a higher relative density than 0,1, otherwise the helmet with foaming PLA will become heavier than existing helmets. The value of 0,1 was chosen since the relative density of the EPS is 0,06.

5.3 Method

To be able to answer the research questions, a compression test is conducted in which samples are tested under different strain-rates. The methods used by Ashby and Gibson (1997) and van den Hazel (2015) are used as guides for the compression experiment. The goal of this experiment is to be able to retrieve the shoulder points from the energy absorption graphs to see how they compare to the EPS. This section will consist of the following parts: Printing the parts (5.3.1), compression testing (5.3.2) and data analysis (5.3.3).

5.3.1 Printing test samples

To be able to understand to what extent the 3D printed foaming PLA was comparable to EPS, a pilot test was conducted. The results of this test can be found in Appendix 5 . From this pilot test, the conclusion was drawn that printing with 100% infill yields compressive strains and densities that are too high in comparison to the EPS foam. EPS reached a maximum force that was not higher than 130 N, whereas the lowest force for PLA was above 1000 N. As a result, adjustments were made to generate samples that were similar to the samples made from EPS. It was also found that under these printing conditions, the amount of foaming was lower in the 220 °C samples. Therefore, for the final test, the temperature of 250 °C was used to ensure that foaming would occur. The dimensions of 13 mm x 13 mm x 26 mm were chosen according to ASTM (2016) for the testing samples. It was ensured that the samples did not buckle, as described in Section 5.1.1. Table 5.3.1 shows an overview of the defined print parameters.

Table 5.3.1, Printing parameters for the benchmarking experiment of the foaming PLA

Printer Model	**UM3**
Printing profile	**Generic PLA**
Printcore	**AA 0,4**
Nozzle Temperature [°C]	190 or 250
Bed Temperature [°C]	60
Fan Speed [%]	100%
Flow rate [%]	100% or 49%
Wall line count [-]	0
Top and bottom layers	2
Layer height [mm]	0,2
Printing Speed [mm/s]	25
Initial layer speed [mm/s]	15
Brim Width [mm]	7
Brim Speed [mm/s]	15
Printing orientation	XZ, See Figure 5.3.1

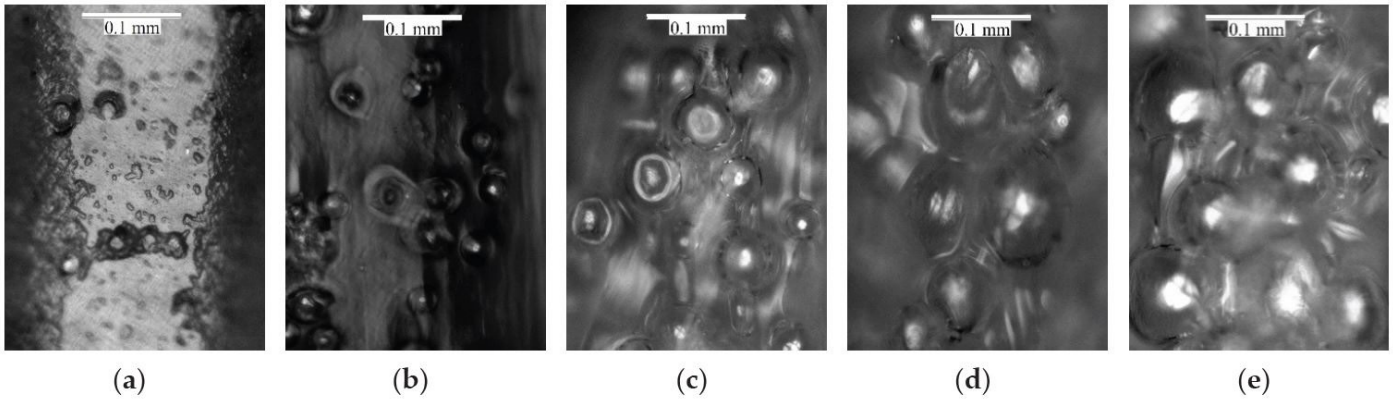

Figure 1. Microscopic images of 3D printed samples in different printing temperature: (**a**) 215 °C, (**b**) 220 °C, (**c**) 225 °C, (**d**) 230 °C, (**e**) 250 °C.

Figure 5.2.1, Microscopic images of 3D printed foaming PLA (Image from Damanpack et al, 2021).

Table 5.3.2 shows the differences between the variable printing settings for each printed sample. Each sample was printed nine times, to accommodate for three different strain-rates resulting in a total of 64 samples. Nine EPS samples were cut out with a knife of an existing helmet liner. It was chosen deliberately to cut the samples with a knife, since van den Bosch (2006) found that EPS' material structure changes when it is cut with heat. The necessary infill was calculated to create samples that were similar to the relative density of the EPS. Two samples were created that were similar to the EPS, the main difference was that one was foamed and the other was not. To gain a broader understanding of the effects of the relative density and the infill amount, a sample with high relative density, one in between the lowest relative density were printed. The different relative densities that were printed are shown in Table 5.3.2. All the samples were printed without walls, in the XZ-direction to test the density and infill. A top and bottom layer were printed as well, to provide a flat surface and an equal distributed load. Figure 5.3.1 illustrates the printing orientation of the samples.

The dimensions of each printed sample was measured three times using a digital calliper with an accuracy of 0,01 mm. The samples were weighed three times using the Kern ABT 320-4M scale which has an accuracy of 0,1 mg. From these measurements the mean height, width, depth, and weight were used to calculate the volume and density of the sample. The density of the sample was calculated using:

$$\rho = \frac{m}{V}$$

With:

ρ = Density [kg/ m^3]

V = Volume [m^3]

M = Weight [kg]

The relative density of the sample was calculated using the formula presented in Chapter 2, Section 2.1.1. To be able to calculate the amount of infill needed for the samples, to obtain the desired relative density, first samples were printed with 100% infill and the corresponding amount of flow rate. These samples were measured and weighed to obtain the relative density. The final densities for the test samples can be found in Appendix 6. The following formula was used to calculate the amount of infill needed to obtain a desired relative density:

$$Infill = \frac{100\% * (\frac{\rho^*}{\rho^s})_n}{(\frac{\rho^*}{\rho^s})_{100}}$$

With:

$(\frac{\rho^*}{\rho^s})_n$ = *desired relative density*

$(\frac{\rho^*}{\rho^s})_{100}$ = *Known relative density*

Table 5.3.2 The variable settings per printed foaming PLA sample

Temperature	Infill	Flow	Calculated relative density
190	6	100	~0,1
190	21	100	~0,2
190	42	100	~0,4
250	6	49	~0,01
250	12	49	~0,1
250	41	49	~0,2
250	80	49	~0,4
EPS	-	-	~0,1

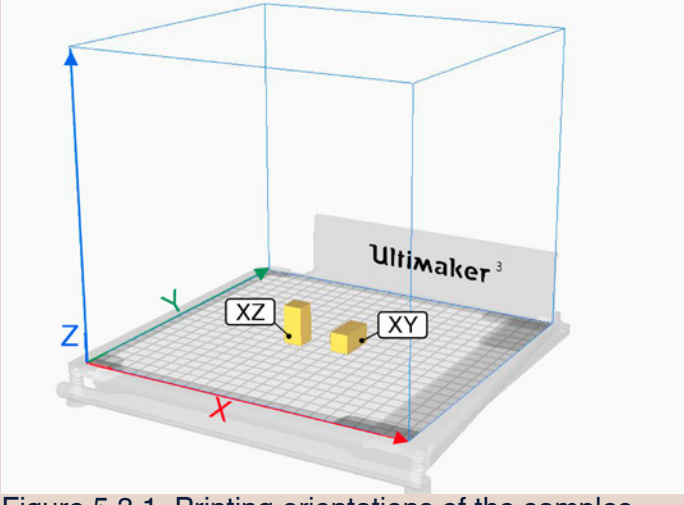

Figure 5.3.1, Printing orientations of the samples

5.3.2 Compression testing

The samples of different densities were tested under compression in the Zwick//Roell Z010 machine with 10kN loadcells, Figure 5.3.2. Three different strain-rates were chosen to test the different densities. The maximum strain-rate was calculated by using the following formula:

$$\epsilon^*(t) = \left(\frac{L(t) - L_0}{L_0}\right) * \frac{d}{dt} = \frac{1}{L_0} * \frac{dL(t)}{dt} = \frac{v(t)}{L_0}$$

With:

ϵ^*(t) = Strain-rate [s^{-1}]

L(t) = The length of a sample at a certain moment in time [m]

L0 = The length of the sample at t = 0 [m]

v(t) = The speed at which the ends of the sample move to/from each other [m/s]

With a maximum crosshead speed of 1000 mm/min (Zwick//Roell, n.d.) and the height of the sample being 26 mm, the maximum strain-rate is 0,64 s-1. Two speeds with a magnitude of 10 lower, were chosen, which is 0,064 s-1 and 0,0064 s-1. Since the machine worked with %/s the values were multiplied by 100%. This gives 64 %/s, 6,4 %/s and 0,64 %/s respectively. The samples were tested until they reached 80% strain or densification. The rest of the machine settings can be found in Table 5.3.3.

5.3.3 Data analysis

The data was analysed in MATLAB and Excel. Excel was used to clean up the data and calculate the stress and strain of the samples. First, the three datasets for each sample were averaged. With the initial measurements of the cross sections and the height, the stress and strain values were calculated. The resulting dataset was cleaned by removing negative values at the beginning. After the densification was reached or 20,8 mm deformation, the machine does not measure higher values anymore, and the values will decline. These declining values after the maximum were also removed from the dataset.
Energy absorption graphs were created in MATLAB using the cleaned data. First, the amount of energy absorbed was calculated. To get the amount of energy absorbed, the area under the energy absorption graph was calculated using the trapezoidal rule:

$$\int_{x_a}^{x_b} f(x)dx = \sum \frac{f(x_{n-1}) + f(x_n)}{2} * \Delta x_n$$

In our case, the x values represent the strain, and the function is the stress. Then, the W/σ ratio was calculated for each point. From the resulting dataset, the highest ratio was found. The index was taken from this value to be able to get the stress and strain at the shoulder point.

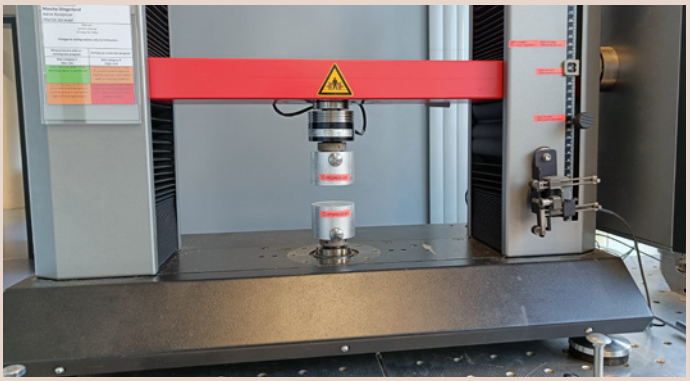

Figure 5.3.2, Zwick//Roell universal testing machine with 10 kN loadcells for compression.

Table 5.3.3 Zwick//Roell machine settings

Machine settings	Values
Loadcells [kN]	10, for compression
Strain-rates [%/s]	64 - 6,4 - 0,64
Maximum deformation (@ 80% strain) [mm]	20,8
Upper force limit [kN]	9

5.4 Results

The results section is split up into two parts. The first part focusses on the material properties of the different samples by presenting the shoulder points and the normalised energy absorbed (5.4.1). The second part will address the visual changes of the materials under compression (5.4.2).

5.4.1 Energy absorbed

Figure 5.4.1 and 5.4.2 show the highest W/σ ratio and the highest amount of energy absorbed at that ratio, plotted against the strain of the samples. Table 5.4.1 holds the individual values for these points. Refer to Appendix 6 for the stress-strain graphs, the energy absorption graphs and a Table with all the values per individual sample. Figure 5.4.1 and 5.4.2 show that in terms of strain, the PLA was fairly close to the EPS. In terms of normalised absorbed energy, the foaming PLA was more similar to the EPS than the non-foaming PLA. The configuration that came closest to the EPS, was the sample printed at 250 °C with a relative density of 0,09. The PLA samples printed at 190 °C with a relative density of 0,19 and the sample printed at 250 °C with a relative density of 0,39 were the least similar to the EPS. Table 5.4.1 shows the exact values for the samples for the specific strain-rate.

Table 5.4.1, specific values for the different samples.

Temperature	**190**	**190**	**190**	**250**	**250**	**250**	**250**	**EPS**
Relative density measured	**0,19**	**0,26**	**0,43**	**0,09**	**0,10**	**0,22**	**0,39**	**0,06**
Strain-rate 0,64%								
W/σ - ratio	0,54	0,61	0,70	0,52	0,69	0,53	0,32	0,43
Strain@ densification	0,64	0,57	0,48	0,61	0,48	0,63	0,73	0,61
Normalised energy absorbed	0,40	1,02	2,18	0,08	0,10	1,00	3,94	0,14
Strain-rate 6,4%								
W/σ - ratio	0,52	0,62	0,60	0,51	0,94	0,51	0,34	0,42
Strain@ densification	0,58	0,54	0,64	0,59	0,51	0,61	0,75	0,61
Normalised energy absorbed	0,41	0,91	3,30	0,08	0,11	1,11	4,50	0,16
Strain-rate 64%								
W/σ - ratio	0,50	0,59	0,75	0,47	1,25	0,55	0,35	0,43
Strain@ densification	0,61	0,56	0,51	0,60	0,52	0,60	0,75	0,63
Normalised energy absorbed	0,42	0,81	2,72	0,09	0,11	1,16	4,86	0,18

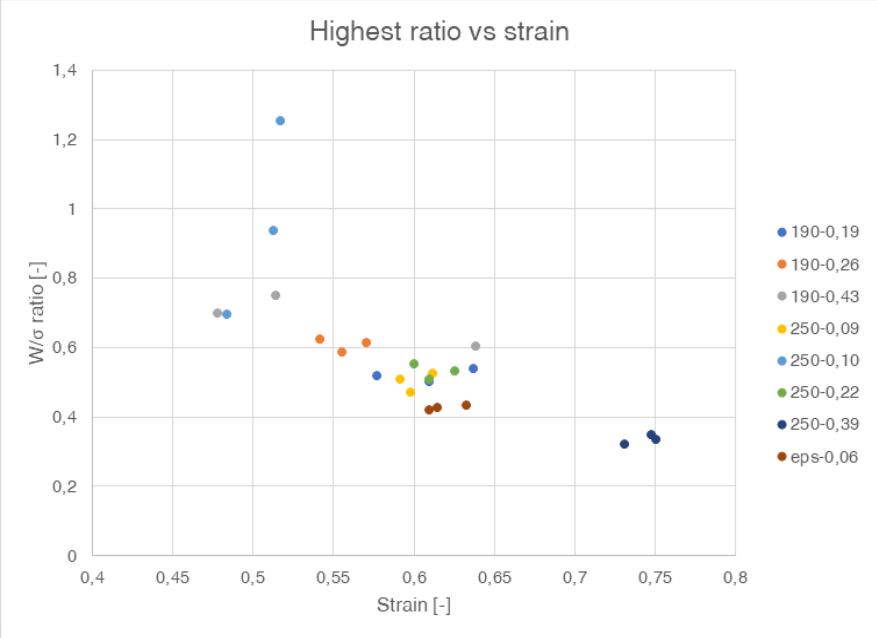

Figure 5.4.1, Highest W/ σ ratio plotted against the strain

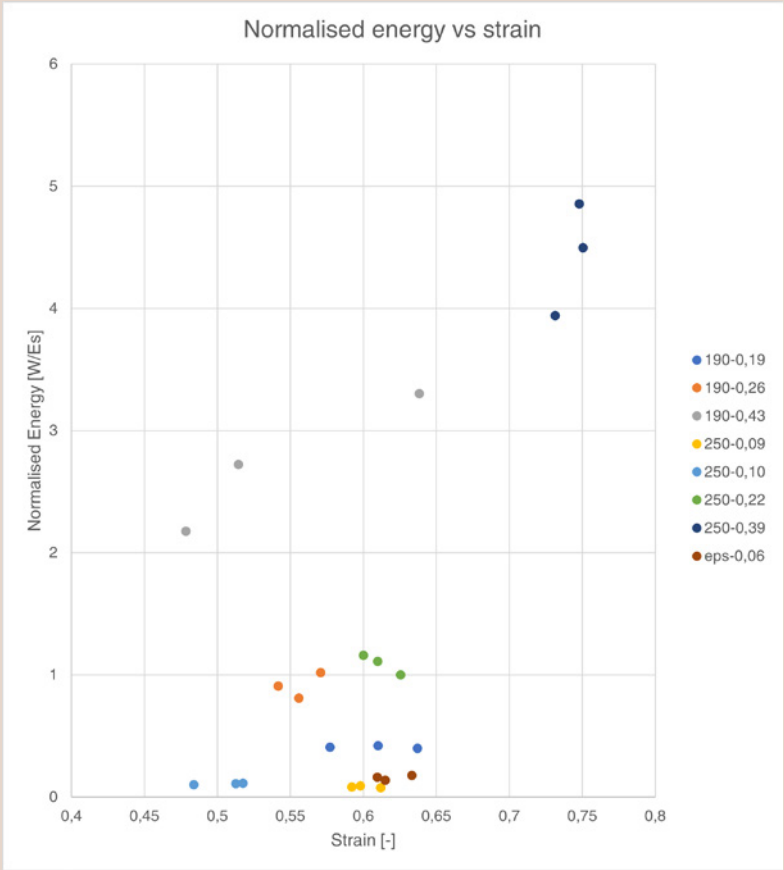

Figure 5.4.2, Highest normalised energy absorbed, shoulder point, plotted against the strain.

5.4.2 Visual deformation

Table 5.4.2 shows that the non-foaming PLA fractured, sometimes resulting in losse plastic pieces. The lightest PLA configuration sprung back a small amount after compression and also folded neatly in comparison to its non-foaming counterpart.

5.5 Discussion

It can be concluded from the results that the two foaming PLA samples with a relative density of 0,09 and 0,10 fell within the boundaries of strain and density. These foaming PLA configurations were also comparable to that of the absorbed energy and the W/σ ratio of EPS. The EPS foam had a W/σ ratio of around 0,43 -0,42 for all the strain-rates. The highest normalised energy absorbed for EPS was for the highest strain-rate, which is 0,18. For the PLA sample with a relative density of 0,09 the W/σ ratio ranged from 0,47 for the highest strain-rate and 0,52 for the lowest strain-rate. The normalised absorbed energy ranged from 0,09 for the highest strain-rate and 0,08 for the lowest strain-rate. For the foaming PLA with a relative density of 0,10 the highest strain-rate had a W/σ ratio of 1,25 and for the lowest strain-rate 0,69. The normalised energy absorbed for the highest strain-rate was 0,11 and for the lowest strain-rate 0,10 for the PLA with a relative density of 0,10. It can be said for both samples that if the strain-rate increased, the absorbed energy also increased. It is worth to note that the differences are fairly small. Therefore, testing with higher strain-rates will be needed to confirm if the amount of energy absorbed indeed increases with higher strain-rates for the two samples.

Between these samples, it can be said that the foaming PLA with a relative density 0,09 came closest to the EPS sample for the W/σ ratio. The 0,10 sample came closest to EPS in terms of normalised energy absorbed. Since the quantity of the W/σ ratio is strain (Fuss et al, 2015), this means that the foaming PLA with a relative density of 0,09 had a strain that is similar to the EPS. Therefore, the conclusion can be drawn that the foaming PLA sample with a relative density of 0,09 is the most similar to the EPS sample for the highest strain-rate.

The LW-PLA foam printed with 80% infill was an outlier in this dataset, since there was not a clear plateau part in the stress-strain curve (Appendix 6). This also caused the shoulder point to be calculated at the highest value of W. The plateau might have not been reached since the material was too stiff (Figure 5.1.1 (2)). Another reason could be, due to the fact that the density of the sample was quite high, the gas within the foam did not contribute much to the overall stiffness of the sample. The sample was dominated by the cell-walls collapsing (Gibson & Ashby, 1997), this causes a plateau that rises with strain.

Even though three strain-rates were tested, they were not that high. The maximum speed of the machine was 1000 mm/min which translates to 0,017 m/s. Therefore with the obtained data, it can only be concluded that the PLA sample with the lightest relative density is comparable to that of EPS from a motorcycle helmet. Due to the similar behaviour of the PLA to EPS at low relative densities, it is a promising material for further research for the application of a motorcycle helmet. For further research, a test according to the ECE-22 standard needs to be done to verify the safety.

What was not taken into account within this test was the pattern of the infill as well as the printing orientation. The infill and printing orientation also impact the absorbed energy. The infill can influence this since it could be seen as a macro-cellular structure, therefore different shapes can have different strengths. The printing orientation could also influence the absorbed energy since 3D printed materials are anisotropic (Ahn et al, 2002). This means that they have more strength in one direction than the other. Kanani & Kennedy (2022) found that if a sample is printed in the XY-direction, it was stronger than a sample printed in XZ-direction (Figure 5.3.1).

Another interesting observation that was made during this experiment, was that the foaming samples folded very neatly. Like a crumple zone in a car, the way the material folds can also influence the amount of energy that it absorbs. Therefore, it could be interesting to further research the folding mechanisms of the foaming material with different infills. For the

Table 5.4.2, Visual deformations of the tested samples under different strain rates					
Temperature	**Relative density**	**No strain**	**0,64 [%/s]**	**6,4 [%/s]**	**64 [%/s]**
190	**0,19**	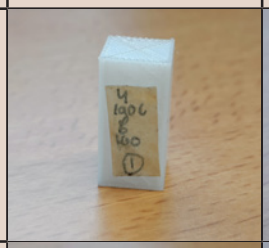	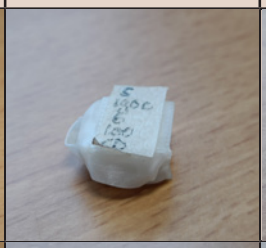		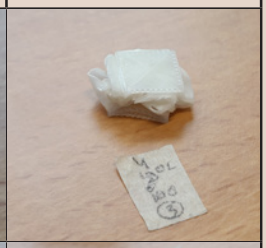
190	**0,26**			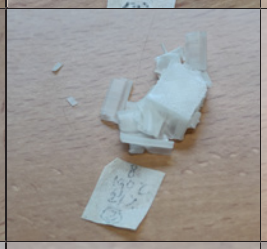	
190	**0,43**	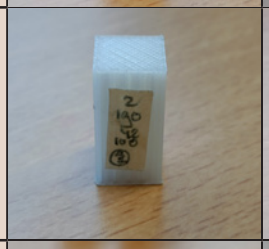	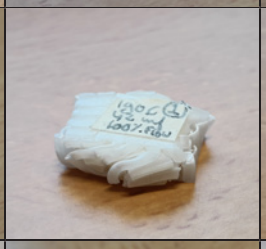	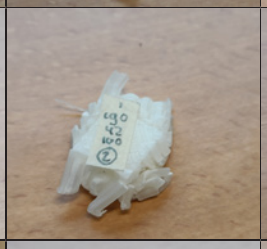	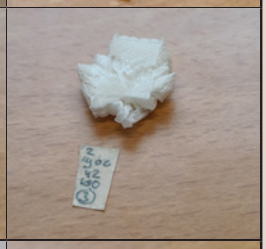
250	**0,09**	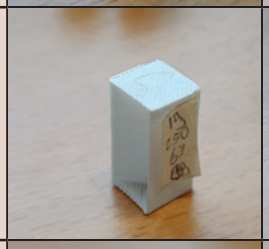			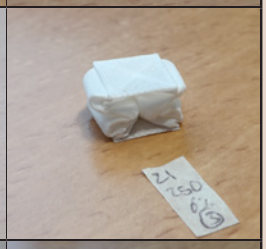
250	**0,10**			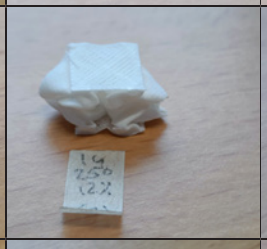	
250	**0,22**	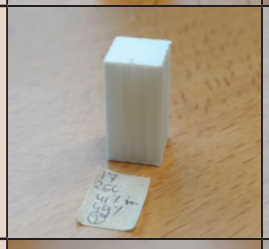	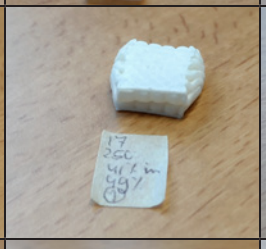	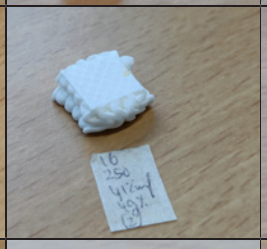	
250	**0,39**	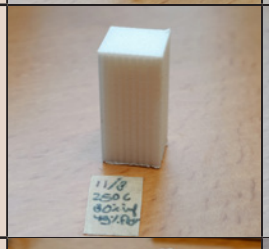		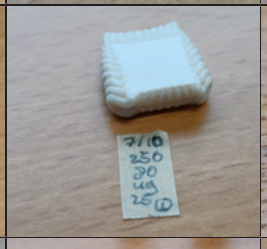	
EPS	**0,06**				

non-foaming samples, the walls did not fold as neatly as the foaming ones. These cracked and chips of the plastic came off. The ECE-22 standard mentions that the material used within a helmet visor should not produce any sharp splinters when it is shattered (UNECE, 2021). Non-foamed PLA may splinter when used in a high impact situation. This is not desirable, so therefore the non-foaming PLA is not suitable for helmet applications.
Lastly, the advantages of the foaming PLA over the non-foaming PLA became clear. The non-foaming PLA was too stiff and heavy for the envisioned application. Apart from this, the splintering is not desired

5.6 Conclusions and future work

This experiment had three goals, the first one is to investigate if the foaming PLA could reach similar energy absorbing properties as the EPS that is already used for motorcycle helmet liners. It can be concluded that the lightest foaming PLA samples (relative densities of 0,09 and 0,10) were able to reach similar values of the W/σ ratio and energy absorbed as values of the EPS. From the two, it was concluded that the sample with the relative density of 0,09 was the most similar to the EPS, due to the similar relative density, W/σ ratio and strain. The non-foaming PLA samples reached values which were too high, and they splintered under compression. The second goal was to investigate how foaming PLA would deform under compression. From the results was concluded that foaming PLA folds when a lower infill percentage was used. There was no splintering, which is desired for the motorcycle helmet application. Lastly, the advantage of foaming PLA over non-foaming PLA was investigated. It can be concluded that the non-foaming PLA splintered under compression and is too stiff which is not desirable for the application. Overall can be concluded that the foaming PLA sample with a relative density of 0,09 is comparable to the EPS. Therefore, it will be used within the demonstrator. It is strongly recommended to further investigate the use of foaming PLA within motorcycle helmets before applying it.
For future work it is interesting to further investigate the foaming PLA samples with a relative density of 0,09 and 0,10 for the helmet application. It is recommended that higher strain-rates are first researched before printing a complete helmet and drop-testing the material. The strain-rates within this experiment are not representative of the strain-rates within an situation as described in ECE-22. If the higher strain-rates also prove to still be similar to the EPS, impact testing can be done by printing bigger samples and testing these within a drop testing rig. It is recommended that the test setup has the conditions as described by ECE-22. It would also be interesting to further investigate different infill patterns to see their influence on the absorbed energy. To do this, the test within this chapter could be redone, but using samples with different infills. It is also recommended to test different temperatures that influence foaming densities of the foaming PLA, since only two variations were used (190 °C and 250°C). This can be done by printing more samples with different densities and testing them as described in the methods section, Section 5.3. Another recommendation is to create samples with variable amounts of foaming within one sample and test these as well. By combining different amounts of foaming, the impact case can be specifically designed. Lastly, it would be interesting to conduct this compression test on the other foaming materials, ASA and TPU to map their mechanical properties for compression.

6. Designing the lining of a motorcycle helmet

This chapter discusses the design process of creating the inner liners for a motorcycle helmet. First, the overall form is discussed (6.1) after which the development of the demonstrator is elaborated (6.2). The chapter ends with a summary and recommendations for further development (6.3).

6.1 Introduction

The compression experiment in Chapter 5 showed that the foaming PLA with a relative density of 0,09 had comparable properties to EPS. Therefore, a proof of concept will be made in which the inner lining of a motorcycle helmet is replaced with foaming materials. This concept will show that using the foaming materials for motorcycle helmets could be a future application. The parts that will be recreated are the impact absorbing layer as well as the comfort layer. The impact absorbing layer will be made using the foaming PLA. The comfort layer will be made from the foaming TPU. For proof of concept, it is chosen to cut a slice of an existing helmet, see Figure 6.1.1. From this slice the impact absorbing foam and comfort liner will be removed and substituted with the found configurations. Figure 6.1.2 shows a sketched overview of the concept.

The main advantage of 3D printing the inner lining of a motorcycle helmet is the fact that it can be customized to the head of the user as was discussed in Chapter 4. Summarized, if a customer's head is 3D scanned, a personalised liner can be created which is more comfortable. The price can also be reduced, by the 3D scanning and locally manufacturing on demand.

Figure 6.1.1: The helmet that will be used as base for the demonstrator.

6.2 Developing the 3D printed liners

To develop the demonstrator, several steps were taken. These steps are discussed in separate sections. First, the process of the 3D-modelling is discussed (6.2.1), followed by 3D printing (6.2.2) and finally, the assembly (6.2.3).

6.2.1 Prepping the existing helmet and 3D modelling

The helmet that was used as a base, was purchased at a second-hand shop. The impact liner was used for the compression test mentioned earlier in the report, in Chapter 5. First, the foam and comfort liner were removed from the helmet to obtain an empty shell. This shell was cut in half with a figure saw of which it was cut in half again. The result, a quarter of a helmet shell.

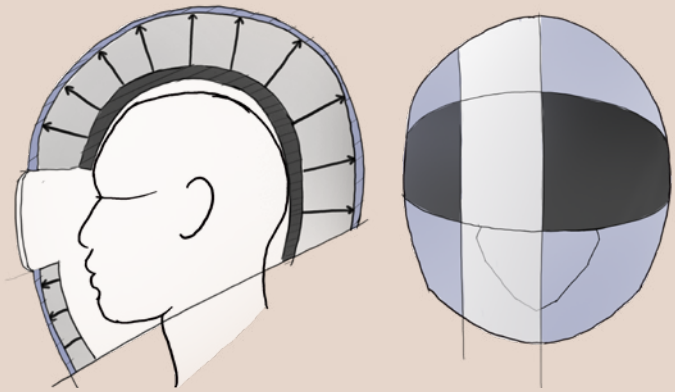

Figure 6.1.2: Sketch illustrating which part of the helmet will be used for the demonstrator, in white. The arrows represent the direction of the infill.

To be able to model the inner linings for the helmet, the obtained slice was 3D scanned using the scaniverse app on an iPad pro with a lidar. The model that was obtained using the scaniverse app was cleaned using mesh mixer. Irregularities such as the table on which the model was scanned among others were removed. To obtain a geometry from the scanned model, the SOLIDWORKS add-in “scan to 3D” was used. With this add-in the holes in the 3D scan could be filled after which surfaces could be obtained. From these surfaces, curves were retrieved which were used to model the new liner with. The overall workflow can be seen in Figure 6.2.1.

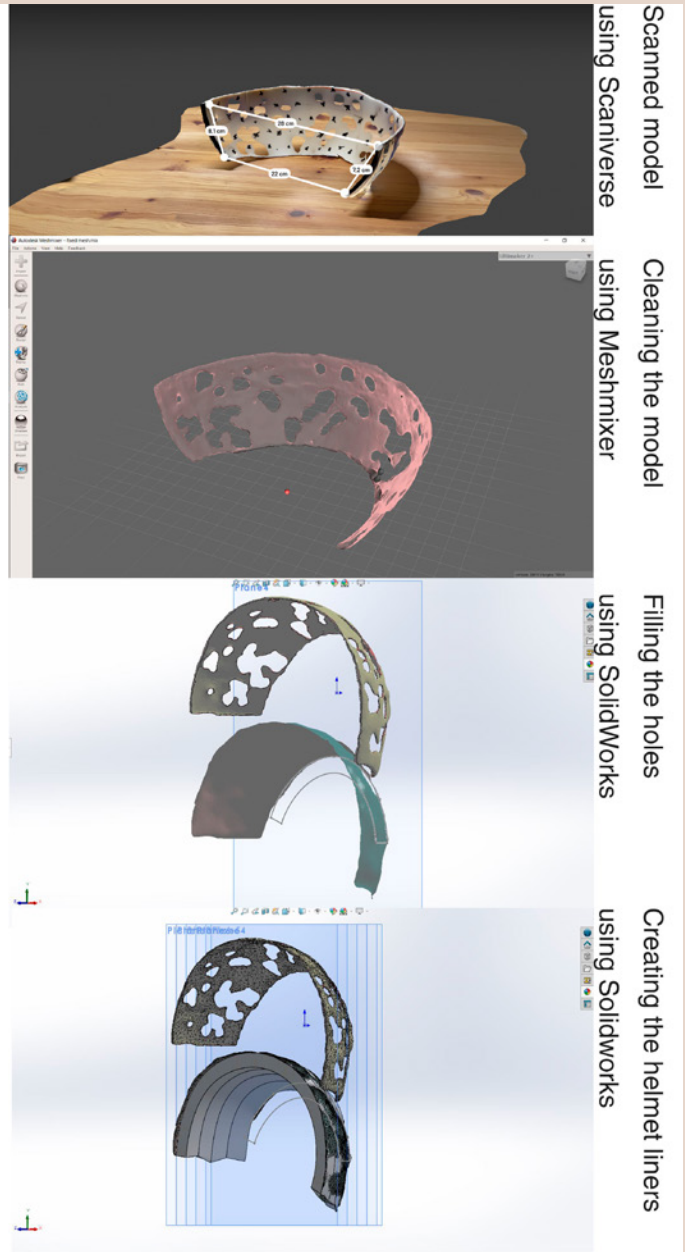

Figure 6.2.1: Workflow of 3D modelling the helmet liners for the helmet slice

The thicknesses of the two liners were chosen by measuring the liners of existing helmets. The measurements of these liners can be found in Appendix 7. The measurements made in Appendix 7 show that the comfort liner in specific varies a lot around the head. For ease, the measurement of 12 mm was used throughout the model, with a taper at the smaller side of the shell for the comfort liner. For the impact liner a consistent thickness of 20 mm was used.

6.2.2 3D printing

To make sure the impact liner was printed in the right orientation, the model was sliced in four separate parts, Figure 6.2.2. This enabled separate pieces to be orientated in such a way that the infill would be perpendicular to the head as tested, Figure 6.1.2. Figure 6.2.3 shows the sliced model with the correctly orientated infill. It is important that the infill is orientated like this, otherwise the results from the last experiment do not apply.

For the comfort liner it was more important that it was soft and comfortable, therefore the gyroid infill was used with an infill of 10%. This gave the final printed part a softer feel, so it was able to mimic the comfort liner. For the foaming TPU it was important that the material was not retracted much, since this can cause the nozzle to clog. To reduce the amount of retraction, the decision was made to print only one outer wall, and to print without supports. An initial test print showed that printing a foaming TPU model at 210 °C , which is the temperature at which the most expansion was found, resulted in too much pressure in the extruder and failed prints. To reduce the amount of pressure that builds up within the nozzle, and ensure that the model is printable, the decision was made to print with 240 °C. The overall printing settings can be found in Table 6.2.1.

Table 6.2.1, Printing parameters for the benchmarking experiment of the foaming PLA

	Foaming PLA	**Foaming TPU**
Printer Model	**UM3**	**UM3**
Printing profile	**Generic PLA**	**Generic TPU 95A**
Printcore	**AA 0,4**	**AA 0,8**
Nozzle Temperature [°C]	250	240
Bed Temperature [°C]	60	20
Fan Speed [%]	100%	100%
Flow rate [%]	49%	65
Wall line count [-]	2	1
Top and bottom layers	2	2
Layer height [mm]	0,2	0,2
Printing Speed [mm/s]	25	25
Initial layer speed [mm/s]	15	15
Infill	6%	10%
Infill pattern	Grid	Gyroid

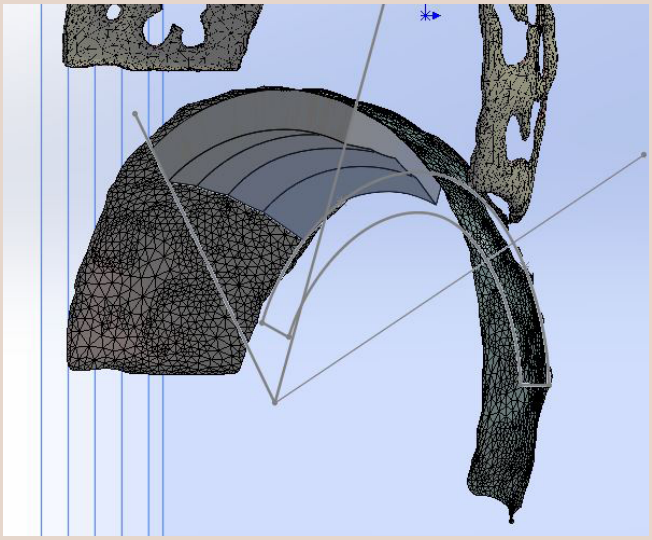

Figure 6.2.2: The grey lines indicate cuts in the 3D model to enable the correct printing orientation.

6.2.3 Assembling the model

To be able to assemble the model, the separate parts were first connected together with each other using Bison Polymax. After which, the foaming PLA models were connected to the outer shell, this was followed by the foaming TPU models which were connected to the PLA. To show that the TPU is the comfort layer, the outer two foaming TPU parts were covered in fabric, the other two parts were left blank to show the foaming TPU. For showing the inside of the printed parts, one piece of the foaming PLA and TPU were not glued within the helmet. The top layer of the foaming PLA part was carefully removed to expose the infill. For the foaming TPU model the side that was facing outward was removed to expose the gyroid infill. These pieces can slide in and out of the helmet, Figure 6.2.4. The final assembled model can be seen in Figure 6.2.4. Overall, the helmet slice was painted black.

6.3 Summary and recommendations for further development

Within this chapter the process of creating a helmet liner was discussed. First, an existing helmet was cut to obtain a part that could be used to create the new liners for. This part was 3D scanned to obtain

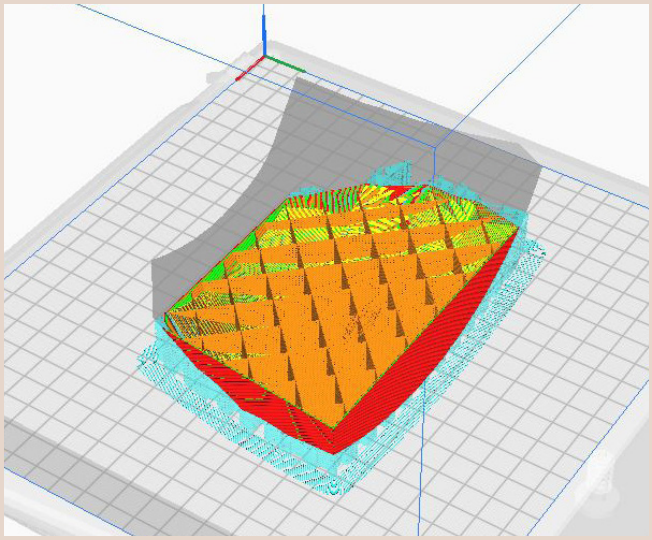

Figure 6.2.3: One of the parts of the impact liner sliced in Cura, with the infill correctly orientated.

the exact geometry. Meshmixer and Solidworks were used to clean the mesh, so a model could be created to fit the 3D scanned helmet part. The created models for foaming PLA and TPU were cut into quarters withing Solidworks to make sure they were printable. In particular for the foaming PLA it was important that the parts had the correct printing orientation for the infill. The printed parts were glued together, and one part of the foaming PLA and TPU were cut to reveal the infill inside. Fabric was added to the TPU liner to emphasize that it is a comfort liner.
To be able to further develop the concept of a 3D printed motorcycle helmet, some suggestions for future work can be made. As mentioned in Chapter 5, it is not clear if the foaming PLA can withstand the ECE-22 norms for motorcycle helmets. Therefore, the first recommended step for further developing this concept is to do more compression tests with higher strain rates. If the feasibility of foaming PLA at higher strain rates is confirmed, a drop test according to the ECE-22 norms can be done. For this test the entire inner linings, made out of PLA and TPU, will need to be printed and fitted within an existing helmet shell. Apart from testing the foaming PLA individually in the compression test, it could also be interesting to combine it with the foaming TPU, to investigate if it has any added benefit for the energy absorbing properties of the system. Prosperi (2021) found that adding a TPU cover to a foaming bicycle helmet improved the energy absorbing properties.
A limitation during the creation of the demonstrator was the fact that the helmet needed to be printed in several parts to orientate the infill as desired. An important development that needs to be done to be able to print the liners in one piece, instead of multiple, is make a slicer or create a plugin, that orientates the infill as defined by the user. At the moment of writing, this is not yet been integrated in any slicer that is available. Another approach of influencing the infill, is to add a cellular structure similar to the used infill on the inside of the 3D model before slicing. Software such as nTopology could be used. During slicing of this model, turn the infill from the slicer off, so the predefined infill can be printed. Moreover, the helmet liner could also be designed in such a way that it is safe to print in separate parts to accommodate the infill orientation.
Lastly, it could be a valuable direction to further investigate the energy absorbing properties of the foaming ASA and TPU for a motorcycle helmet, to do this the energy absorption tests from Chapter 5 can be repeated.
The development of a 3D printed motorcycle helmet could be interesting for companies such as Hexr (n.d.) and Kav Sports (n.d.) to explore further, since they already have experience with 3D printing of bicycle helmets.

Figure 6.2.4, The assembled demonstrator.

Conclusion

This last part of the thesis covers the conclusion, recommendations for further research and my personal reflection on the project.

7. Thesis conclusion

This chapter concludes the overall project. First, the project goals are repeated and the final results are evaluated by summing up the conclusions of each part of the thesis. This is followed by recommendations for future work and finally, a reflection on the project is given.

7.1 Conclusion

The goals of this thesis were as follows:

Get an understanding of existing knowledge about foaming materials for FDM printing.

Characterize the influence of printing parameters on the expansion of the foaming materials.

Propose and explore an application for the foaming materials for FDM printing.

By conducting literature research, several experiments and activities the aforementioned goals were achieved. The first goal was achieved through a literature review. First, an in depth review was given of the material properties of foaming materials outside the scope of 3D printing, to understand potential applications for the foaming materials for FDM printing. This was followed by an overview of the influence of five printing parameters on a final printed model, Table 2.2.1 (Chapter 2). Lastly, an overview was created of the known and unknown material properties for the three foaming materials, PLA, ASA and TPU, which can be found in Table 2.3.1 (Chapter 2). The existing applications within the literature were mapped for these materials to understand how the foaming materials could be applied.

The second goal was achieved, by researching the effect of: nozzle temperature, printing speed and flow rate, on the expansion of the materials. The results from these experiments gave a deeper understanding of the expansion of the materials, after which these could be used in the creation of the demonstrator. The found guidelines were summarized in Figure 3.6.1 (Chapter 3).

The third goal was achieved by proposing the application of using foaming PLA for the impact liner for motorcycle helmets. The compression testing indicated that foaming PLA with a relative density of 0,09 and 0,10 and an infill of 6% and 12% respectively were found to be close to the values of EPS, which is currently used in most motorcycle helmets. With this test, an overview of the material properties for foaming PLA in compression, were presented in Chapter 5. The foaming PLA with a relative density of 0,09 was applied within a demonstrator to present a proof of concept for using foaming materials in a motorcycle helmet. The knowledge from the printing parameter experiments were applied within the demonstrator. The infill needs to be perpendicular to the head, to obtain the same forces as in the compression test. This means that either the slicing software needs to be further developed, or the model needs to be adjusted to be able to print it.

Overall, it can be concluded that this thesis contributed to the knowledge of foaming materials for FDM printing. Firstly, Table 2.3.1 (Chapter 2) shows the available material properties of the foaming materials for FDM printing in the literature. From the table was seen that there are still many knowledge gaps for the material properties in tension and compression. Secondly, the influence of printing parameters were mapped and presented in Figure 3.6.1 (Chapter 3) were found. These guidelines can be used by designers to print with the foaming materials. The results from the compression experiment provide more insight into the compressive material properties of the foaming PLA, Figure 5.4.1, 5.4.2 and Table 5.4.1 (Chapter 5). Lastly, the application for the helmet showed that the foaming materials could be used within a motorcycle helmet.

Overall, this thesis investigated the printing parameters for foaming materials which were used to create samples with specific densities for a compression experiment. With the found printing parameters and results from the compression test a helmet demonstrator was created to show a possible application for the foaming materials for FDM printing. The obtained results in this thesis provide a starting point for further investigation of print parameters, material properties and applications of foaming materials. More concrete recommendations for future work are given in the next section.

7.2 Future work

For each goal, recommendations for future work can be made. First of all, due to the scope of this project, the focus was on foaming materials for FDM printing. For future work it could be interesting to investigate the printing parameters for other printers and foaming filament brands to see the difference in expansion between these. For example, an enclosure around the print bed affects the airflow, thus influencing the expansion of the material. For different brands of foaming filament, manufacturers can add different foaming agents to the materials, possibly causing different amounts of expansion, or even different behaviours.

Secondly, additional printing parameters could be further investigated to gain a better understanding on the influence of the expansion of the material, for example the influence of the bed temperature on the expansion of the first few layers of the material. Another printing parameter that could be investigated is the influence of the infill. For example, the influence of the expansion of the infill on the total part. It could be interesting to print the infill with a lot of foaming, and the outer layers without foaming to see how this would influence the final print. Following this, it is relevant to further investigate the material properties in compression and tension for the foaming materials discussed within this thesis, to get an even more in depth view of them. Table 2.3.1 (Chapter 2) can be used as starting point for identifying the knowledge gaps. By obtaining a more in depth view, it can become clear in which additional fields these materials could be useful.

Third, the material properties of the foaming PLA were only further investigated for different strain-rates under compression. It would be recommended to further investigate the compressional properties of the foaming TPU and ASA.

Fourth, since there was no impact test conducted, it cannot be said that the foaming PLA can definitely be used for motorcycle helmets. Therefore, it is recommended that first the compression test is repeated with higher strain rates, in order to verify if the material could be suitable for a motorcycle helmet application. After this is verified, a complete helmet could be created to test according to the ECE-22 standard.

7.3 Reflection on the project

In this section I would like to briefly reflect on my experience of conducting this project and what I have learned. First of all, one of my personal learning goals was to find out if doing research would be something I would enjoy. From this project, I got some insight into doing research which gave me some insights on whether to continue my academic career. I concluded that at this moment, I am not interested in continuing an academic career. I missed designing products until production, instead of staying conceptual. Maybe I will further pursue an academic career later, since I learned that I like investigating topics and trying to understand them.

I also learned that when planning a project, one can never have enough buffer around doing experiments. For the first temperature experiment, I had to redo it two times. For the other experiments I always had to do a pilot experiment before being able to conduct the final experiment. These pilot experiments really helped in understanding what the outcomes would be, and if needed I could adjust the experiment before conducting the final experiment. On the other hand, I also learned to just go with the flow. If something happens, then you have to learn to adjust your project accordingly. I think that was one of the toughest things I struggled with. I was sometimes so invested in my original planning that I did not always give myself enough time to step back and reflect. Even though I tried doing this by doing a weekly reflections, it might have been better to add in monthly reflections or reflections after a finished activity to really give myself the opportunity to think about what I had learned.

Besides, I learned that I really missed working within a team. Within a team, there are always others who understand the project as well as you do, and can help you brainstorm and plan the project. Within a graduation project, you become the expert about your topic. It is possible to brainstorm with your supervisors or peers, but no-one really understands it on a level you do. This can sometimes become a bit lonely. Even though, you conduct your graduation project alone, I learned that it is very important to have peers around you during your graduation. I think graduation would have been a lot more difficult if I did not have peers around me who were also graduating. We looked out for each other, and helped each other where needed. For example, by brainstorming together or discussing each other's plannings presentations.

Lastly, I learned that a graduation project is just a project. With this I mean that even though it is the end of your master education and a big milestone, you should not forget that it is still a learning opportunity. Therefore, for any student starting their graduation project, do not stress about it too much.

References

123-3D.nl. (n.d.). *Extruder 3D-printer onderdelen Nozzles 123-3d.nl.* Retrieved March 6, 2023, from https://www.123-3d.nl/3D-printer-onderdelen/Extruder/Nozzles-p13196.html

3D ninja. (n.d.). *Ultimaker s5*. Retrieved April 3, 2023, from https://www.3dninja.nl/product/ultimaker-s5/

571.218 Standard No. 218; Motorcycle helmets. (2022).

Agarwal, K. M., Shubham, P., Bhatia, D., Sharma, P., Vaid, H., & Vajpeyi, R. (2022). Analyzing the Impact of Print Parameters on Dimensional Variation of ABS specimens printed using Fused Deposition Modelling (FDM). *Sensors International, 3,* 100149. https://doi.org/10.1016/J.SINTL.2021.100149

Ahn, S., Montero, M., Odell, D., Roundy, S., & Wright, P. K. (2002). Anisotropic material properties of fused deposition modeling ABS. *Rapid Prototyping Journal, 8*(4), 248–257. https://doi.org/10.1108/13552540210441166

Alternate. (n.d.). *Creality Ender-3 S1 Plus 3d-printer.* Retrieved March 7, 2023, from https://www.alternate.nl/Creality/Ender-3-S1-Plus-3d-printer/html/product/1872310

ANSYS inc. (2022a). ASA (Extrusion, injection and blow molding) [Dataset]. In *Granta Edu pack 2022 R1, level 3* (22.1.2). ANSYS.

ANSYS inc. (2022b). PLA (general purpose) [Dataset]. In *Granta Edu pack 2022 R1, level 3 (22.1.2).* ANSYS.

ANSYS inc. (2022c). TPU (r) (molding) [Dataset]. In *Granta Edu pack 2022 R1, level 3* (22.1.2). ANSYS.

ANSYS inc. (2022d). Expanded PS foam (closed cell, 0.050) [Dataset]. In *Granta Edu pack 2022 R1, level 3* (22.1.2). ANSYS.

Arai. (n.d.). *One-Piece Multi-density EPS liners*. Retrieved March 7, 2023, from https://araiamericas.com/node/274

Ashby, M. F. (2016). *Materials Selection in Mechanical Design* (5th ed.).

Ashby, M., Shercliff, H. and Cebon, D. (2014) "*Materials: Engineering, Science, Processing and Design*", (3rd ed.). Elsevier, Butterworth-Heinemann.

Astm. (2016). *Standard Test Method for Compressive Properties Of Rigid Cellular Plastics* 1. https://www.astm.org/d1621-16.html

Avalle, M., Belingardi, G., & Montanini, R. (2001). Characterization of polymeric structural foams under compressive impact loading by means of energy-absorption diagram. *International Journal of Impact Engineering, 25*(5), 455–472. https://doi.org/10.1016/S0734-743X(00)00060-9

Bhavsar, P., Sharma, B., Moscoso-Kingsley, W., & Madhavan, V. (2020). Detecting first layer bond quality during FDM 3D printing using a discrete wavelet energy approach. *Procedia Manufacturing, 48*, 718–724. https://doi.org/10.1016/J.PROMFG.2020.05.104

Chen, X., & Lee, S. (2022a). Morphology and Compressive Property of 3D-printed 3-pointed Star Shape Prepared Using Lightweight Thermoplastic Polyurethane. *Fibers and Polymers.* https://doi.org/10.1007/s12221-022-4833-5

Chen, X., & Lee, S. (2022b). Physical Property of 3D-Printed N-Pointed Star-Shaped Outsole Prepared by FDM 3D Printer Using the Lightweight TPU. *Polymers, 14(15)*, 3189. https://doi.org/10.3390/polym14153189

ColorFabb. (n.d.-a). LW-ASA Black. Retrieved October 14, 2022, from https://colorfabb.com/lw-asa-black

ColorFabb. (n.d.-b). LW-PLA NATURAL. Retrieved October 14, 2022, from https://colorfabb.com/lw-pla-natural

ColorFabb. (n.d.-c). VARIOSHORE TPU BLACK. Retrieved October 14, 2022, from https://colorfabb.com/varioshore-tpu-black

ColorFabb. (2022a, October 27). Technical Datasheet LW-ASA. https://colorfabb.com/media/datasheets/tds/colorfabb/TDS_E_ColorFabb_LW-ASA.pdf

ColorFabb. (2022b, October 27). Technical Datasheet LW-PLA. https://colorfabb.com/media/datasheets/tds/colorfabb/TDS_E_ColorFabb_LW-PLA.pdf

ColorFabb. (2019, October 9). Technical Datasheet, Colorfabb Varioshore TPU. https://colorfabb.com/media/datasheets/tds/colorfabb/TDS_E_ColorFabb_varioShore_TPU.pdf

Damanpack, A. R., Sousa, A., & Bodaghi, M. (2021). Porous PLAs with controllable density by FDM 3d printing and chemical foaming agent. *Micromachines*, 12(8). https://doi.org/10.3390/mi12080866

Dainese. (n.d.). *What's a helmet made of?* Https://Demonerosso.Dainese.Com/Whats-a-Helmet-Made-Of#:~:Text=From%20just%20fiberglass%20in%20the,Helmet%20we%20are%20dealing%20with.

Daniel [ModBot]. (2021, November 13). *3d Printing Lightweight ASA (LW-ASA) Best Filament For Props & Cosplay?* [Video]. YouTube. Retrieved 22 September 2022, from https://www.youtube.com/watch?v=5eKimoriMJM&list=PLVa9HLpUaRf6faEOieiYQ-BZkvJf6O3sJ&index=8&ab_channel=ModBot

Dey, A., & Yodo, N. (2019). *Manufacturing and Materials Processing A Systematic Survey of FDM Process Parameter Optimization and Their Influence on Part Characteristics.* https://doi.org/10.3390/jmmp3030064

Dong, K., Ke, H., Panahi-Sarmad, M., Yang, T., Huang, X., & Xiao, X. (2021). Mechanical properties and shape memory effect of 4D printed cellular structure composite with a novel continuous fiber-reinforced printing path. *Materials and Design*, 198. https://doi.org/10.1016/j.matdes.2020.109303

Doshi, M., Mahale, A., Kumar Singh, S., & Deshmukh, S. (2022). Printing parameters and materials affecting mechanical properties of FDM-3D printed Parts: Perspective and prospects. *Materials Today: Proceedings, 50,* 2269–2275. https://doi.org/10.1016/j.matpr.2021.10.003

Doubrovski, Z., Verlinden, J. C., & Geraedts, J. M. P. (2011). Optimal design for additive manufacturing: Opportunities and challenges. P*roceedings of the ASME Design Engineering Technical Conference, 9*, 635–646. https://doi.org/10.1115/DETC2011-48131

Ellena, T., Mustafa, H., Subic, A., & Pang, T. Y. (2018). A design framework for the mass customisation of custom-fit bicycle helmet models. I*nternational Journal of Industrial Ergonomics, 64*, 122–133. https://doi.org/10.1016/J.ERGON.2018.01.005

Esun. (2022). Safety Data Sheet(SDS) According to GHS *Section 1-Identification of the substance/preparation and of the company/undertaking Product identifier Section 2-Hazards Identification.* https://www.esun3d.com/uploads/eSUN_ePLA-LW-filament_MSDS_V3.0.pdf

Esun. (2021). *ePLA-LW-light weight PLA) Technical datasheet.* https://www.esun3d.com/uploads/eSUN_ePLA-LW-Filament_TDS_V4.0.pdf

Fuss, F. K., Belbasis, A., van den Hazel, B., & Ketabi, A. (2015). Design Strategy For Selecting Appropriate Energy Absorbing Materials and Structures: Data Library and Customised Selection Criteria. P*rocedia Technology, 20*, 98–103. https://doi.org/10.1016/j.protcy.2015.07.017

Gibson, L. J., & Ashby, M. F. (1997). C*ellular Solids: Structure and Properties* (2nd ed.). Cambridge University Press. https://doi.org/10.1017/CBO9781139878326

Gotthans, J., Gotthans, T., & Marsalek, R. (2021, April 19). Prediction of Object Position from Aerial Images Utilising Neural Networks. 2*021 31st International Conference Radioelektronika*, RADIOELEKTRONIKA 2021. https://doi.org/10.1109/RADIOELEKTRONIKA52220.2021.9420193

Hermann, S. (2020a, February 15). C*olorFabb LW-PLA - Testing Foaming PLA.* CNC Kitchen. Retrieved October 13, 2022, from https://www.cnckitchen.com/blog/colorfabb-lw-pla-testing-foaming-pla

Hermann, S. (2020b, November 28). *Testing colorFabb varioShore TPU - Foaming 3D printing filament.* CNC Kitchen. Retrieved October 13, 2022, from https://www.cnckitchen.com/blog/testing-colorfabb-varioshore-tpu-foaming-3d-printing-filament

Hexr. (n.d.). *Hexr*. Retrieved April 5, 2023, from https://hexr.com/collections

Horvath, J. (2014). Mastering 3D Printing. *Mastering 3D Printing*. https://doi.org/10.1007/978-1-4842-0025-4

Igor Gaspar [My Tech Fun]. (2021, September 23). *LW-PLA vs LW-ASA by Colorfabb, which one is stronger?* [Video]. YouTube. Retrieved 22 September 2022, from https://www.youtube.com/watch?v=24jSxUJ0AT0&list=PLVa9HLpUaRf6faEOieiYQ-BZkvJf6O3sJ&index=5&ab_channel=MyTechFun

ISO/TC 261. (2021, November). *Additive manufacturing — General principles — Fundamentals and vocabulary* (ISO/ASTM 52900:2021(en)). https://www.iso.org/obp/ui/#iso:std:iso-astm:52900:ed-2:v1:en

Kaçergis, L., Mitkus, R., & Sinapius, M. (2019). Influence of fused deposition modeling process parameters on the transformation of 4D printed morphing structures. *Smart Materials and Structures*, 28(10). https://doi.org/10.1088/1361-665X/ab3d18

Kanani, A.Y., & Kennedy, A. (2022). Effect of the Material Extrusion Process Parameters on the Compressive Properties of Additively Manufactured Foamed and Nonfoamed Polylactic Acid Structures. *3D Printing and Additive Manufacturing*. https://doi.org/10.1089/3dp.2022.0091

Kanani, A.Y, Rennie, A. E. W., & Abd Rahim, S.Z.B. (2022). Additively manufactured foamed polylactic acid for lightweight structures. *Rapid Prototyping Journal*. https://doi.org/10.1108/RPJ-03-2022-0100

Kav Sports. (n.d.). *Kav Sports*. Retrieved April 7, 2023, from https://kavsports.com/pages/helmet-technology

Khan, S., Joshi, K., & Deshmukh, S. (2021). A comprehensive review on effect of printing parameters on mechanical properties of FDM printed parts. *Materials Today: Proceedings, 50*, 2119–2127. https://doi.org/10.1016/J.MATPR.2021.09.433

Kim, M. K., Lee, I. H., & Kim, H. C. (2018). Effect of fabrication parameters on surface roughness of FDM parts. *International Journal of Precision Engineering and Manufacturing, 19*(1), 137–142. https://doi.org/10.1007/s12541-018-0016-0

Knackmuhs, J. , Mayer, L. , Rouch, G. , & Whitehead, I. (2022). *Designing a Fixed-Wing 3D Printed Aircraft*. http://creativecommons.org/publicdomain/zero/1.0/

Kristiawan, R. B., Imaduddin, F., Ariawan, D., Ubaidillah, & Arifin, Z. (2021). A review on the fused deposition modeling (FDM) 3D printing: Filament processing, materials, and printing parameters. *Open Engineering, 11*(1), 639–649. https://doi.org/10.1515/eng-2021-0063

Loughborough University. (n.d.). *About additive manufacturing*. Retrieved November 22, 2022, from https://www.lboro.ac.uk/research/amrg/about/

Liu, B. C., Ivers, R., Norton, R., Boufous, S., Blows, S., & Lo, S. K. (2008). Helmets for preventing injury in motorcycle riders. *Cochrane Database of Systematic Reviews*. https://doi.org/10.1002/14651858.CD004333.pub3

Lu, G., & Yu, T. (2003). *Energy Absorption of Structures and Materials* (Vol. 1). Woodhead Publishing Ltd.

Lucci, C., Piantini, S., Savino, G., & Pierini, M. (2021). Motorcycle helmet selection and usage for improved safety: A systematic review on the protective effects of helmet type and fastening. *Traffic Injury Prevention, 22*(4), 301–306. https://doi.org/10.1080/15389588.2021.1894640

Marlinfw. (n.d.). M109 - *Wait for hotend temperature.* Retrieved March 7, 2023, from https://marlinfw.org/docs/gcode/M109.html

Michau, M. (2021). *Digital Design for Diabetes 3D Printing Variable-Density Diabetic Orthotics to Mitigate Lower-Limb Amputations in New Zealand Supervised by Simon Fraser and Tim Miller*. https://openaccess.wgtn.ac.nz/articles/thesis/Digital_Design_for_Diabetes_3D_Printing_Variable-Density_Diabetic_Orthotics_to_Mitigate_Lower-Limb_Amputations_in_New_Zealand/16681951

Nofar, M., Utz, J., Geis, N., Altstädt, V., & Ruckdäschel, H. (2022). Foam 3D Printing of Thermoplastics: A Symbiosis of Additive Manufacturing and Foaming Technology. *Advanced Science,* 9(11). https://doi.org/10.1002/ADVS.202105701

Nolan. (n.d.). *N100-5*. Retrieved April 5, 2023, from https://www.nolan.it/it/caschi-apribili/n100-5

Nurul Fazita, M. R., Abdul Khalil, H. P. S., Nor Amira Izzati, A., & Rizal, S. (2018). Effects of strain rate on failure mechanisms and energy absorption in polymer composites. In *Failure Analysis in Biocomposites, Fibre-Reinforced Composites and Hybrid Composites* (pp. 51–78). Elsevier. https://doi.org/10.1016/B978-0-08-102293-1.00003-6

Parrotte, M. (n.d.). *WHICH HELMET STANDARD IS THE BEST? SNELL, DOT, ECE, SHARP, OR FIM? WE RATE ALL 5*. Retrieved March 7, 2023, from https://agvsport.com/blog/which-helmet-standard-is-the-best-snell-dot-ece-sharp-or-fim.html#:~:text=There%20are%20four%20separate%20tests,some%20other%20motorcycle%20helmet%20certificates

Pérez, M., Medina-Sánchez, G., García-Collado, A., Gupta, M., & Carou, D. (2018). Surface quality enhancement of fused deposition modeling (FDM) printed samples based on the selection of critical printing parameters. *Materials, 11*(8). https://doi.org/10.3390/ma11081382

Pezutti-Dyer, F., & Buechley, L. (2022, February 13). Extruder-Turtle: A Library for 3D Printing Delicate, Textured, and Flexible Objects. *ACM International Conference Proceeding Series*. https://doi.org/10.1145/3490149.3501312

Polák, R., Sedláček, F., Raz, K., Polak, R., & Sedlacek, F. (2017). *Determination of FDM Printer Settings with Regard to Geometrical Accuracy.* 561–0566. https://doi.org/10.2507/28th.daaam.proceedings.079

Prosperi, G. (2021). *3D printing of a cycling helmet with bioinspired structure LW-PLA*. https://webthesis.biblio.polito.it/20169/

Polymaker. (2021). *Safety Data Sheet 1. Product and Company Identification*. https://cdn.shopify.com/s/files/1/0548/7299/7945/files/PolyLite_LW-PLA_SDS_US_EN_V1.1.pdf?v=1641783192

Qiao, P., Yang, M., & Bobaru, F. (2008). Impact Mechanics and High-Energy Absorbing Materials: Review. *Journal of Aerospace Engineering, 21*(4), 235–248. https://doi.org/10.1061/(asce)0893-1321(2008)21:4(235)

Ramli, R., & Oxley, J. (2016). Motorcycle helmet fixation status is more crucial than helmet type in providing protection to the head. *Injury, 47*(11), 2442–2449. https://doi.org/10.1016/j.injury.2016.09.022

Roof. (n.d.). *RO5 BOXER V8 MATT BLACK.* Retrieved April 5, 2023, from https://www.roof.fr/en/boxer-v8/406-ro5-boxer-v8-noir-mat.html

Shoei Europe. (n.d.). *SHOEI P.F.S. / Personal Fitting System.* Retrieved April 5, 2023, from https://www.shoei-europe.com/shop/en/shoei-p.f.s./personal-fitting-system#:~:text=The%20Personal%20Fitting%20System%20can,some%20models%20from%20previous%20generations.&text=The%20determination%20of%20the%20head,about%2020%20to%2030%20minutes.&text=The%20recommended%20retail%20price%20for%20the%20fitting%20is%2060%20EUR.

Siviour, C. R., & Jordan, J. L. (2016). High Strain Rate Mechanics of Polymers: A Review. *Journal of Dynamic Behavior of Materials, 2*(1), 15–32. https://doi.org/10.1007/s40870-016-0052-8

Snell Foundation. (2019). *STANDARD FOR PROTECTIVE HEADGEAR.* https://smf.org/standards/m/2020/M2020_Final.pdf

Soe, K. T., Zhang, Y. X., & Zhang, L. (2022). Material properties and high-velocity impact responses of a new hybrid fiber-reinforced engineered cementitious composite (ECC). In *Advances in Engineered Cementitious Composite: Materials, Structures, and Numerical Modeling* (pp. 77–120). Elsevier. https://doi.org/10.1016/B978-0-323-85149-7.00004-5

Solomon, I. J., Sevvel, P., & Gunasekaran, J. (2020). A review on the various processing parameters in FDM. *Materials Today: Proceedings, 37*(Part 2), 509–514. https://doi.org/10.1016/j.matpr.2020.05.484

Spoerk, M., Gonzalez-Gutierrez, J., Sapkota, J., Schuschnigg, S., & Holzer, C. (2018). Effect of the printing bed temperature on the adhesion of parts produced by fused filament fabrication. *Plastics, Rubber and Composites, 47*(1), 17–24. https://doi.org/10.1080/14658011.2017.1399531

Takahashi, H., & Miyashita, H. (2016). Thickness control technique for printing tactile sheets with fused deposition modeling. *UIST 2016 Adjunct - Proceedings of the 29th Annual Symposium on User Interface Software and Technology,* 51–53. https://doi.org/10.1145/2984751.2985701

Takahashi, H., & Miyashita, H. (2017). Expressive fused deposition modeling by controlling extruder height and extrusion amount. C*onference on Human Factors in Computing Systems - Proceedings, 2017*-May, 5065–5074. https://doi.org/10.1145/3025453.3025933

Tempelman, E., Shercliff, H., & van Eyben, B. N. (2014). *Manufacturing and Design* (1st ed.). Elsevier. https://doi.org/10.1016/C2011-0-08438-7

Topçu, I. B., & Unverdi, A. (2018). Scrap tires/crumb rubber. In W*aste and Supplementary Cementitious Materials in Concrete: Characterisation, Properties and Applications* (pp. 51–77). Elsevier. https://doi.org/10.1016/B978-0-08-102156-9.00002-X

Turner, B. N., & Gold, S. A. (2015). A review of melt extrusion additive manufacturing processes: II. Materials, dimensional accuracy, and surface roughness. In *Rapid Prototyping Journal* (Vol. 21, Issue 3, pp. 250–261). Emerald Group Holdings Ltd. https://doi.org/10.1108/RPJ-02-2013-0017

Ultimaker B.V. (2022). *Ultimaker Cura 5.10* (5.1.0). Ultimaker.

UNECE. (2021). *UN Regulation No. 22 - Rev.5 - 06 series | UNECE*. https://unece.org/transport/documents/2021/08/standards/un-regulation-no-22-rev5-06-series

Urréchaga, E. M., Kodadek, L. M., Bugaev, N., Bauman, Z. M., Shah, K. H., Abdel Aziz, H., Beckman, M. A., Reynolds, J. M., Soe-Lin, H., Crandall, M. L., & Rattan, R. (2022). Full-face motorcycle helmets to reduce injury and death: A systematic review, meta-analysis, and practice management guideline from the Eastern Association for the Surgery of Trauma. *The American Journal of Surgery, 224*(5), 1238–1246. https://doi.org/10.1016/j.amjsurg.2022.06.018

van den Bosch, H. L. A. (2006). *Crash helmet testing and design specifications*. https://doi.org/10.6100/IR613094

van den Hazel, B. (2015). *IMPACT MECHANICS OF HELMET COMPONENTS*. https://essay.utwente.nl/69908/1/CONF-Report_internship%20Bennie%20van%20den%20Hazel.pdf

Voordeelhelmen.nl. (n.d.a). *Shoei helme*n. Retrieved March 7, 2023, from https://www.voordeelhelmen.nl/allemerken/shoei-helmen/?p=2&product_list_order=price_asc

Voordeelhelmen.nl. (n.d.b). *X-Lite helme*n. Retrieved March 7, 2023, from https://www.voordeelhelmen.nl/allemerken/x-lite-helmen/

Williams, E., Long, S., Tatum, M., Anderson, D. D., & Thomas, G. (2021). *DMD2021-1034 DESIGNING A 3D PRINTED BONE SIMULANT FOR WIRE NAVIGATIONTRAINING*.http://asmedigitalcollection.asme.org/BIOMED/proceedings-pdf/DMD2021/84812/V001T01A002/6805505/v001t01a002-dmd2021-1034.pdf

Wu, J. (2018). Study on optimization of 3D printing parameters. *IOP Conference Series: Materials Science and Engineering, 392*(6). https://doi.org/10.1088/1757-899X/392/6/062050

Žarko, J., Vladić, G., Pál, M., & Dedijer, S. (2017). Influence of printing speed on production of embossing tools using FDM 3d printing technology. *Journal of Graphic Engineering and Design, 8*(1), 19–27. https://doi.org/10.24867/JGED-2017-1-019

Zhong, F., Liu, W., Zhou, Y., Yan, X., Wan, Y., & Lu, L. (2020). Ceramic 3D printed sweeping surfaces. *Computers and Graphics (Pergamon), 90*, 108–115. https://doi.org/10.1016/j.cag.2020.05.007

Zwick//Roell. (n.d.). *ProLine*. Retrieved March 7, 2023, from https://www.zwickroell.com/nl/producten/statische-materiaaltestmachines/universele-testmachines-voor-statische-toepassingen/proline/

Appendices

Designing and exploring an application for foaming 3D-printer filaments project title

Please state the title of your graduation project (above) and the start date and end date (below). Keep the title compact and simple. Do not use abbreviations. The remainder of this document allows you to define and clarify your graduation project.

start date 05 - 09 - 2022 17 - 03 - 2023 end date

INTRODUCTION **

Please describe, the context of your project, and address the main stakeholders (interests) within this context in a concise yet complete manner. Who are involved, what do they value and how do they currently operate within the given context? What are the main opportunities and limitations you are currently aware of (cultural- and social norms, resources (time, money,...), technology, ...).

There are different types of 3D-printers available on the market. The most popular printer is the fused deposition modeling (FDM) printer. The printer and its filament can be made relatively cheap, making it an accessible way for people to get into contact with 3D-printing. Companies are also using 3D-printing to make prototypes and such. Filament is the material that is used in FDM printers to print with. There are several types of filament on the market, usually made out of a certain type of plastic, which can be categorized in; professional, non-professional, filled, conductive biodegradable, and so on (All3DP, 2021). Therefore, FDM printing already provides a lot of opportunities for companies as well as hobbyists to print products with a wide range of filaments available, facilitating different material properties. Usually, the properties of the material do not change significantly during printing: the properties of the filament are roughly identical to the properties of the printed material. However, recent developments in filaments are bringing a change to this. A new category of filaments that expand (foam) during the printing process has become available. This creates the opportunity to creating a wide variety of printed material properties while using a limited set of filament.

The filaments that will be used during the project are LW-PLA, LW-ASA and VarioShore TPU from ColorFabb, of which the technical data sheets were released in 2019 and 2020 (ColorFabb, 2019a, ColorFabb 2020 & ColorFabb, 2019b respectively). As can be seen from the release years, these materials are fairly new and therefore not much is known about these filaments. These filaments have the ability to foam in a controlled manner due to the addition of a blowing agent (Hermann, 2020a). During this project the opportunities and limitations of this filament will be explored. The material comes out foaming from the nozzle and has different characteristics than non-foaming filaments. Since the materials are new, it is not yet well known what changing the printing process parameters have for effect on the material.

Due to the foaming characteristic, different applications could be explored such as, sound dampening, vibration dampening and transparentness among others. An interesting aspect of this filament is that it needs a certain nozzle temperature to start foaming. For all the materials this is around 230C (ColorFabbb, n.d. -a&b, ColorFabb 2020) under this temperature it almost does not foam, Figure 1. A foreseeable challenge due to the foaming nature of the material, is that it might be less controllable because it expands when it leaves the nozzle (ColorFabb, n.d.-a)

The stakeholders that could benefit from applications for this type of filament are (professional) users of 3D-printers. Currently, the suggested use for these filaments are for lightweight structures such as model planes or costumes. By investigating the effect of changing different parameters, a new meaningful application can be found.

(Sources can be found on the next page in Figure 2)

space available for images / figures on next page

introduction (continued): space for images

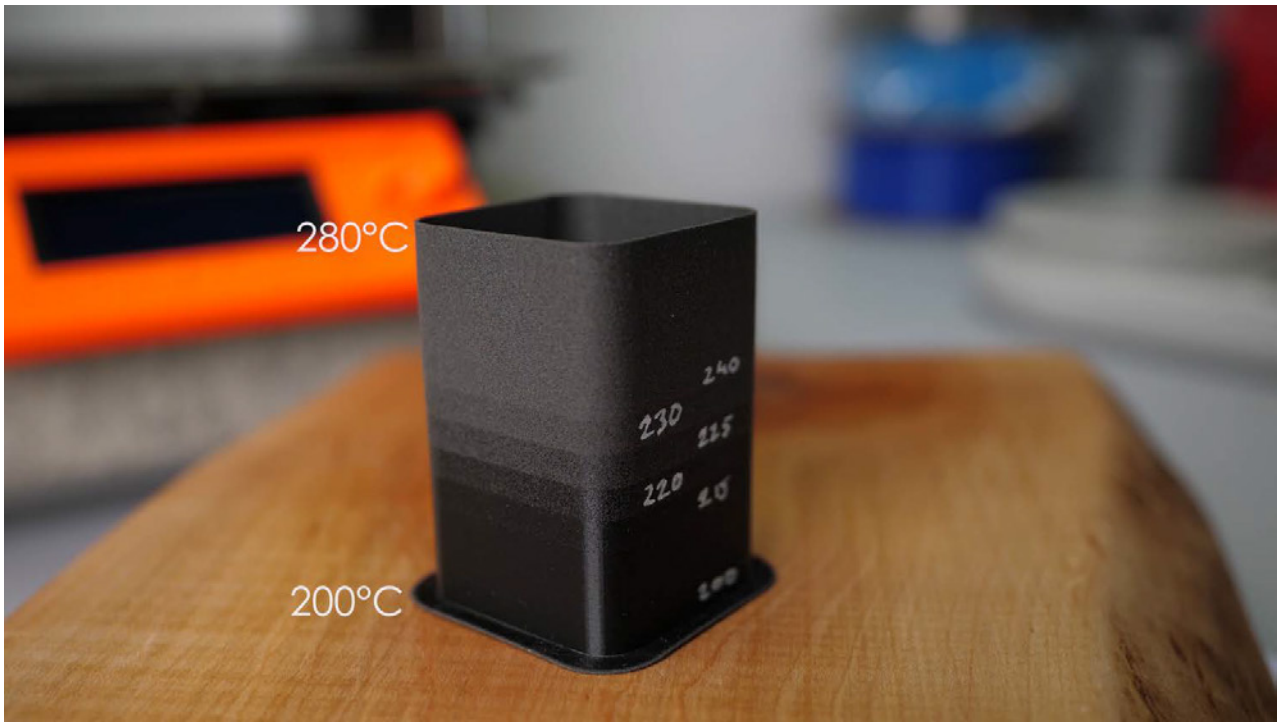

image / figure 1: Example of different stages of foaming for LW-PLA (Hermann, 2020b)

All3DP. (2021, December 27). *The Best 3D Printer Filament: The Types in 2022*. Retrieved 27 June 2022, from https://all3dp.com/1/3d-printer-filament-types-3d-printing-3d-filament/

ColorFabb. (n.d.-a). *LW-PLA GRIJS ZILVER*. Retrieved 27 June 2022, from https://colorfabb.com/nl/lw-pla-gray-silver

ColorFabb. (n.d.-b). *VARIOSHORE TPU BLUE*. Retrieved 27 June 2022, from https://colorfabb.com/nl/varioshore-tpu-blue

ColorFabb. (2019a, April 4). *Technical datasheet colorFabb LW-PLA* (v1.0) [This datasheet holds the technical data for LW-PLA]. ColorFabb. https://colorfabb.com/media/datasheets/tds/colorfabb/TDS_E_ColorFabb_LW-PLA.pdf

ColorFabb. (2019b, October 9). *Technical datasheet colorFabb varioShore TPU* (v1.0) [This sheet holds the technical data for the varioShore TPU]. ColorFabb. https://colorfabb.com/media/datasheets/tds/colorfabb/TDS_E_ColorFabb_varioShore_TPU.pdf

ColorFabb. (2020). *Technical datasheet colorFabb LW-ASA* (v1.0) [This sheet holds the technical data for LW-ASA]. ColorFabb. https://colorfabb.com/media/datasheets/tds/colorfabb/TDS_E_ColorFabb_LW-ASA.pdf

Hermann, S. (2020a, February 15). *A 4th dimension for 3D prints - Colorfabb Light-Weight, foaming PLA* [Video]. YouTube. https://www.youtube.com/watch?v=2tmgzwgi2UI&t=666s&ab_channel=CNCKitchen

Hermann, S. (2020b, February 15). *LW-PLA Temperature Test Tower* [Picture]. CNC Kitchen. https://www.cnckitchen.com/blog/colorfabb-lw-pla-testing-foaming-pla

image / figure 2: Sources used in the introduction

PROBLEM DEFINITION **

Limit and define the scope and solution space of your project to one that is manageable within one Master Graduation Project of 30 EC (= 20 full time weeks or 100 working days) and clearly indicate what issue(s) should be addressed in this project.

During this project, the goal is to research the possibilities of the foaming filaments. Because the foaming filaments are only out for three to two years now, not much research has been done on the applications of this filament. Therefore, the design goal is to find opportunities for the foaming filament.

During the project, the printing process parameters will be regarded. Since the filaments are very new, it is not yet known what influence these parameters have on the material. Examples of printing parameters are; Layer thickness, Infill, speed, orientation of the part, and extrusion temperature (Doshi et all, 2022 & Yadav et all, 2020).

LW-PLA, LW-ASA and varioShore TPU will be further researched. During the first weeks of exploration a choice is made to further continue with one of these three filaments. These materials will be researched using a printer which has the ability to extrude two filaments e.g. Ultimaker.

- Doshi, M., Mahale, A., Kumar Singh, S., & Deshmukh, S. (2022). Printing parameters and materials affecting mechanical properties of FDM-3D printed Parts: Perspective and prospects. Materials Today: Proceedings, 50, 2269–2275. https://doi.org/10.1016/j.matpr.2021.10.003
- Yadav, D., Chhabra, D., Kumar Garg, R., Ahlawat, A., & Phogat, A. (2020). Optimization of FDM 3D printing process parameters for multi-material using artificial neural network. Materials Today: Proceedings, 21, 1583–1591. https://doi.org/10.1016/j.matpr.2019.11.225

ASSIGNMENT **

State in 2 or 3 sentences what you are going to research, design, create and / or generate, that will solve (part of) the issue(s) pointed out in "problem definition". Then illustrate this assignment by indicating what kind of solution you expect and / or aim to deliver, for instance: a product, a product-service combination, a strategy illustrated through product or product-service combination ideas, ... In case of a Specialisation and/or Annotation, make sure the assignment reflects this/these.

The goals of this project are:
-1. In general explore the possibilities of the three aforementioned filaments.
-2. Develop a method and characterize the properties of the materials and processes.
-3. Design a demonstrator with one of the materials that can showcase the most interesting findings.

A literature study will be done on the properties of structures that also have a foaming structure, but are created using different technologies. These insights will be linked to the possible parameters of the printing process. Further practical experiments will feed into the search for possible applications and opportunities.
After this research phase and mapping the opportunities and applications, I will develop methods and characterize the most interesting properties of these materials. The most interesting material will be chosen to further continue with to make a demonstrator out of and to further investigate. At the end of the research phase, I expect to have characterized most of the properties of the material and what the influences are of the printing and process parameters.
At the end of the project I expect to deliver a demonstrator which can showcase my most interesting findings.

PLANNING AND APPROACH **

Include a Gantt Chart (replace the example below - more examples can be found in Manual 2) that shows the different phases of your project, deliverables you have in mind, meetings, and how you plan to spend your time. Please note that all activities should fit within the given net time of 30 EC = 20 full time weeks or 100 working days, and your planning should include a kick-off meeting, mid-term meeting, green light meeting and graduation ceremony. Illustrate your Gantt Chart by, for instance, explaining your approach, and please indicate periods of part-time activities and/or periods of not spending time on your graduation project, if any, for instance because of holidays or parallel activities.

start date 5 - 9 - 2022 17 - 3 - 2023 end date

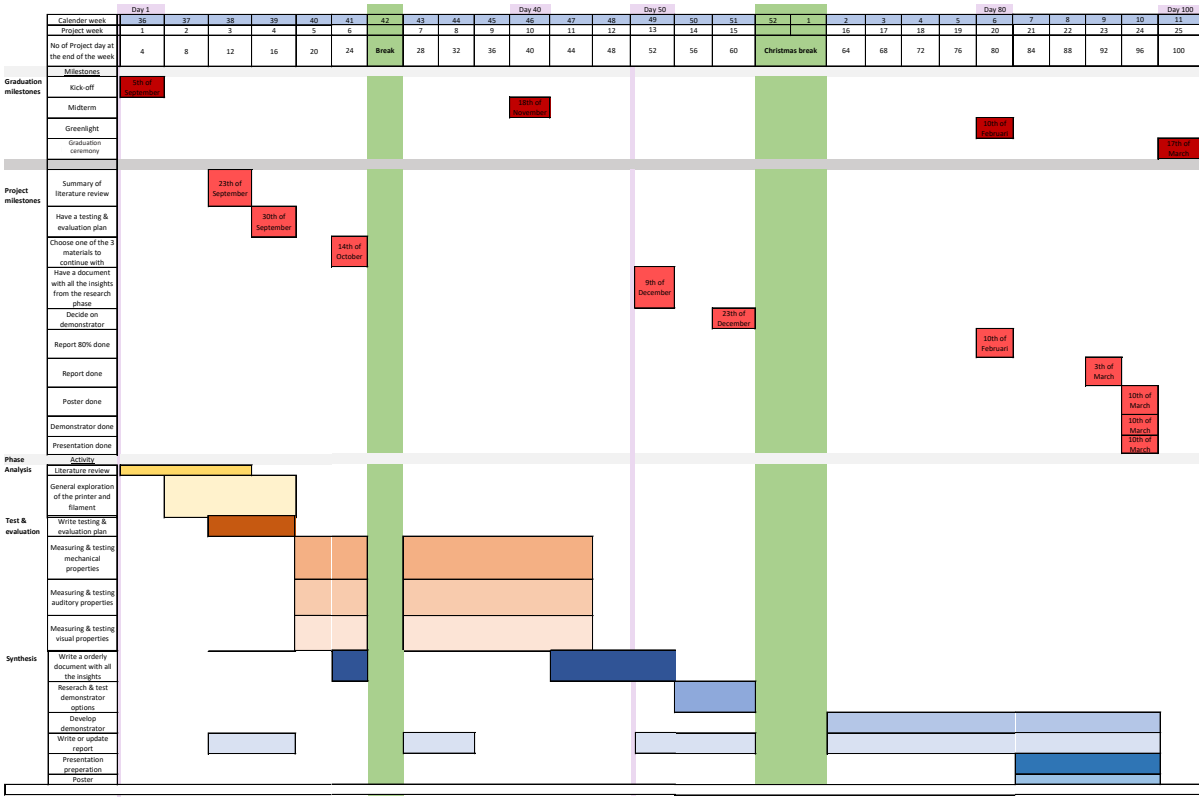

I will graduate part-time, therefore I will work on my graduation 4 days in a week. In the 4th row from the top, the number of graduation days at the end of the week are listed.

My general approach for this project is to do a process that is scrum and the double diamond model combined. That is why I also put in extra project related milestones. This is to keep myself on track and make sure I close each phase of the project. Each week I will asses what needs to be done to reach the nearest milestone and make a weekly, more detailed, planning. At the end of the week I will reflect on my activities and make a new week planning for the coming week. In past projects such as ACD and BEP this worked well for me and therefore I will continue this workflow.

The double diamond model is applied in such a way that when I arrive at a milestone I converge by documenting the phase I went trough and start with diverging for the next phase.
A short overview of each phase will be given:
- Analysis: This phase is to collect as much knowledge beforehand on the material as possible. I will also look into different fields where they use foaming material. During this phase I will also generally experiment with the printer and material to get familiar with it. It closes with a summary of the literature review and experimentation.
- Test & Evaluation: This phase is meant to test with the materials more in depth. The first two weeks are used to test with all three materials. At the end of these weeks a choice will be made to further investigate one material. This phase closes with a document that reports on all the insights.
- Synthesis : This phase is meant to develop a demonstrator in which I can showcase all the interesting properties of the material that I found. It closes with the final presentation, poster, thesis and demonstrator.

MOTIVATION AND PERSONAL AMBITIONS

Explain why you set up this project, what competences you want to prove and learn. For example: acquired competences from your MSc programme, the elective semester, extra-curricular activities (etc.) and point out the competences you have yet developed. Optionally, describe which personal learning ambitions you explicitly want to address in this project, on top of the learning objectives of the Graduation Project, such as: in depth knowledge a on specific subject, broadening your competences or experimenting with a specific tool and/or methodology, ... Stick to no more than five ambitions.

I set-up this project because I am interested in the 3D-printing field. I have my own 3D-printer and enjoy it a lot. During my elective space I chose the elective Digital materials which showed that there is way more possible with 3D-printing than I had initially thought. Therefore, my first learning goal is to explore and learn more about the possibilities of 3D-printing. Another reason why I set-up this project is that I want to apply my current knowledge about FDM 3D-printing as well as broaden it for the future. I think that in the coming years 3D-printing will become an important part of the prototyping process and therefore I think it is important to have knowledge in this field. Besides the process I am also interested in materials and their properties. Therefore, another learning goal is to apply and improve my current knowledge about materials and material testing.

I decided that I want to do a research project. Therefore, I consciously chose to not directly include a company within my project. In my former experiences within ACD and AED companies were quite restricting in what they wanted from the project and what was in their scope of interest. A research project gives more freedom for testing, prototyping and exploring new paths. Besides a higher degree of freedom within a research project, I also want to explore if research is something I am interested in. I have been doubting if I want to do a PhD or not since I have not much experience in doing research. Therefore, I want to use my master thesis to learn what doing research within the field of industrial design is like.

A competence I want to prove in my master thesis is that I am able to work methodologically. In the past I got complements from coaches that I can work thoroughly and methodologically, within this project I want to showcase this as well.

FINAL COMMENTS

In case your project brief needs final comments, please add any information you think is relevant.

Appendix 2 Search terms

Search terms
LW-PLA
ColorFabb
Varioshore TPU
LW-ASA
Printing parameters FDM
Polywood
Wood filled PLA.
Extruder height
Contour printing
Vase mode
Thin wall printing
Continuous line 3d printing
Continuous FDM print path.
Surface treatment FDM
Surface roughness of FDM
fdm printing review
shape memory polymer(s)
lattice structures additive manufacturing
lattice structures
Energy absorption
Energy absorbing
Impact absorption

Appendix 3 Energy absorbing applications

Personal protective equipment

Personal protective equipment is defined by the United states Department of labour (n.d.) as : “Personal protective equipment, commonly referred to as “PPE”, is equipment worn to minimize exposure to hazards that cause serious workplace injuries and illnesses.” PPE comes in many forms, in this case I will consider PPE also outside of the workplace so braces or helmets used within sports.

In the application of energy absorption PPE, is used to protect the user from intense impact (Lu and Yu, 2003). For example, helmets need to protect the users head in case the user falls, or when something drops on their head (Lu and Yu, 2003) . Apart from helmets, there are also many protection pads for the body, which have a similar function.

Vehicles

Motorised vehicles are also engineered to be able to sustain impact. Within the car industry alone, there is much attention for making the best energy absorbing structures to be able to protect the passengers. Usually this is done by engineering structures that fold up in a certain way as to be able to absorb as much energy as possible (Lu and Yu, 2003). Outside of the car industry, vehicles that are used for industrial purposes, such as digging machines, also have specialised cages (Lu and Yu, 2003) to protect the passenger in case something drops on it or if the vehicle rolls over.

Infrastructures

In earthquake areas, many buildings are built to be able to absorb the energy of earthquakes. This is usually done with specially engineered materials and structures. Another example of infrastructure that needs to withstand high amounts of energy are crash bars, alongside the highway. They need to catch the impact of a car or lorry in case it loses control (Lu and Yu, 2003).

Packaging

Packaging of precious products are also used to be energy absorbing. This is to protect it from transport and handling. For packaging usually paper materials or plastics are being used (Lu and Yu, 2003). These can also be manufactured in special structures to be able to withstand even more energy (Lu and Yu, 2003).

Lu, G., & Yu, T. (2003). *Energy Absorption of Structures and Materials* (Vol. 1). Woodhead Publishing Ltd.

United States Department of Labour. (n.d.). *Personal Protective Equipment.* Retrieved March 7, 2023, from https://www.osha.gov/personal-protective-equipment

Appendix 4 Gcode example

This appendix shows a snipped of Gcode in which triangles were printed with different temperatures. The red coloured text shows the command that changes the nozzle temperature before starting with a new triangle. Several lines were removed to to keep the example short.

```
;START_OF_HEADER
;HEADER_VERSION:0.1
;FLAVOR:Griffin
;GENERATOR.NAME:Cura_SteamEngine
;GENERATOR.VERSION:main
;GENERATOR.BUILD_DATE:2022-07-19
;TARGET_MACHINE.NAME:Ultimaker 3
;EXTRUDER_TRAIN.0.INITIAL_TEMPERATURE:190
;EXTRUDER_TRAIN.0.MATERIAL.VOLUME_USED:2534
;EXTRUDER_TRAIN.0.MATERIAL.GUID:506c9f0d-e3aa-4bd4-b2d2-23e2425b1aa9
;EXTRUDER_TRAIN.0.NOZZLE.DIAMETER:0.4
;EXTRUDER_TRAIN.0.NOZZLE.NAME:AA 0.4
;BUILD_PLATE.TYPE:glass
;BUILD_PLATE.INITIAL_TEMPERATURE:60
;PRINT.TIME:2366
;PRINT.GROUPS:4
;PRINT.SIZE.MIN.X:32.49
;PRINT.SIZE.MIN.Y:20.225
;PRINT.SIZE.MIN.Z:0.27
;PRINT.SIZE.MAX.X:186.549
;PRINT.SIZE.MAX.Y:179.206
;PRINT.SIZE.MAX.Z:25
;END_OF_HEADER
;Generated with Cura_SteamEngine main
T0
M82 ;absolute extrusion mode
G92 E0
M109 S190
G280 S1
G0 Z20.001
G1 F1500 E-6.5
;LAYER_COUNT:100
;LAYER:0
M107
M204 S1000
M205 X20 Y20
G0 F4500 X70.478 Y151.824 Z0.27
G0 X67.412 Y143.431
;TYPE:SKIRT
G1 F1500 E0
G1 F900 X68.038 Y143.838 E0.01517
G1 X68.615 Y144.309 E0.0303
G1 X69.139 Y144.84 E0.04546
G1 X69.604 Y145.424 E0.06062
G1 X70.003 Y146.054 E0.07577
G1 X70.332 Y146.723 E0.09092
G1 X70.588 Y147.424 E0.10608
G1 X70.768 Y148.148 E0.12123
G1 X70.869 Y148.887 E0.13639
G1 X70.89 Y149.633 E0.15155
G1 X70.831 Y150.376 E0.16669
.
.
.
.
.
.
.
;MESH:Triangle 20mm.STL(2)
M109 S200
G0 F4500 X164.55 Y171.768
G0 X165.62 Y171.785
;TYPE:WALL-OUTER
G1 F1500 E124.42284
G1 F900 X160.677 Y153.336 E124.81086
G1 X179.126 Y158.279 E125.19888
G1 X165.62 Y171.785 E125.58691
G1 X160.677 Y153.336 Z0.36 E125.97493
G1 X179.126 Y158.279 Z0.45 E126.36295
G1 X165.62 Y171.785 Z0.54 E126.75099
;TIME_ELAPSED:688.490544
;LAYER:1
M106 S85
M204 S714
;MESH:Triangle 20mm.STL(2)
```

Appendix 5 Pilot compression test

Compression test was done according to the instructions from ASTM 2016

Astm. (2016). *Standard Test Method for Compressive Properties Of Rigid Cellular Plastics 1*. https://www.astm.org/d1621-16.html

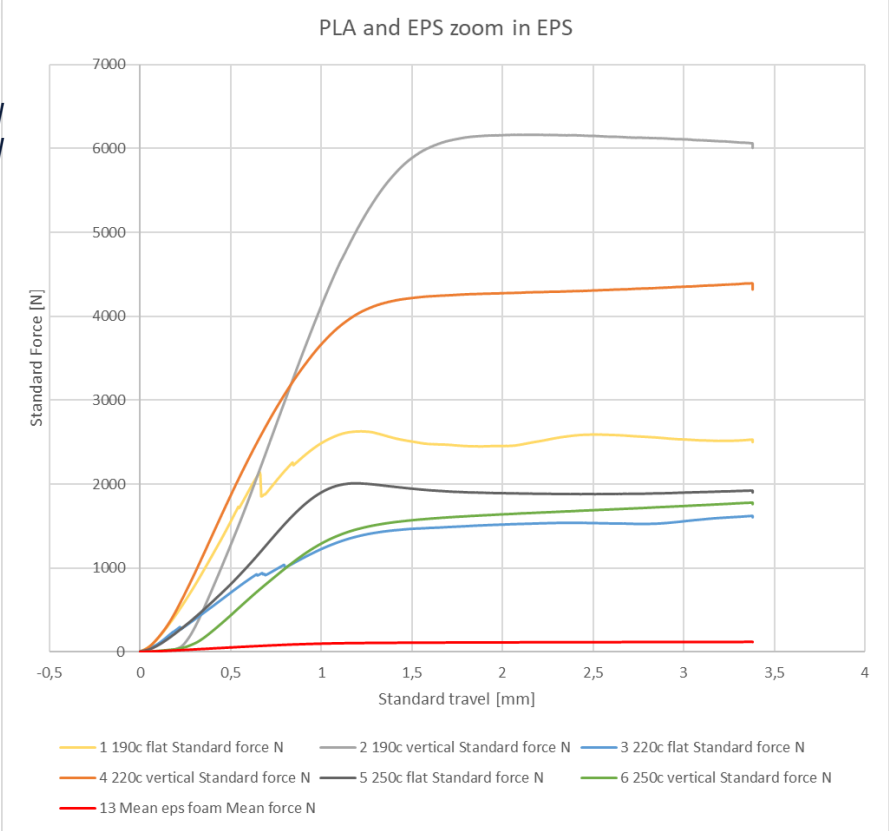

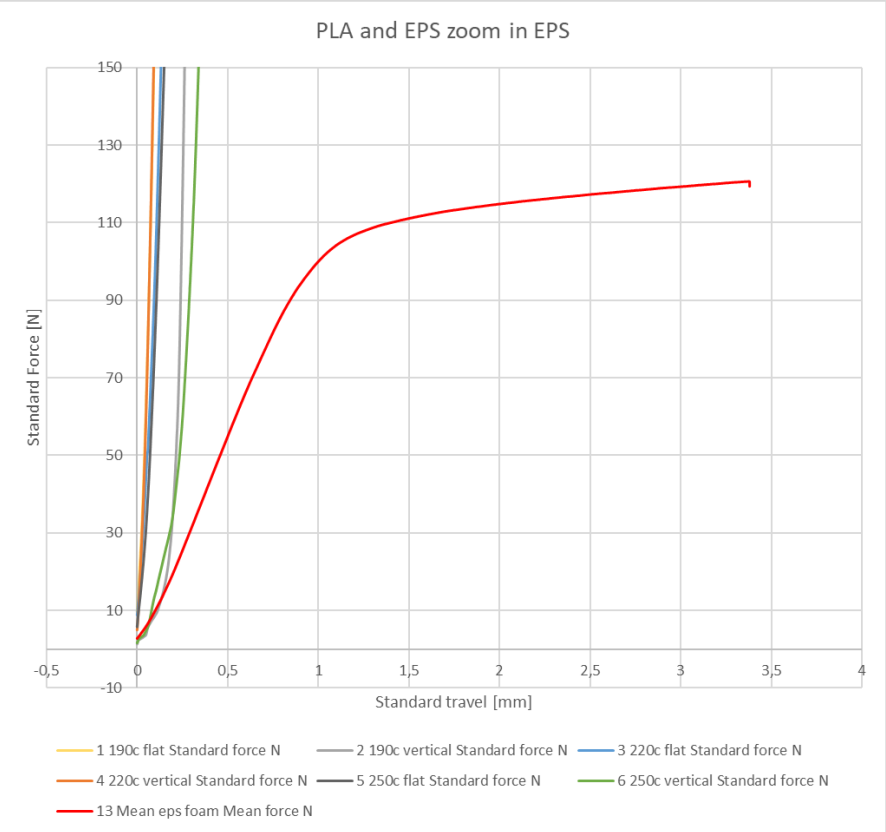

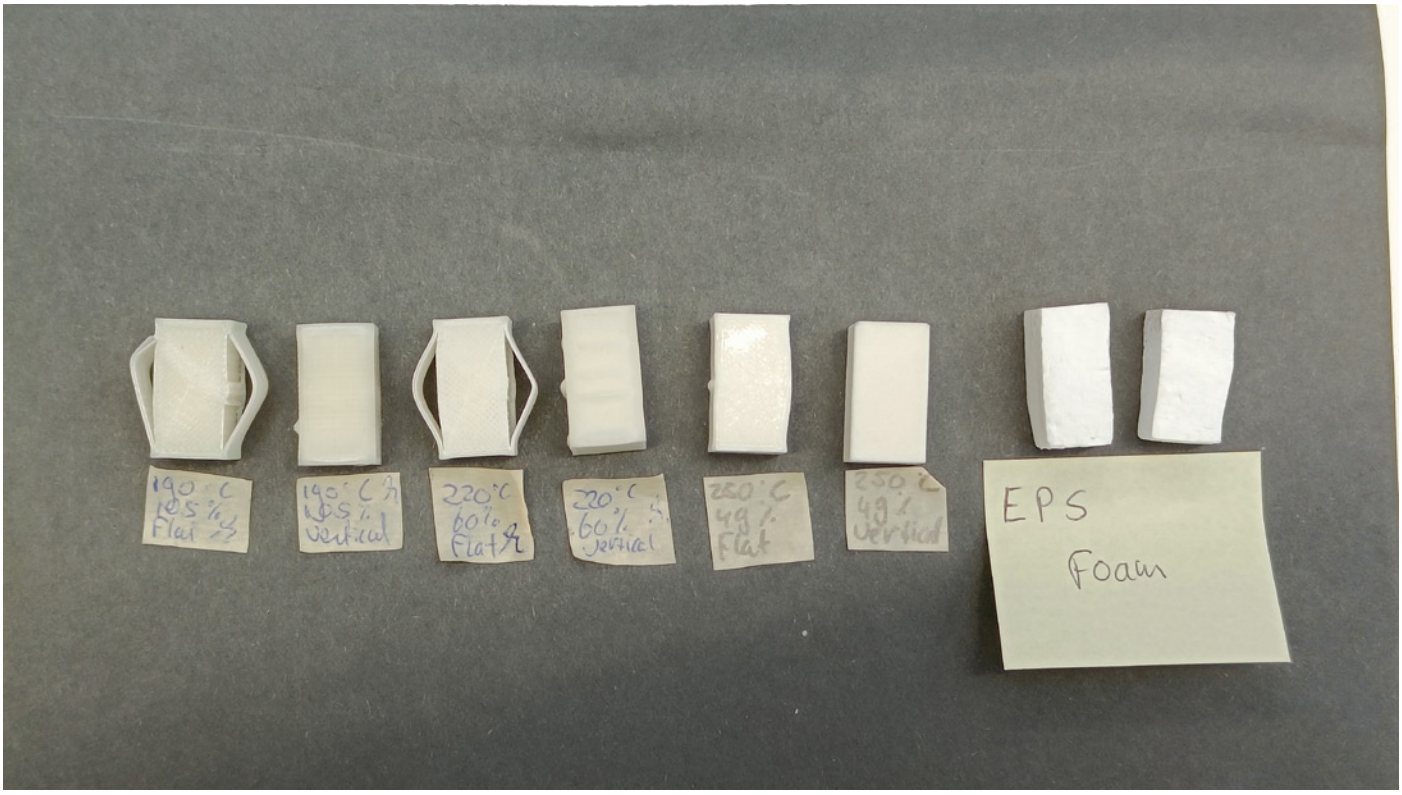
EPS
Foam

Appendix 6, more results compression test, stress-strain and energy absorption curves

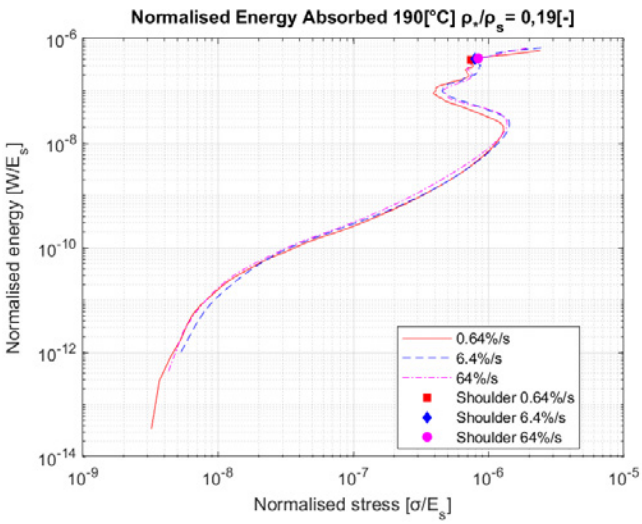

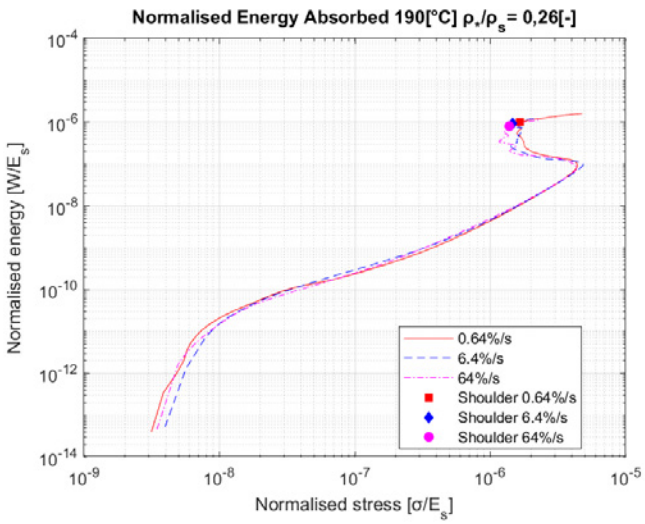

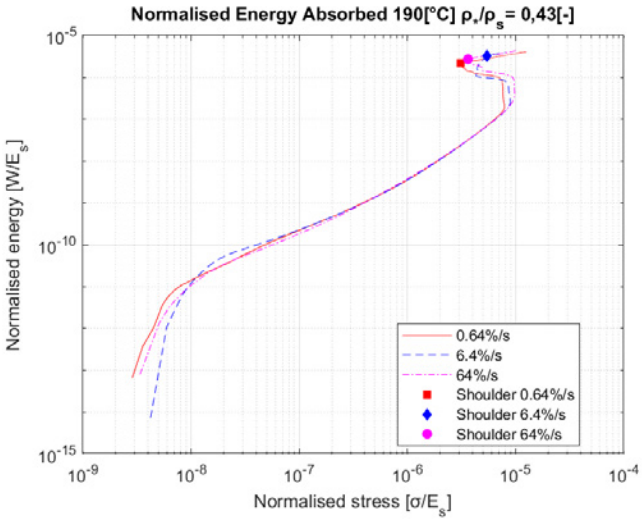

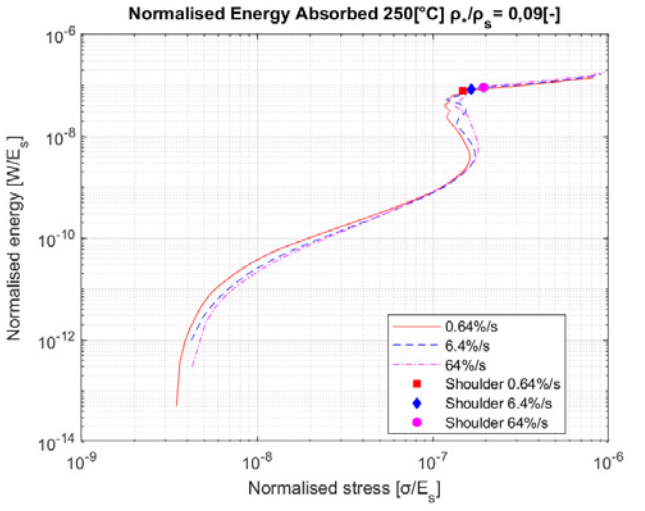

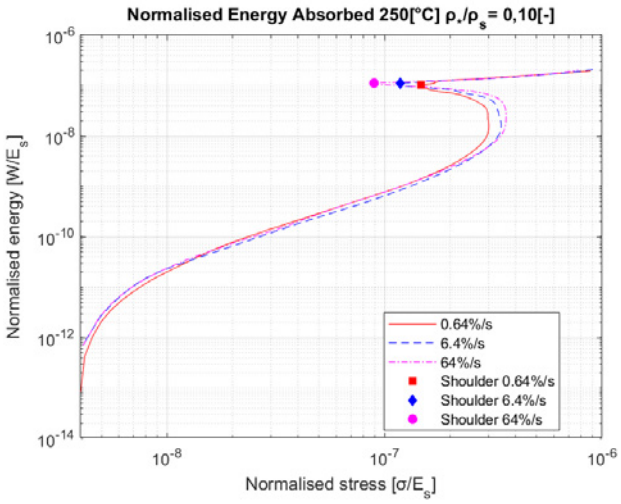
Normalised Energy Absorbed 250[°C] ρ*/ρs = 0,10[-]
Normalised energy [W/Es]
Normalised stress [σ/Es]
0.64%/s
6.4%/s
64%/s
Shoulder 0.64%/s
Shoulder 6.4%/s
Shoulder 64%/s

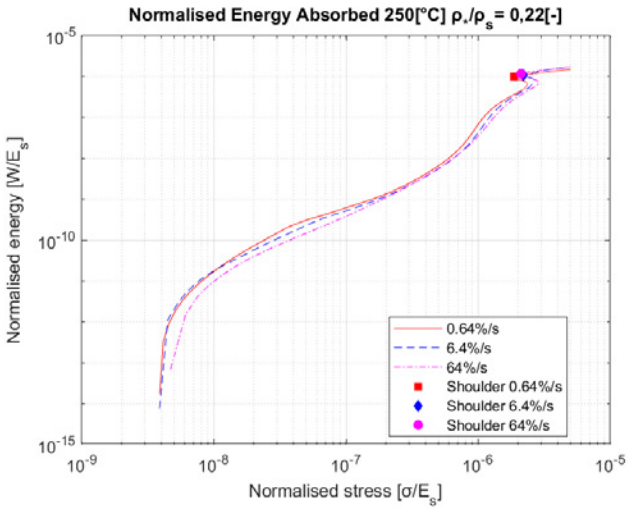
Normalised Energy Absorbed 250[°C] ρ*/ρs = 0,22[-]
Normalised energy [W/Es]
Normalised stress [σ/Es]
0.64%/s
6.4%/s
64%/s
Shoulder 0.64%/s
Shoulder 6.4%/s
Shoulder 64%/s

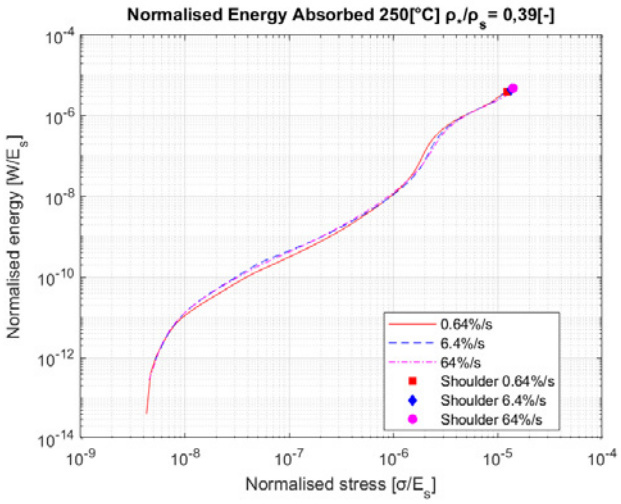
Normalised Energy Absorbed 250[°C] ρ*/ρs = 0,39[-]
Normalised energy [W/Es]
Normalised stress [σ/Es]
0.64%/s
6.4%/s
64%/s
Shoulder 0.64%/s
Shoulder 6.4%/s
Shoulder 64%/s

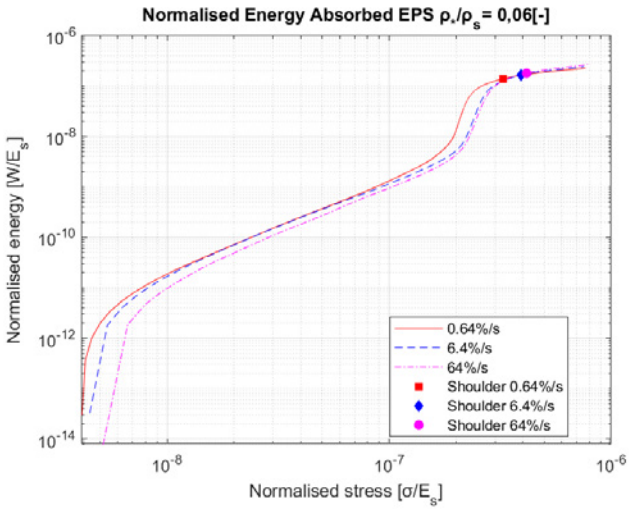
Normalised Energy Absorbed EPS ρ*/ρs = 0,06[-]
Normalised energy [W/Es]
Normalised stress [σ/Es]
0.64%/s
6.4%/s
64%/s
Shoulder 0.64%/s
Shoulder 6.4%/s
Shoulder 64%/s

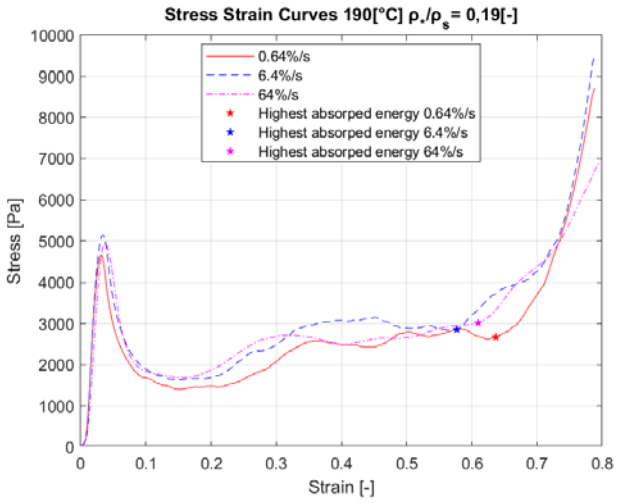
Stress Strain Curves 190[°C] ρ*/ρs = 0,19[-]
Stress [Pa]
Strain [-]
0.64%/s
6.4%/s
64%/s
Highest absorped energy 0.64%/s
Highest absorped energy 6.4%/s
Highest absorped energy 64%/s

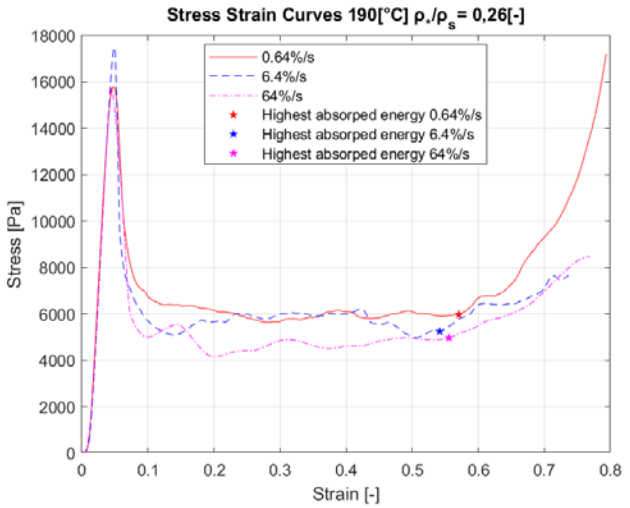
Stress Strain Curves 190[°C] ρ*/ρs = 0,26[-]
Stress [Pa]
Strain [-]
0.64%/s
6.4%/s
64%/s
Highest absorped energy 0.64%/s
Highest absorped energy 6.4%/s
Highest absorped energy 64%/s

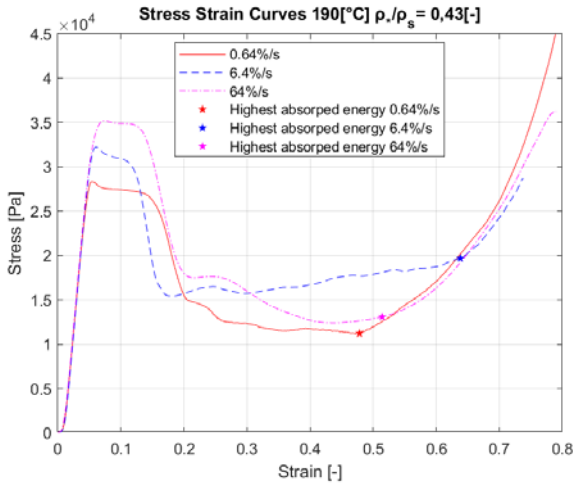
Stress Strain Curves 190[°C] ρ*/ρs = 0,43[-]
×10^4
0.64%/s
6.4%/s
64%/s
Highest absorped energy 0.64%/s
Highest absorped energy 6.4%/s
Highest absorped energy 64%/s
Stress [Pa]
Strain [-]

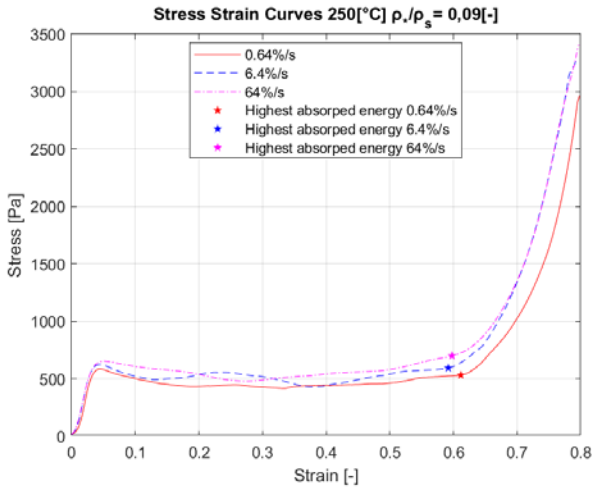
Stress Strain Curves 250[°C] ρ*/ρs = 0,09[-]
0.64%/s
6.4%/s
64%/s
Highest absorped energy 0.64%/s
Highest absorped energy 6.4%/s
Highest absorped energy 64%/s
Stress [Pa]
Strain [-]

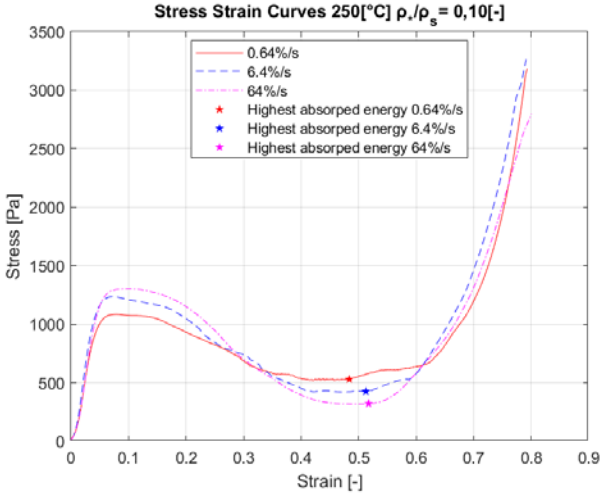
Stress Strain Curves 250[°C] ρ*/ρs = 0,10[-]
0.64%/s
6.4%/s
64%/s
Highest absorped energy 0.64%/s
Highest absorped energy 6.4%/s
Highest absorped energy 64%/s
Stress [Pa]
Strain [-]

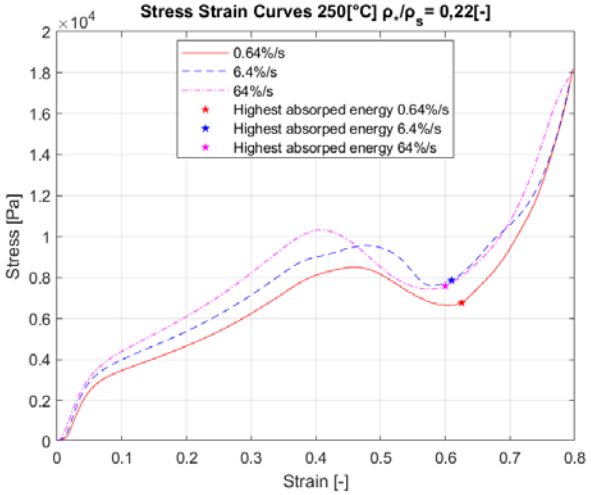
Stress Strain Curves 250[°C] ρ*/ρs = 0,22[-]
×10^4
0.64%/s
6.4%/s
64%/s
Highest absorped energy 0.64%/s
Highest absorped energy 6.4%/s
Highest absorped energy 64%/s
Stress [Pa]
Strain [-]

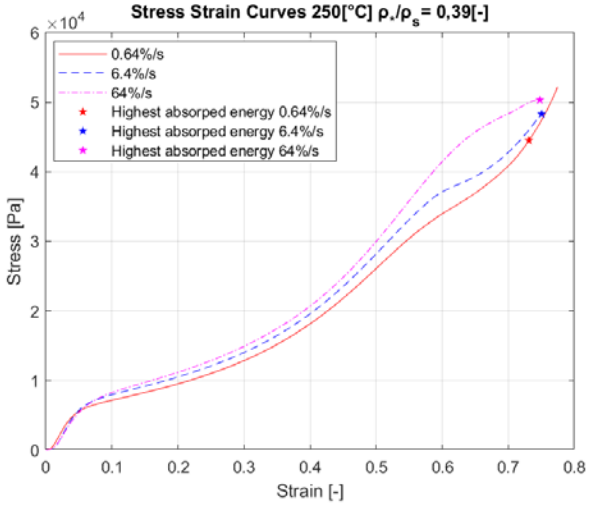
Stress Strain Curves 250[°C] ρ*/ρs = 0,39[-]
×10^4
0.64%/s
6.4%/s
64%/s
Highest absorped energy 0.64%/s
Highest absorped energy 6.4%/s
Highest absorped energy 64%/s
Stress [Pa]
Strain [-]

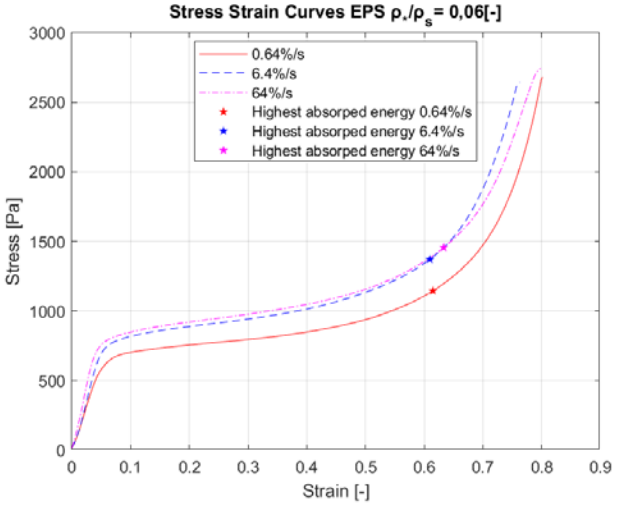
Stress Strain Curves EPS ρ*/ρs = 0,06[-]
0.64%/s
6.4%/s
64%/s
Highest absorped energy 0.64%/s
Highest absorped energy 6.4%/s
Highest absorped energy 64%/s
Stress [Pa]
Strain [-]

strain-rate 0,64	**190-0,19-1**	**190-0,26-1**	**190-0,43-1**	**250-0,09-1**	**250-0,10-1**	**250-0,22-1**	**250-0,39-1**	**eps-0,06-1**
Energy absorbed @ densification	1433,9	3665,1	7830	278,2531	367,8015	3603,3	14194	488,2724
Energy ratio	0,5373	0,6132	0,6992	0,5236	0,6947	0,533	0,319	0,4266
Strain @densification	0,6371	0,5707	0,4784	0,6118	0,4837	0,6256	0,7313	0,6149
stress @ densification	2668,8	5876,8	11199	531,4049	529,4625	6760,6	44490	1144,5
Deformation @ densification	16,648839	14,87308	12,45435	15,902721	12,61113	16,16828	19,01624	15,9061
Normalised energy absorbed	0,3983056	1,018083	2,175	0,0772925	0,102167	1,000917	3,942778	0,139506
strain-rate 6,4	**190-0,19-2**	**190-0,26-2**	**190-0,43-2**	**250-0,09-2**	**250-0,10-2**	**250-0,22-2**	**250-0,39-2**	**eps-0,06-2**
Energy absorbed @ densification	1473,8	3272,6	11892	300,8613	399,2081	3997,8	16184	573,5873
Energy ratio	0,5165	0,6236	0,6047	0,5068	0,9368	0,5083	0,3351	0,4185
Strain @densification	0,5772	0,5417	0,6384	0,592	0,5127	0,6099	0,7505	0,6096
stress @ densification	2853,3	5247,8	19665	593,6989	426,1531	7864,4	48298	1370,6
Deformation @ densification	15,055941	14,12031	16,67735	15,314382	13,34957	15,89467	19,513	15,72565
Normalised energy absorbed	0,4093889	0,909056	3,303333	0,0835726	0,110891	1,1105	4,495556	0,163882
strain-rate 64	**190-0,19-3**	**190-0,26-3**	**190-0,43-3**	**250-0,09-3**	**250-0,10-3**	**250-0,22-3**	**250-0,39-3**	**eps-0,06-3**
Energy absorbed @ densification	1511,4	2918,1	9804,5	329,3607	403,5589	4182,2	17487	627,9851
Energy ratio	0,5012	0,5865	0,7499	0,4703	1,2528	0,5509	0,3475	0,4313
Strain @densification	0,61	0,5557	0,5144	0,5979	0,5174	0,6	0,7479	0,6332
stress @ densification	3015,7	4975	13074	700,2932	322,1282	7,5913	50324	1456,1
Deformation @ densification	15,899311	14,54514	13,3664	15,539421	13,38686	15,558	19,58085	16,41536
Normalised energy absorbed	0,4198333	0,810583	2,723472	0,0914891	0,1121	1,161722	4,8575	0,179424
Density of sample	234,7782	321,4296	530,2186	116,9516	128,6414	273,4618	483,6184	64,1593

Appendix 7, Helmet measurements

Measurements of the EPS impact liner and comfort liner from different helmets in mm		
	EPS	Comfort liner
MT integral helmet	24,69 20,00 21,31 23,50	12,15 8,71 10,18 27,70 (cheek)
Nolan helmet	21,70 25,19 33,20 24,95	33,50 (cheek) 33,03 (cheek) 10,13 9,64 8,55
Nexx	30,09 23,23 27,8 15	11,59 10,02 31,86(cheek) 29,36(cheek) 31,84(cheek)
Xlite	23,35 36,71 18,44 20,73	36,75(cheek) 37,14(cheek) 10,78 11,00